Title
Identification of cholestenoic acid as a ligand for the nuclear hormone receptor DAF-12 in Caenorhabditis elegans

Author
Held, Jason M

Publication Date
2006

Peer reviewed|Thesis/dissertation

Identification of Cholestenoic Acid as a Ligand for the Nuclear Hormone Receptor

DAF-12 in *Caenorhabditis elegans*

by

Jason M. Held

DISSERTATION

Submitted in partial satisfaction of the requirements for the degree of

DOCTOR OF PHILOSOPHY

in

Pharmaceutical Sciences and Pharmacogenomics

in the

GRADUATE DIVISION

of the

UNIVERSITY OF CALIFORNIA, SAN FRANCISCO

To Joanne,

for all the love and support

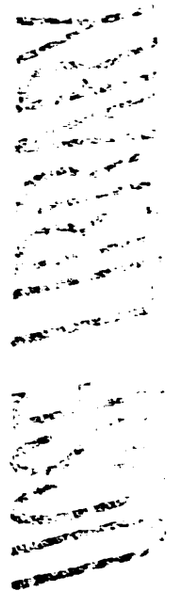

ACKNOWLEDGEMENTS

I would like to acknowledge my advisors Dr. Brad Gibson and Dr. Gordon Lithgow for their support and flexibility to let me choose a project that was outside of the realm of experiments typical in their labs. I would also like to sincerely acknowledge Dr. Matt Gill for his mentoring and his ability to tell a scientific narrative.

I would also like to thank Mark White as well as Amanda Foster for providing generous amounts of extracts to analyze, Dr. Gary Scott for his unwavering support, Dr. Nancy Phillips for nuggets of knowledge about lipids and analytical chemistry, Dr. Anders Olsen for advice on thesis composition, Lori LaVine for advice on how to prevent explosions, Dr. Al Fisher and Dr. Di Chen for their encyclopedic knowledge of DAF mutants, Dr. Pankaj Kapahi for his exuberant encouragement, Dr. Simon Allen for taking the time to help troubleshoot HPLC problems, Dr. Xin Guo for an introduction to mass spectrometry, and Kally Pan for critical review of portions of this thesis.

I would also like to thank all the members of the Gibson and Lithgow labs for useful discussions, especially Eric Johansen for organic chemistry terminology, as well as Vicky Loel, Justine Bock, and Andrej Novak for their help whenever it was needed.

ABSTRACT

Identification of Cholestenoic Acid as a Ligand for the Nuclear Hormone Receptor DAF-12 in *Caenorhabditis elegans*

Jason M. Held

The orphan nuclear DAF-12 regulates *C. elegans* dauer formation, lipid metabolism, and lifespan in response to the environmental cues of population density, temperature, and food availability. The identity of the DAF-12 ligand has not yet been discovered despite significant evidence that it is sterol-derived and metabolized by DAF-9, a cytochrome P450. We have previously identified that lipophilic nematode extracts can rescue dauer formation in *C. elegans*. Chemical characterizations of these extracts demonstrate that the ligand for DAF-12 contains a carboxyl moiety and we show that *C. elegans* can carboxylate sterols. A candidate ligand screen of sterol acids found that the C27 bile acid cholestenoic acid (5-cholesten-3β-ol-(25S)-carboxylic acid) promotes reproductive growth in dauer-constitutive mutants in a *daf-9* and *daf-12* dependent manner by acting as a DAF-12 ligand. Gas chromatography–mass spectrometry analysis of the dauer-rescuing lipophilic extracts identified several regioisomers of cholestenoic acid that are not present in extracts from hormone deficient *daf-9* mutants. These findings confirm an endocrine link between DAF-12 and upstream signaling pathways that regulate dauer formation and lifespan determination. Identification of cholestenoic acid provides an important tool to further decipher the mechanism of these phenotypes and suggests that carboxylated sterols play an important role in the life history of *C. elegans*.

Dr. Bradford W. Gibson, Thesis Advisor

TABLE OF CONTENTS

LIST OF FIGURES

CHAPTER I

Introduction

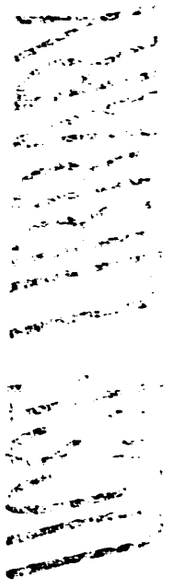

Dauer formation is a complex phenotype

In order to survive, organisms must respond to their complex environment by detecting external cues and translating them into appropriate physiological responses. In *Caenorhabditis elegans* (*C. elegans*), an example of this is dauer formation. Under favorable conditions the worm develops through four larval stages (L1-L4) to adult (Figure 1.1). However, an alternate third larval stage known as the dauer stage is initiated during unfavorable environmental conditions (Figure 1.1) (Cassada and Russell, 1975). When conditions become favorable again, the worm can resume development at L4 and become a reproductive adult. Several signals are synergistically integrated by the worm to determine whether to develop into a dauer: high concentration of a pheromone that signals overcrowding, limited food signal, and high temperature (Golden and Riddle, 1984; Ailion and Thomas, 2000). Dauer formation is a complex phenotype in which the worm arrests development, shifts its metabolism towards fat and carbohydrate storage, increases stress-protective enzymes, modifies its behavior, and develops a cuticle especially resistant to environmental chemicals (Albert and Riddle, 1988; Riddle and Albert, 1997).

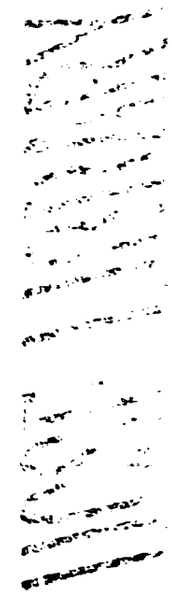

Genetic analysis of dauer formation

Mutant screens have identified over 40 genes that are involved in regulating dauer formation. These genetic pathways have defined mutations causing inappropriate dauer formation (dauer constitutive – Daf-c) (Albert et al., 1981) or failure to form dauers (dauer defective – Daf-d) (Swanson and Riddle, 1981). By combining multiple mutations,

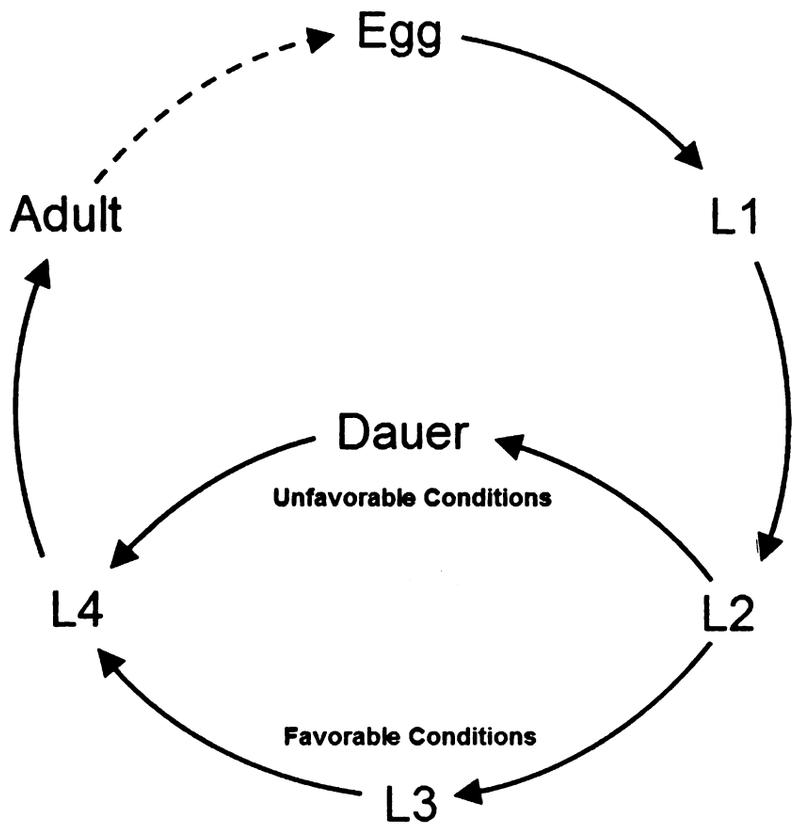

Figure 1.1 The life cycle of *C. elegans*. Under favorable conditions the worm develops from egg to adult through four larval stages, L1-L4. Under stressful conditions the worm can enter diapause after L2 and become a dauer. Upon return of favorable conditions the worm can resume development to L4 and become an adult.

epistatic analysis has determined how genes are ordered relative to one another in the dauer signaling pathway and has revealed that three separate signaling pathways regulate dauer formation (Figure 1.2) (Vowels and Thomas, 1992; Malone et al., 1996; Riddle and Albert, 1997). One pathway is an insulin signaling pathway in which *daf-2*, an insulin-like receptor/IGF-1 homolog, acts via the FOXO-family transcription factor *daf-16* (Vowels and Thomas, 1992; Gottlieb and Ruvkun, 1994). A second pathway is a transforming growth factor-β (TGFβ) pathway in which *daf-7*, a TGFβ ligand, interacts with Type I and Type II TGFβ receptors *daf-4* and *daf-1* to regulate transcription via the Smads *daf-3*, *daf-8*, and *daf-14* and the Sno/Ski homolog *daf-5* (Patterson and Padgett, 2000). The third signaling pathway has been less tractable genetically but includes the guanylate cyclase *daf-11* and heat-shock protein 90 *daf-21* (Birnby et al., 2000). The genes in these pathways transduce the environmental signals that mediate the decision to proceed with normal reproductive growth or initiate dauer formation.

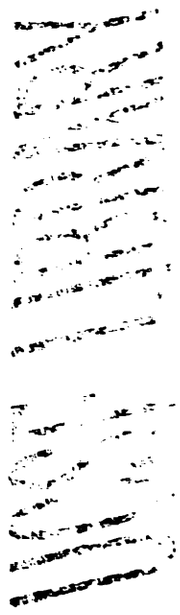

daf-12 was isolated in the first mutant screen for dauer formation (Riddle et al., 1981) and epistasis experiments have revealed that *daf-12* is the most downstream Daf gene. With a nuclear receptor occupying the terminal position in the dauer formation pathway (Figure 1.2) (Riddle and Albert, 1997), this signaling pathway is much like other mammalian signaling pathways in which the insulin/FOXO and TGFβ pathways are known to converge with nuclear receptor signaling (Yanagisawa et al., 1999; Subramaniam et al., 2001; Dowell et al., 2003). Most *daf-12* mutants are Daf-d, initially suggesting that the role of DAF-12 was to allow for entry into diapause. However, a subset of *daf-12* mutations are Daf-c suggesting that since *daf-12* has both Daf-c and Daf-d phenotypes it plays an instructive role in the dauer formation process and directs

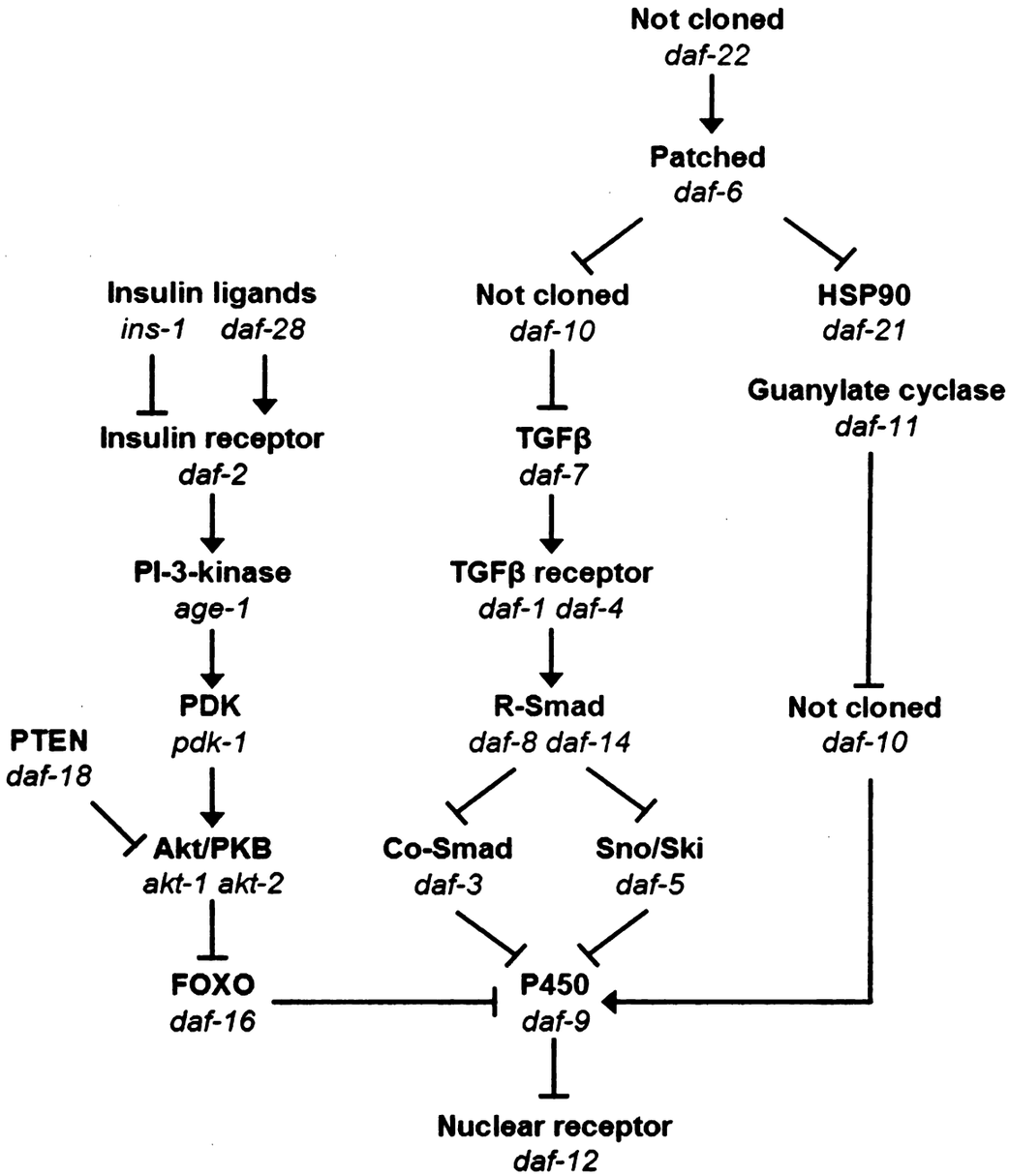

Figure 1.2 Genetic pathway for dauer larva formation. Epistasis analysis has revealed genetic components that regulate dauer formation. The pathway is drawn to show wild type gene functions that stimulate (arrow) or inhibit (T bar) subsequent steps in the pathway. There are three main branches: insulin signaling, TGFβ signaling, and a HSP90/guanylate cyclase pathway.

both programs of reproductive growth as well as entry into diapause (Antebi et al., 1998; Antebi et al., 2000; Gerisch and Antebi, 2004; Mak and Ruvkun, 2004).

The role of DAF-12 in worm biology

In addition to dauer formation, DAF-12 has been implicated in several other aspects of worm physiology during development, including gonad formation. During L3 the gonad of the worm grows from a four cell primordium in the ventral midbody outward along the body wall. It then makes a 90 degree turn and migrates along the epidermis a short distance to the dorsal muscle bands where it make another 90 degree turn back towards the midbody. This creates an overall path shaped like a U. Many *daf-12* mutants have a Mig phenotype (Migration of cells abnormal) in which the gonad initially moves outwardly along the ventral midbody but fails to make either 90 degree turn. This creates a linear gonad rather than a U-shaped one (Antebi et al., 1998). DAF-12 is thought to regulate the first 90 degree turn by upregulating the receptor UNC-5, a receptor for the netrin guidance cue UNC-6 (Su et al., 2000).

In addition to gonad formation, DAF-12 is involved in the coordination of developmental timing in *C. elegans*. DAF-12 works with *lin-14* and *lin-28* along with microRNAs (miRNAs) *let-7* and *lin-4* to properly regulate developmental timing (Antebi et al., 1998). *lin-4* is expressed in L1 and downregulates *lin-14*, promoting the progression from the L1 to the L2 stage (Wightman et al., 1993). *lin-4* also downregulates *lin-28* to allow development to L3 (Moss and Tang, 2003) in an interaction that involves DAF-12 via an unknown mechanism (Seggerson et al., 2002). *let-7* is required for the transition from L4 to adult (Reinhart et al., 2000) and the timing

of its expression is dependent on *daf-12* (Johnson et al., 2003). A recent model of these interactions suggests that *let-7* miRNA and DAF-12 are in a feedback loop in which *daf-12* is required to turn on *let-7* but once *let-7* miRNA accumulates it represses DAF-12 production (Grosshans et al., 2005).

DAF-12 is also implicated as a regulator of lifespan in *C. elegans* (Tatar et al., 2003; Kenyon, 2005). The role of DAF-12 in the aging process is complex since most *daf-12* mutations either shorten lifespan or have no effect (Larsen et al., 1995; Gems et al., 1998) yet others lead to increased lifespan (Fisher and Lithgow, 2006). Furthermore, *daf-12* has been found to interact with the *daf-2* insulin-like pathway to regulate lifespan. *daf-2* alone is long-lived and *daf-2;daf-12* double mutants either cause suppression of *daf-2* lifespan extension in one class of *daf-2* mutants or synergistically increase lifespan in another class of *daf-2* mutants (Larsen et al., 1995; Gems et al., 1998). DAF-12 also plays a key role in the lifespan extension that occurs when germline precursor cells are removed by laser ablation (Hsin and Kenyon, 1999). Germline lifespan extension is dependent on the nuclear-localization of the FOXO-family transcription factor DAF-16; however, mutations in *daf-12* suppress both DAF-16 nuclear-localization and lifespan extension (Arantes-Oliveira et al., 2002). Interestingly, *daf-12* is not required for the DAF-16 nuclear-localization that occurs in long-lived *daf-2* mutants, suggesting that this suppression is specific to the lifespan signal of the reproductive pathway (Berman and Kenyon, 2006). DAF-12 itself has an essential role in promoting longevity since *daf-12* mutants suppress the lifespan extension in a germline deficient animal with a constitutively nuclear-localized DAF-16 (Berman and Kenyon, 2006).

DAF-12 characterization

The molecular characterization of DAF-12 provides insight into how DAF-12 is involved in so many aspects of worm physiology. DAF-12 is a nuclear receptor with a typical nuclear receptor architecture consisting of a hypervariable amino terminus (N-terminus), a conserved zinc finger DNA-binding domain (DBD), a hinge region, and a carboxy-terminal ligand-binding domain (LBD) (Figure 1.3 A) (Mangelsdorf and Evans, 1995; Antebi et al., 2000; Snow and Larsen, 2000). Nuclear receptors are often involved in complex signaling pathways, and the many phenotypes that *daf-12* affects suggest that *daf-12* is no different.

Nuclear receptors in *C. elegans*

DAF-12 may be the best characterized nuclear receptor in *C. elegans*, but it is certainly not the only one playing key roles in the biology of *C. elegans*. Nuclear receptors have undergone a tremendous expansion in *C. elegans* to 284 putative receptors versus the 48 found in humans (Sluder et al., 1999; Sluder and Maina, 2001). These receptors have been shown to be involved in neuronal development (Qin and Powell-Coffman, 2004), larval molting (Gissendanner and Sluder, 2000; Kostrouchova et al., 2001), sex determination (Carmi et al., 1998), xenobiotic response (Lindblom et al., 2001), and lipid metabolism (Van Gilst et al., 2005a; Van Gilst et al., 2005b). Like all nuclear receptors in *C. elegans*, however, DAF-12 remains an orphan receptor.

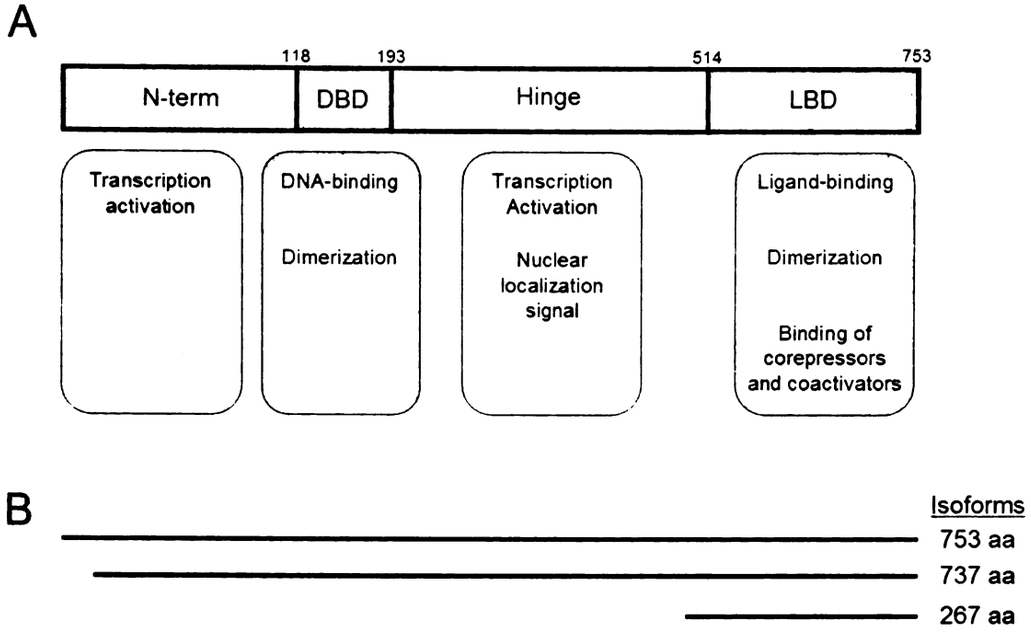

Figure 1.3 Molecular characterization of DAF-12. (A) DAF-12 is a nuclear receptor with a typical domain structure including a variable N-terminal region, a DNA-binding domain (DBD), a hinge region, and a ligand-binding domain (LBD). The amino acids from full-length DAF-12 that correspond to each domain are listed above. Typical domain functions are listed below. (B) Splice variants of DAF-12 are 753, 737, and 267 amino acids. Lines represent the domains of DAF-12 (from A) present in each isoform.

DAF-12 expression

DAF-12 has three splice variants: two that are 753 and 737 amino acids and contain both the LBD and DBD and another variant with only the LBD that is 267 amino acids (Figure 1.3 B) (Antebi et al., 2000; Snow and Larsen, 2000). There is no clear understanding of the role that the LBD-only version of DAF-12 plays, but it may perform an autoregulatory function much like the mammalian SHP nuclear receptor that has no DBD (Seol et al., 1996) or the non-DNA-binding domain form of the *Drosophila* E75B hormone receptor that has been demonstrated to act as a dominant negative receptor (White et al., 1997). Northern blot analysis of *daf-12* mRNA levels shows that DAF-12 expression occurs in all developmental stages but is highest in L2 pre-dauers and egg, and lowest in animals that recently recovered from the dauer stage (Snow and Larsen, 2000). Interestingly, the ratio of transcripts containing both the LBD and DBD versus the truncated LBD-only transcript do not change significantly at any time (Snow and Larsen, 2000). DAF-12 protein expression has been studied using a *daf-12* gene that has a green fluorescent protein (GFP) inserted just after the N-terminus and is found to be nuclear-localized. DAF-12::GFP is expressed in a wide number of cells from egg through adult but expression is highest in L2 and lowest in dauers. DAF-12::GFP is expressed in the somatic gonad precursors, nervous system, seam cells, hypodermis, and pharyngeal muscle (Antebi et al., 2000; Snow and Larsen, 2000). Translational regulation of DAF-12 has been demonstrated to be at least partially dependent on the translational factor 4E *ife-4* (Dinkova et al., 2005).

DNA-binding domains and the DAF-12 DBD

Nuclear receptors commonly regulate target gene expression through direct binding of the receptor DBD to DNA. The DNA binding sites typically consist of two hexamers arranged either as direct or inverted repeats spaced 1 to 5 bases apart or as a single hexamer (Rastinejad et al., 1995; Zhao et al., 1998). The occupied binding site can vary depending on whether the receptor is acting in a homo-, hetero-, or monomeric mode of action. DAF-12 has a high-affinity site that is a direct repeat AGTGCA spaced 5 bases apart (Shostak et al., 2004) and has also been shown to bind to a TGTGTG sequence (Ao et al., 2004). More than 50 genes exhibiting DAF-12-dependent regulation have been identified, encoding genes of many putative functionalities (Shostak et al., 2004; Fisher and Lithgow, 2006).

Ligand-binding domains and the DAF-12 LBD

Nuclear receptors act as agonist-induced factors to modulate target gene transcription via allosteric interactions of the LBD. Receptor agonists and antagonists interact with the LBD via two sets of α-helices that form the faces of the ligand binding pocket (LBP) (Figure 1.4). In the unliganded state, the α-Helix 12 (H12) in the C-terminal portion of the receptor is unordered and extends away from the LBP. With H12 displaced, the entire corepressor binding surface is exposed. A conserved helix, LXX I/H I XXX I/L, of the corepressor fits into the LBP in the absence of a ligand (Perissi et al., 1999). Upon ligand binding H12 folds back over the LBP with the ligand entirely buried in a predominantly hydrophobic pocket (Bourguet et al., 1995; Wurtz et al., 1996; Gampe, Jr. et al., 2000; Egea et al., 2000). The packing of H12 over a portion of the corepressor binding site

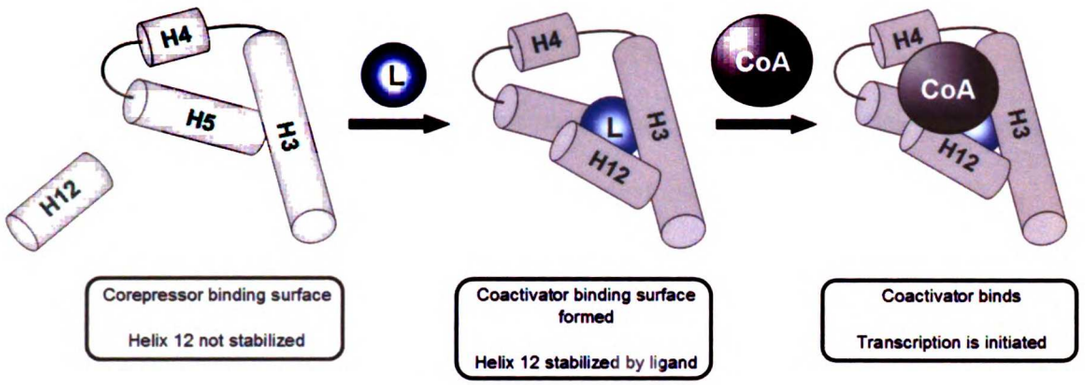

Figure 1.4 Model of ligand-dependent nuclear receptor transcriptional activation. Typically α-helix 3 (H3), H4, and H5 of the nuclear receptor LBD form a pocket to which corepressors bind when no ligand is present. Upon ligand binding, the corepressor is released and H12 packs onto the hydrophobic surface of the ligand creating a new binding site with affinity for coactivators. Coactivators then recruit basal transcriptional machinery for transcriptional activation.

causes corepressor release and formation of a new surface that has high affinity for the shorter coactivator LXXLL interaction domain motif and recruits coactivators (Nolte et al., 1998; Shiau et al., 1998; Darimont et al., 1998; Xu et al., 1999). For DAF-12, a single coregulator has been identified from a yeast two-hybrid screen. Named DIN-1 (DAF-12-interacting protein 1), it is an evolutionarily conserved putative corepressor similar to SHARP. It is Daf-d suggesting that DIN-1 binds DAF-12 under dauer formation conditions in which DAF-12 is unliganded (Ludewig et al., 2004). No DAF-12 coactivator has been identified.

The coactivators or corepressors that directly bind the LBD are crucial for nuclear receptor-dependent transcriptional regulation. Nuclear receptors modify chromatin structure by the innate histone deactylase activity of the receptor (McKenna et al., 1999a) or via association with histone deacetylases and histone acetyltransferases (Glass and Rosenfeld, 2000). Following chromatin decondensation, a second complex, either the thyroid receptor-associated proteins (TRAP) (Yuan et al., 1998) or the vitamin D receptor-interacting proteins (DRIP) (Rachez et al., 1998), establishes the link between the receptor and basal transcriptional machinery (McKenna et al., 1998; Freedman, 1999; McKenna et al., 1999b). In mammals, this transcriptional machinery includes the steroid receptor coactivators (SRCs) (Onate et al., 1995), cointegrators p300 (Eckner et al., 1994) and CBP (Chrivia et al., 1993), SWI/SNF homologs (Yoshinaga et al., 1992), and E3 ubiquitin-protein ligase coactivators (Cavailles et al., 1995). The transcriptional output of a nuclear receptor can further be influenced by post-translational modifications (Pagano et al., 1994; Hammer et al., 1999; Boudjelal et al., 2000; Fu et al., 2004).

Mutations in *daf-12*

Mutations in *daf-12* have been classified into six categories based on their effects on dauer and gonadal phenotypes. Significant mutations in the DBD such as those in predicted DNA contact residues (S137F and R143K) or a Zn coordinating Cys (C121Y) have strong Daf-d and gonadal phenotypes (Figure 1.5) (Antebi et al., 2000). The importance of the LBD to the function of DAF-12 has been made clear by two mutants (Q618stop and R688stop) that truncate the LBD between H5 and H9 and likely effect ligand binding, receptor dimerization, and transactivation. These mutants both have dauer and gonadal phenotypes, though they are less severe than that of DBD mutants (Antebi et al., 2000). A LBD mutant with a single amino acid change in an H4 residue (G582K) thought to stabilize the LBD as well as a LBD truncated at H10 (Q707stop) have near normal dauer formation but do have gonadal phenotypes suggesting that different DAF-12 factors separately regulate dauer and gonad formation (Antebi et al., 2000). Finally, mutation of a single Arg residue in H12 (R564) to either a Cys or His confers a Daf-c phenotype (Antebi et al., 2000). R564 likely makes direct hydrogen bonds with the DAF-12 ligand and is predicted to make DAF-12 ligand-insensitive (Wagner et al., 1995; Antebi et al., 2000).

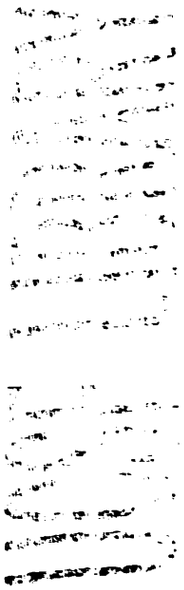

DAF-12 ligand: sterol hypothesis

Several pieces of evidence support the hypothesis that the DAF-12 ligand is sterol-derived. First, *C. elegans* requires exogenous cholesterol for normal growth in laboratory conditions and has been shown to be unable to synthesize sterols *de novo* (Hieb and Rothstein, 1968; Chitwood, 1999). Growing worms with the enantiomer of

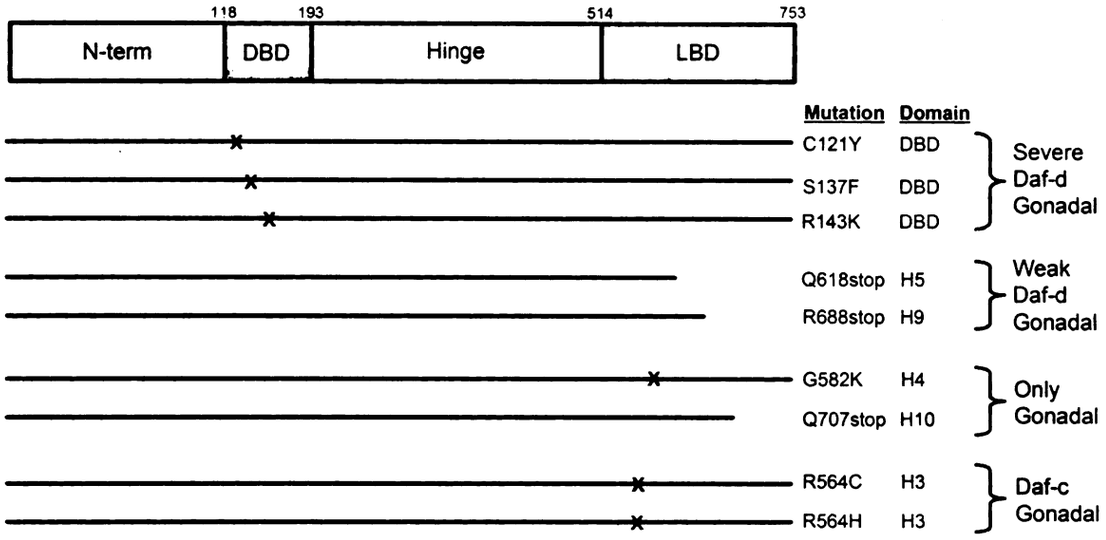

Figure 1.5 DAF-12 mutations lead to a variety of phenotypes. Mutations of important DBD residues (C121Y, S137F, R143K) lead to severe Daf-d and gonadal phenotypes whereas truncation of the LBD before H9 (Q618stop and R688stop) leads to weak Daf-d and gonadal phenotypes. A variety of DAF-12 mutants have been isolated that have unusual phenotypes such as G582K and Q707stop which affect H4 and H10 and lead to only gonadal phenotpyes. The conversion of R564 in H3 to either C or H leads to Daf-c, rather than Daf-d mutants. Line length represents length of mutant isoform and the domains contained. Point mutation locations are indicated by "X".

cholesterol causes lethality and developmental arrest (Crowder et al., 2001). Bioinformatic analysis suggests that the *C. elegans* genome does not contain homologs of squalene synthase or squalene cyclase, the key enzymes for the generation of lanosterol from squalene which is the first mammalian step in cholesterol biosynthesis (Entchev and Kurzchalia, 2005). Furthermore, cholesterol deprivation in wild type animals leads to a variety of phenotypes including developmental arrest and reduced fertility (Shim et al., 2002; Merris et al., 2003). Finally, developmental delay is observed in *ncr-1* and *ncr-2* mutants in which lysosomal transport of sterols is compromised, while *ncr-1;ncr-2* double mutants are Daf-c (Sym et al., 2000; Li et al., 2004).

Endocrine partnership of DAF-9 with DAF-12

A secondary endocrine system involving a lipophilic hormone has been proposed to link the transcriptional outputs of DAF-12 with upstream Daf signaling pathways via the cytochrome P450 DAF-9 (Figure 1.6). In favorable environments, DAF-9 is thought to be active and producing the DAF-12 ligand (Gerisch and Antebi, 2004; Mak and Ruvkun, 2004). This ligand binds DAF-12 and initiates transcription of genes that drive reproductive development. In unfavorable environments in which the worm becomes a dauer, DAF-9 is thought to be inactive and no DAF-12 ligand is produced (Gerisch and Antebi, 2004; Mak and Ruvkun, 2004). Unliganded DAF-12 then drives transcription of genes involved in dauer formation.

Over 80 cytochrome P450s have been identified in the genome of *C. elegans* (*C. elegans* Sequencing Consortium, 1998; Nelson, 1999) yet *daf-9* is the only P450 that has been identified with a dauer phenotype. This suggests that *daf-9* plays a critical or

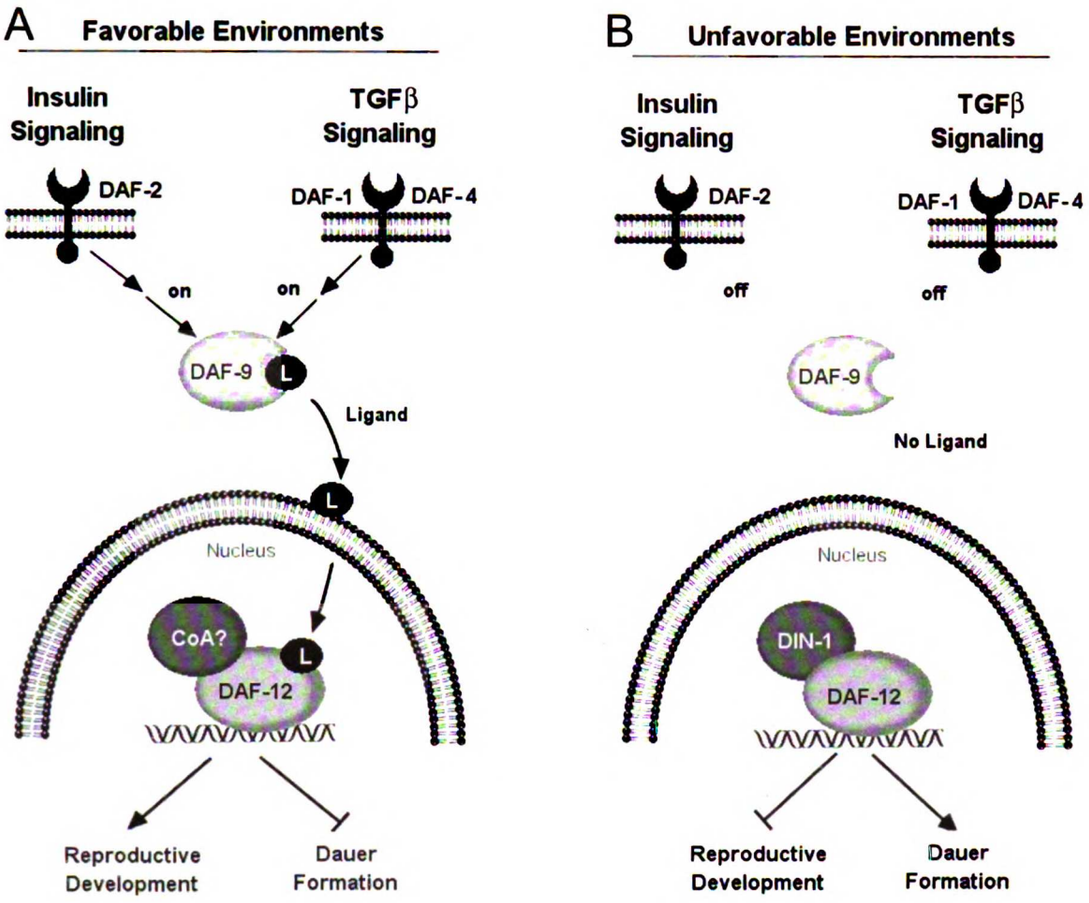

Figure 1.6 Enodcrine model of DAF-9 and DAF-12. The cytochrome P450 DAF-9 is hypothesized to integrate upstream dauer signaling such as insulin (DAF-2) and TGFβ (DAF-1, DAF-4) pathways by modulating DAF-12 ligand production. (A) In favorable environments, DAF-9 is active and generates DAF-12 ligand which binds to DAF-12 in the nucleus and causes transcription of genes that bring about reproductive growth and development. (B) In unfavorable environments, DAF-9 is inactive and no ligand is generated. Unliganded DAF-12, bound to its corepressor DIN-1, drives transcription of dauer-formation genes.

rate-limiting step in DAF-12 ligand production (Albert and Riddle, 1988). P450s are well known to mediate production of lipophilic hormones in mammals and *Drosophila* (Miller, 1988; Warren et al., 2002). *daf-9* has homology to the steroid and fatty acid hydroxylase family suggesting that an enzymatic hydroxylation step is likely important for ligand production (Gerisch et al., 2001; Jia et al., 2002). Strong *daf-9* alleles are Daf-c, suggesting that they are unable to synthesize a DAF-12 ligand. Interestingly, these mutants resemble the dauer and gonadal migration phenotypes of the R564 Daf-c *daf-12* mutants that are thought to be ligand-insensitive (Gerisch et al., 2001; Jia et al., 2002). Weak alleles of *daf-9* that are thought to be slightly compromised in their ability to synthesize the DAF-12 ligand have an enhanced dauer phenotype with cholesterol deprivation, which further supports the sterol hypothesis (Gerisch et al., 2001; Jia et al., 2002). Based on epistasis, *daf-9* has been placed upstream of *daf-12* but downstream of all other Daf genes (Figure 1.2) (Gerisch et al., 2001; Jia et al., 2002).

DAF-9 has been found to be highly expressed in the hypodermis from mid-L2 through L4 (Gerisch and Antebi, 2004; Mak and Ruvkun, 2004). Hypodermal expression of DAF-9 is absolutely dependent on DAF-12, suggesting a feedback control mechanism between nuclear receptor and P450 that is commonly found in hormonal pathways in mammals (Gerisch and Antebi, 2004; Mak and Ruvkun, 2004). Under favorable conditions (20°C, low pheromone, abundant food and cholesterol) *daf-9* is weakly expressed and under stressful dauer forming conditions (27°C, high pheromone, low food and cholesterol) *daf-9* expression is switched off (Gerisch and Antebi, 2004). Interestingly, under mildly stressful conditions not severe enough to cause dauer entry the level of hypodermal DAF-9 expression increases 8 to 13 fold over that of favorable

conditions (Gerisch and Antebi, 2004). This suggests that when the decision to become a reproductive adult or a dauer is relatively close, the worm makes an all-out drive to become an adult (Gerisch and Antebi, 2004).

A second location of DAF-9 expression is in a pair of neuron-like cells in the head called the XXXL/R cells (Gerisch et al., 2001; Gerisch and Antebi, 2004; Mak and Ruvkun, 2004) in which DAF-9 is in close coordination with SDF-9, a protein tyrosine phosphatase-like molecule that enhances DAF-9 activity (Ohkura et al., 2003). The DAF-9 levels in the XXXL/R cells are constant throughout development and do not vary with different levels of stress suggesting that these cells may produce a tonic level of the DAF-12 ligand (Gerisch and Antebi, 2004).

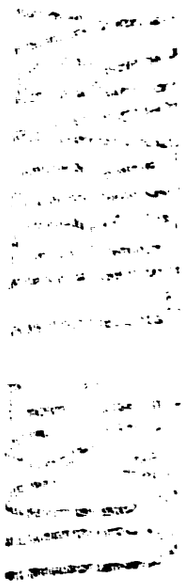

Gamravali is a potential DAF-12 ligand

It has been observed that sterol-deprived worms grown in the presence of the Δ^7 4-methyl sterol lophenol arrest as dauer larvae in a *daf-12*-dependent manner (Matyash et al., 2004). These lophenol-induced dauers are rescued by the addition of exogenous cholesterol or by the addition of a nematode lipid extract, termed *gamravali* (Matyash et al., 2004). It was suggested that this extract contained a candidate DAF-12 ligand that was thought to be a polyhydroxylated sterol based on crude purification (Matyash et al., 2004). However it was later published that this extract was unable to rescue dauer formation in *daf-9* mutants as would be expected if it contained a DAF-12 ligand (Entchev and Kurzchalia, 2005).

The previously ch

The previously characterized bioactive extracts

In order to identify the DAF-12 ligand we have previously isolated a nematode-derived lipophilic extract that possesses the activity predicted of a hormone produced by DAF-9 and acting on DAF-12 (Gill et al., 2004). This extract is able to rescue the dauer arrest of Daf-c mutants from the insulin and TGFβ signaling pathways as well as *daf-9* mutants. Furthermore it does not alter the phenotype of a ligand-insensitive *daf-12* mutant. The identity of the endogenous ligand of DAF-12 has been elusive, but would provide an excellent tool to help further understand the mechanism of development, aging, and lifespan extension in *C. elegans*. We aim to identify the bioactive component within this extract – this is the focus of my thesis. Here we describe the chemical characterization of bioactivity in this extract and find that sterol acids exist in worms. We find that the sterol acid (25S)-cholestenoic acid can rescue the Daf-c phenotype of *daf-2* and *daf-9* mutant worms by acting as a DAF-12 ligand and does not rescue a ligand-insensitive *daf-12* mutant. (25S)-cholestenoic acid acts, likely as a DAF-12 ligand *in vivo*, to downregulate DAF-9 expression and as a ligand *in vitro.* We also find regioisomers of (25S)-cholestenoic acid in bioactive worm extracts, but not in extracts from hormone deficient *daf-9(-)* mutants. (25S)-cholestenoic acid is the first ligand identified for any nuclear receptor in *C. elegans*.

Collaboration

This project was extremely collaborative in nature and although the majority of the work described in this document is my own, I would like to clarify where I received technical

and collaborative help. My two primary collaborators at the Buck Institute were Dr. Matthew S. Gill, an endocrinologist, and Mr. Mark P. White, a technician in the lab.

For the generation of extracts on a routine basis, White, Gill, and I grew large scale worm cultures to freeze and extract. White and Gill were primarily responsible for the ether extraction, and White or I aminopropyl fractionated the extract. I then performed all analytical experiments on these extracts such as thin-layer chromatography (TLC), high-performance liquid chromatography (HPLC), gas-chromatography mass spectrometry (GC-MS), and derivatization. When bioassay was required after chemical analysis, either Gill or I performed the dauer rescue bioassay.

In Chapter 2, Gill developed the dauer rescue bioassay and characterized the initial rescue of Daf-c phenotypes and which worm conditions maximized bioactive potency. Gill also discovered that extracts rescue the gonad formation of *daf-9* mutants. However, all data shown in the results section including solid-phase extraction (SPE), HPLC, and GC-MS data is my own with the help of Gill in making the extract and bioassay. The *daf-9(gk160) daf-12(m20)* mutant that we used was initially created by Dr. Alfred L. Fisher (formerly Buck Institute, currently University of Pittsburgh).

In Chapter 3, I performed all derivatizations and most of the associated bioassays. I also initiated, characterized, optimized, and performed the aminopropyl SPE until it became a routine procedure. I also initiated and performed all the TLC experiments. I performed all aspects of the [4-^{14}C]-radiolabeled cholesterol supplementation experiment.

In Chapter 4, the decision to screen bile acids including Δ^5 cholestenoic acid was a joint collaborative decision between Gill and me. When we determined that cholestenoic acid rescued the *daf-9(gk160)* mutant I began experiments to identify

endogenous cholestenoic acid-like compounds in worms and Gill began more detailed characterization of cholestenoic acid Daf-c rescue. Gill identified the differential effects of the R and S forms of cholestenoic acid and initiated the R and S competition experiments. All of the data shown in the figures, including pictures, are my own replicates of data for *daf-2(e1368)*, *daf-9(gk160)*, and *daf-12(rh273)* and I specifically focused on gathering new knowledge about the sensitivity of *daf-2(e1368)* and *daf-9(gk160)* rescue by (25S)-cholestenoic acid. As attributed in the text, Gill extended the number of Daf-c mutants rescued by cholestenoic acid. Also attributed to Gill in the text is his development of a cell-based assay that determined *in vitro* that (25S)-cholestenoic acid transactivated DAF-12 but not the ligand-insensitive R564H mutant version. This assay also demonstrated that transactivation was competed off by excess (25R)-cholestenoic acid. I performed all aspects of the TLC and HPLC procedures that correlated the chemical properties of cholestenoic acid and the bioactive component. I also extended the *in vivo* characterization of cholestenoic acid by examining its effects on the DAF-9::GFP and DAF-12::GFP strains.

In Chapter 5 and 6, I performed all the sample derivatization, mass spectrometry, and data analysis for bile acid and sterol standards. I also performed all downstream analysis on the aminopropyl SPE fractionated extracts. This included derivatization, HPLC, mass spectrometry, and data analysis such as quantitation and spectral interpretation. I also determined if 3-hydroxy forms of 3-keto sterols could be produced by our derivatization procedure. Gill screened for sterols that rescued the Daf-c phenotype of *daf-2(e1368)* and made the initial discovery that lathosterol rescues the

Daf-c phenotype. I replicated this data and also tested several other compounds such as $\Delta^{8(14)}$ sterol and the LXR oxysterol ligands (22R), 25, and 27-hydroxycholesterol.

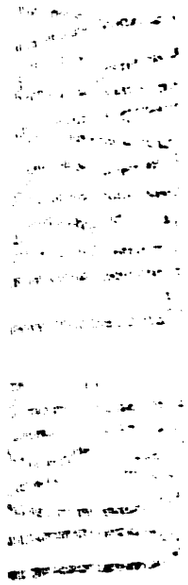

CHAPTER II

Purification of lipophilic activity in *C. elegans* extracts

ABSTRACT

DAF-12 is a nuclear receptor that acts as a ligand-induced transcription factor. We have found that crude *C. elegans* extracts can rescue the Daf-c phenotype of *daf-2(e1368)* and *daf-9(gk160)* but not the *daf-12(rh273)* mutant strain that is predicted to have a ligand-insensitive DAF-12. Therefore we hypothesized that the bioactive component in these extracts was the DAF-12 ligand. As an initial step to identify the bioactive component, we wanted to reduce the number of analytes for downstream analysis and found that HPLC was a useful initial step to purify the crude extracts. We also made extracts from *daf-9(-)* worms, the P450 enzyme just upstream of DAF-12, since the bioactive and *daf-9(-)* extracts should differ by only the metabolic products of DAF-9.

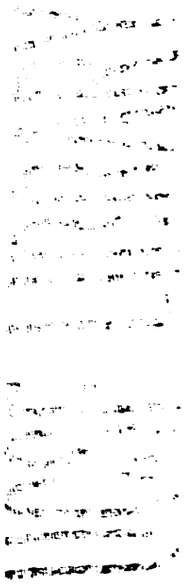

INTRODUCTION

Nuclear receptor ligand identification

The identification of a novel small molecule that not only binds but transactivates a nuclear receptor is often a complicated task for even well-characterized mammalian systems. Historically, the biochemical relationship of nuclear receptors and ligands was advanced by work seeking to explain how hormones affected physiology and a biochemical model of hormone action was proposed in which the hormone acted via direct interaction with a protein receptor (Agarwal, 1978). In the early nuclear receptor-ligand interactions that were described, the hormone was initially characterized followed by isolation of the receptor it bound and cloning of the receptor (Simons, Jr. and Thompson, 1981; Gehring and Hotz, 1983). The glucocorticoid receptor was the first nuclear receptor identified this way (Hollenberg et al., 1985; Weinberger et al., 1985). The concept of an "orphan" receptor, a receptor with no known cognate ligand, did not occur until novel nuclear receptors were identified in the genome (Giguere et al., 1988). Only after a seven year search were biologists able to develop ligand identification techniques and begin to characterize the ligands for these receptors (Kliewer et al., 1995; Forman et al., 1995a; Forman et al., 1995b).

Some of the techniques used to identify nuclear receptor ligands are compound library screening (Schapira et al., 2003; Nicolaou et al., 2003), molecular modeling (Wurtz et al., 2000; Webb et al., 2003; Schapira et al., 2003; Jacobs et al., 2003), candidate testing (Menke et al., 2002; Otte et al., 2003; Bramlett et al., 2003), screening of endogenous extracts (Dussault et al., 2003), mass spectrometry (Elviri et al., 2001; Potier et al., 2003; Bitsch et al., 2003; Lengqvist et al., 2005a; Lengqvist et al., 2005b),

differential proteolysis (Zeng et al., 1994), and even finding accidental ligands in a crystal structure of the receptor (Stehlin et al., 2001; Dhe-Paganon et al., 2002; Krylova et al., 2005). In general, nuclear receptor ligands are often difficult to isolate and characterize from natural products (O'Malley, 1990; Soontjens et al., 1996) and the vast majority of ligands have been found by screening known mammalian metabolites in a cell-based assay for transactivation of the target receptor.

Nuclear receptor ligand identification in *C. elegans*

There are several hurdles to applying the common candidate screening approach to identify the DAF-12 ligand. First, although DAF-12 does have mammalian homologs, it is difficult to obtain the huge number of specialized trace level metabolites that are typically screened in order to find candidate ligands. It is also difficult to guess which subset of candidates should be tested in a screen since although sterols play a role in dauer formation, common sterols have been tested and do not show any sign of rescuing worms from dauer. Furthermore, worms have evolved novel enzymatic regulation of sterols, likely lost many aspects of the ecdysone signaling mechanism that is critical for fly development, and utilize a completely novel pheromone critically important for their development, making it a very real possibility that the DAF-12 ligand is a unique compound to worms. Secondly, nuclear receptors often have a very specific set of chemical requirements for binding selectivity and it is unlikely that DAF-12 would have the same ligand specificity as a mammalian receptor. And, unlike screens of known compounds that are well characterized for their presence, abundance, and even tissue distribution in mammals, there is very little known about general metabolism in

C. elegans. Therefore any candidate found would have to be identified and characterized in worms. Thirdly, screening compounds requires a cell culture system to express the receptor and detect transactivation. However, no *C. elegans* cell culture system exists. Some attempts have been made to culture *C. elegans* cells, but they are difficult to work with and are differentiated into cell types that are not relevant for DAF-12 analysis (Christensen et al., 2002). It is unclear if using a non-*C. elegans* cell system would have the right cofactors necessary for the stabilization of the LBD or if the increased temperature (37°C for mammalian cell culture versus 25° for worm growth) would affect DAF-12 folding or ligand binding.

Initial characterization of a dauer-rescuing extract from *C. elegans*

We have previously identified a crude lipophilic nematode extract that influences dauer formation in a manner that is consistent with a hormone produced by the cytochrome P450 DAF-9, and acts on DAF-12. This extract rescues the Daf-d phenotype of *daf-2(e1368)* mutants (Figure 2.1 A) in a dose-dependent manner (Figure 2.1 B). Interestingly, extracts from a putative null *daf-12* mutant, *daf-12(m20)*, has more dauer-rescuing potency than N2 (wild type) and the potency from L3/L4 *daf-12(m20)* worms is maximal (Figure 2.1 C). We believe this is due to negative feedback regulation from the receptor knockout which results in an upregulation of ligand production, so we focused on growing L3/L4 *daf-12(m20)* worms from which to make extracts.

Several nuclear receptor ligands have been identified by fractionating a complex endogenous extract and tracking where active components elute. In almost every case, a heterologous transfection system is used that has a nuclear receptor and DNA response

A

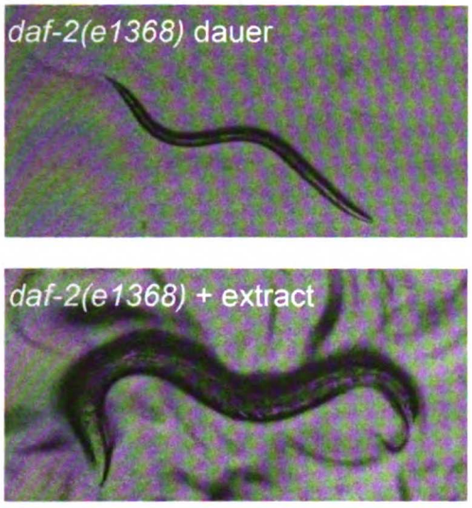

B

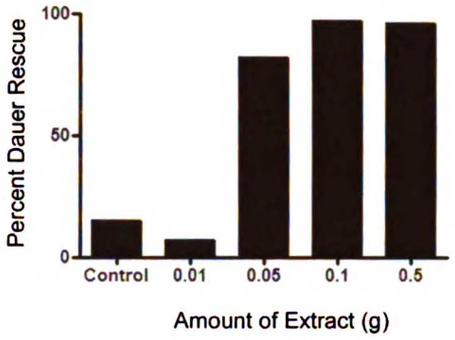

C

Extract Genotype	Extract Development Stage	% Dauers	% Rescued
N2	L1/L2	75	25
	L3/L4	94	6
	Adult	100	-
daf-12(m20)	L1/L2	76	18
	L3/L4	12	72
	Adult	97	2

Figure 2.1 *daf-12(m20)* extracts contain a putative DAF-12 ligand.

(A) Images of a *daf-2(e1368)* dauer and an extract-treated *daf-2(e1368)* rescued to adulthood. (B) Dose response curve of extract rescue. (C) Comparison of *daf-2(e1368)* rescue from extracts of different strains and larval stages.

element reporter to detect ligand-dependent transactivation (Zeng et al., 1994; Blumberg et al., 1996; Blumberg et al., 1998; de Urquiza et al., 2000; Goldstein et al., 2003). After unsuccessful attempts activating DAF-12 in a cell-based assay with extracts, we switched to dauer rescue as a bioassay since it is an easy phenotype to score. Initially both normal phase and reversed phase solid-phase extraction (SPE) were used to crudely fractionate the extract (Figure 2.2). This fractionation determined that the bioactive component was both hydrophobic and polar since it eluted with 100% methanol in reversed phase and 100% ether in normal phase (Figure 2.2). With the incredible number of biochemical components in the metabolome of the cell that might potentially be the ligand, our first focus was to further reduce the chemical complexity of the extracts in an unbiased separation strategy. It is well proven that a highly efficient preparative step is high-performance liquid chromatography (HPLC). Though reversed phase has become the most common HPLC separation phase in recent times, the value of normal phase HPLC as an additional stage of separation is well established for natural product isolation and lipid analysis.

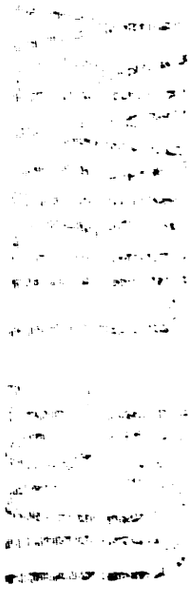

Comparing DAF-9 extracts with bioactive extracts

The wide availability of *C. elegans* mutants has also been used to reduce complexity since in many cases the identification of a natural product requires that the bioactive component be purified to very close to homogeneity in order for it to be characterized. This requires a large amount of starting material and an extremely intensive purification strategy. This has been the case recently even in worms, with the purification of the worm pheromone named daumone. Evidence of the arduousness of this task is the fact

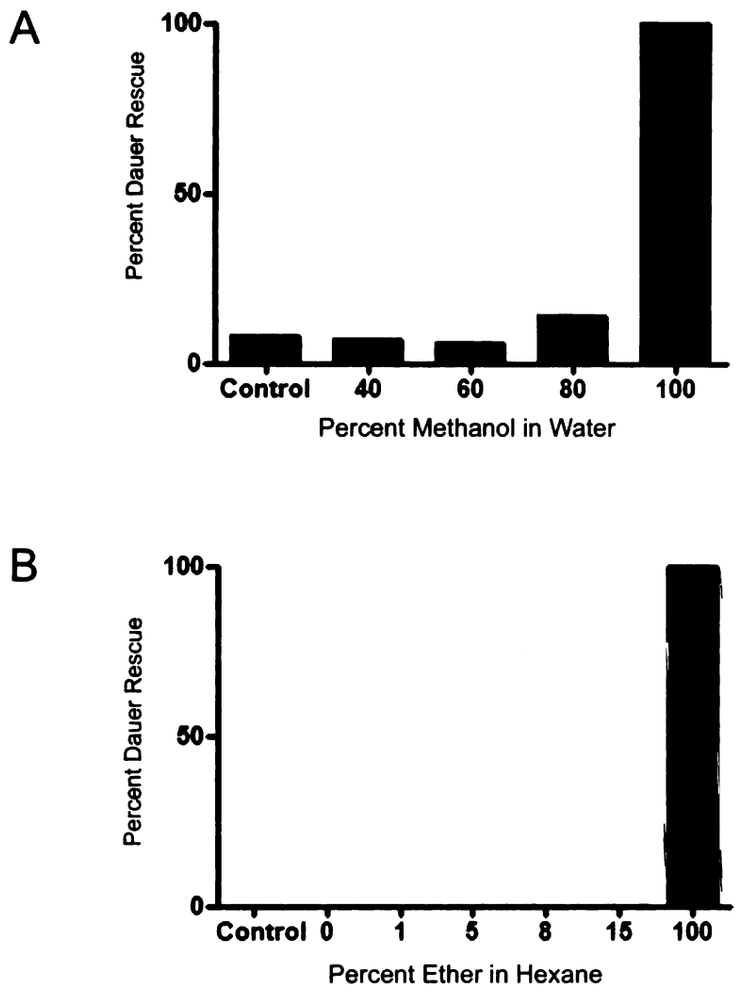

Figure 2.2 SPE fractionated extracts rescue the *daf-2(e1368)* Daf-c phenotype. (A) Bioactivity of reversed phase fractionation of *daf-12(m20)* extracts using a C18 SPE column. (B) Bioactivity of normal phase fractionation of *daf-12(m20)* extracts using a silica SPE column.

that it took over 20 years from the initial chemical characterization and crude purification of the bioactivity (Golden and Riddle, 1982) to its chemical identification (Jeong et al., 2005). In order to try to circumvent some of these difficulties we took advantage of available *C. elegans* mutants to make extracts from a worm that does not have the bioactive component. Therefore, we have taken the strategy in all cases to compare bioactive *daf-12(m20)* extract with a *daf-9(-)* mutant. Since DAF-9 is the putative enzyme that makes the DAF-12 ligand, it would be expected that a *daf-9(-)* mutant would not have bioactivity, which is the case (Figure 2.3 A). The *daf-9(gk160)* mutant strain in Figure 2.3 A is a putative null and is Daf-c, making it impossible to grow up to the same L3/L4 stage as the *daf-12(m20)* worms. However, A. Fisher crossed this mutant into a *daf-12(m20)* mutant background which is Daf-d and epistatically downstream of *daf-9*. Therefore the *daf-9(gk160) daf-12(m20)* worm bypasses the dauer stage yet does not produce any bioactive ligand (Figure 2.3 A).

We place the bioactivity of the extract downstream of *daf-9* because the bioactive extracts from *daf-12(m20)* extracts are able to rescue the *daf-9(gk160)* Daf-c dauer phenotype (Figure 2.3 B). Extracts from *daf-9(gk160) daf-12(m20)* are not able to rescue *daf-9(gk160)*, as expected (Figure 2.3 B). Interestingly, the *daf-12(m20)* extracts do not rescue the Daf-c phenotype of a DAF-12 mutant (R564H) that is predicted to be ligand-insensitive. Extract is also able to rescue the gonadal migration phenotype of *daf-9* (Figure 2.3 C) but not the gonadal migration defect in the DAF-12 ligand-insensitive mutant. These data suggest that the activity of the extract is not only downstream of DAF-9 but upstream of DAF-12 (Figure 2.3 D). By focusing on the differences between *daf-12(m20)* and *daf-9(gk160) daf-12(m20)* extracts we hope to simplify the

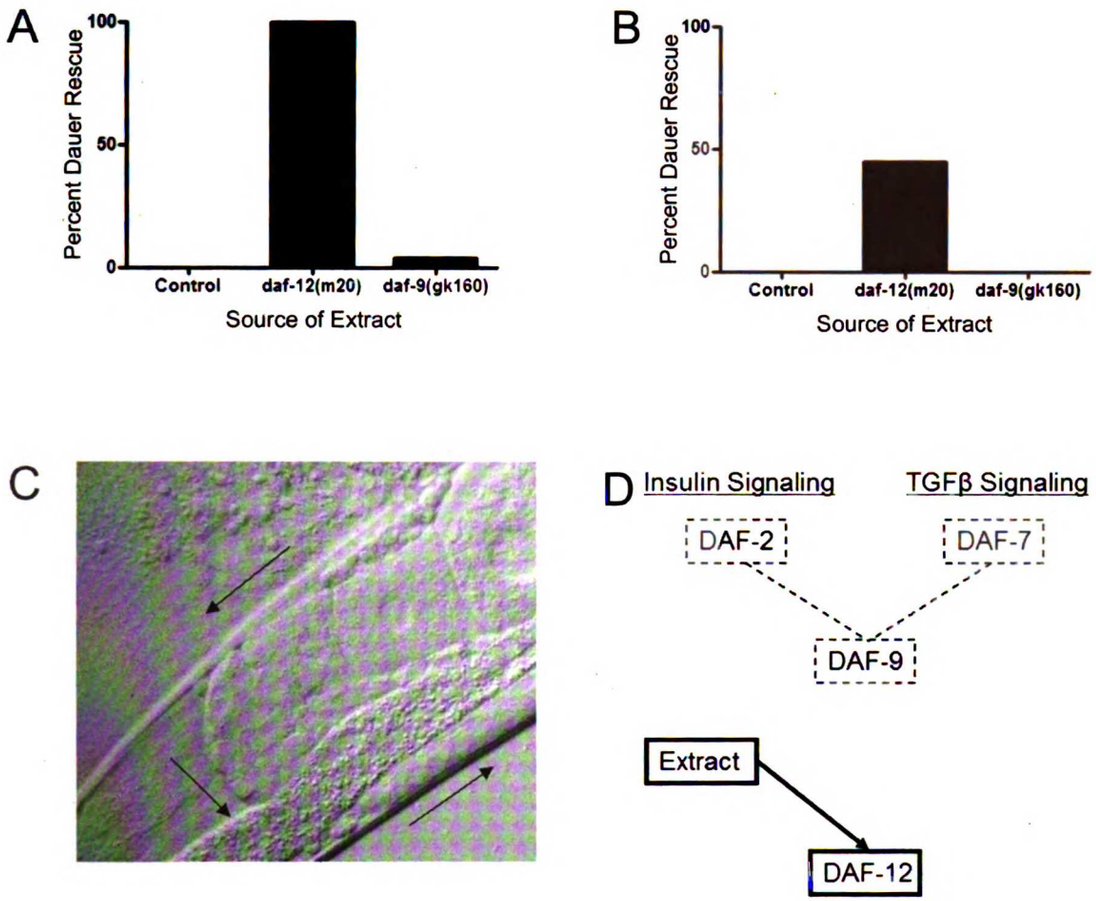

Figure 2.3 The activity of *daf-12(m20)* extracts is downstream of DAF-9. (A) Rescue of the Daf-c phenotype of *daf-2(e1368)* by extracts from *daf-12(m20)* but not *daf-9(gk160) daf-12(m20)* extracts. (B) Rescue of the Daf-c phenotype of *daf-9(gk160)* by *daf-12(m20)* extracts, but not *daf-9(gk160) daf-12(m20)* extracts. (C) Image of a gonad from a *daf-9(gk160)* worm which is properly reflexed after treatment with *daf-12(m20)* extract. (D) Model of *daf-12(m20)* extract rescue under dauer-inducing conditions in which the bioactive component of the extract acts downstream of DAF-9 to modulate DAF-12's action.

identification process of the DAF-12 ligand since we predict that the *daf-9(gk160) daf-12(m20)* extracts presumably only differ in their chemical complement from *daf-12(m20)* bioactive worms by the absence of DAF-9 metabolic products.

RESULTS

RESULTS

Reversed phase (C18) HPLC

As a first step, reversed phase HPLC was used to fractionate the extract based on hydrophobicity. Using a C18 column, extracts from *daf-12(m20)* and *daf-9(gk160) daf-12(m20)* were compared using an acetonitrile:water solvent system. The UV chromatograms from *daf-12(m20)* and *daf-9(gk160) daf-12(m20)* extracts are very similar (Figure 2.4 A and B) and this similarity is consistent from extract to extract. Most compounds elute during the middle of the gradient, and as the gradient reaches 100% acetonitrile at about minute 40, the number of compounds eluting falls off dramatically. To find which fraction(s) contained the bioactive component(s), one minute fractions from the HPLC run were collected, dried down, and resuspended in 10 μL DMSO for *daf-2(e1368)* bioassay. Two discrete fractions consistently had dauer rescue bioactivity, with a fraction between that did not rescue. The consistent presence of two bioactive fractions suggested that either there was more than one bioactive compound in our extracts, or that a precursor to the DAF-12 ligand also had bioactivity in *daf-2(e1368)*. However, since the HPLC solvents were not buffered and the pH was unmodified we questioned if the two bioactive peaks were an artifact of differential ionization of a single acidic or basic compound. For example the ionized COO^- or NH_4^+ form of a molecule may retain differently than the un-ionized COOH or NH_3 form. In order to test this, 0.1% trifluoroacetic acid was added to each solvent to change the pH from roughly neutral to 2 in order to fully protonate or deprotonate any biologically relevant chemical species. This resulted in a single peak of bioactivity in the HPLC suggesting that the bioactive component(s) were either acidic or basic (Figure 2.4 C).

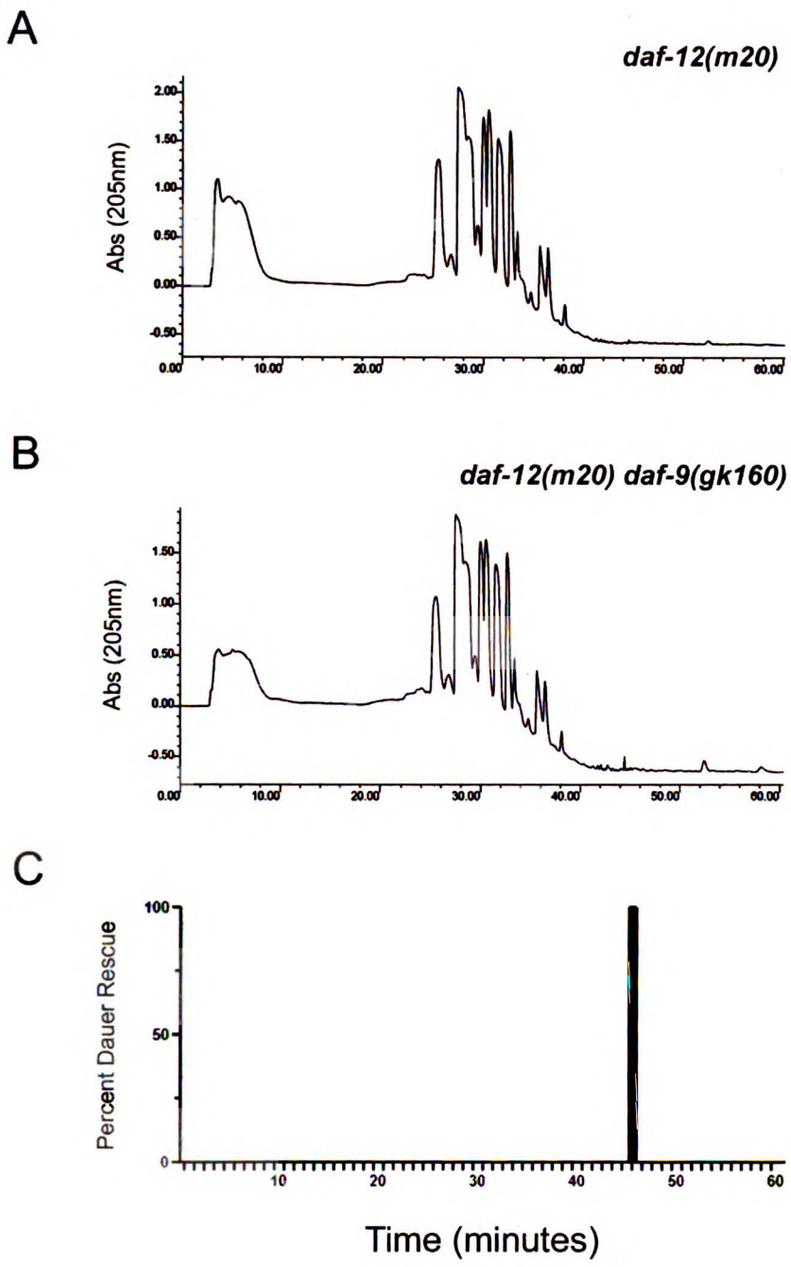

Figure 2.4 Reversed phase HPLC of extracts. (A) *daf-12(m20)* chromatogram. (B) *daf-9(gk160) daf-12(m20)* chromatogram. (C) Bioassay of 1 minute HPLC fractions from *daf-12(m20)* extracts on *daf-2(e1368)* worms.

An isocratic mode of separation was attempted next since isocratic separation typically resolves components better than a gradient HPLC method and therefore improves separation. A 76:24 acetonitrile:water gradient eluted bioactivity about 30 minutes after injection (data not shown); however, bioactivity did not elute in a tight peak. Furthermore, where there was limited variability of retention times using gradient reversed phase HPLC, the retention of bioactivity in isocratic HPLC was extremely variable and required substantial effort to bioassay the large number of potentially bioactive fractions. What made the isocratic mode unfeasible, however, was the significant increase (fivefold) in the amount of extract necessary to simply identify the bioactive fractions. This increase in extract required for isocratic reversed phase HPLC made it not feasible to use on a routine basis since worms to make extracts were in limited quantities and we wanted to maximize extract for the downstream analysis of bioactive fractions.

Reversed phase (diphenyl) HPLC

Diphenyl columns are a unique form of reversed phase separation. In comparisons to C18 that rely on purely hydrophobic interactions to separate analytes, the π-π interaction mechanism of diphenyl separation greatly enhances selectivity for unsaturated compounds. Since sterols are often unsaturated and differ significantly in their unsaturated characteristics, we tested diphenyl separation to fractionate the extracts. Compounds were well separated and bioactivity eluted at 25-26 minutes (Figure 2.5).

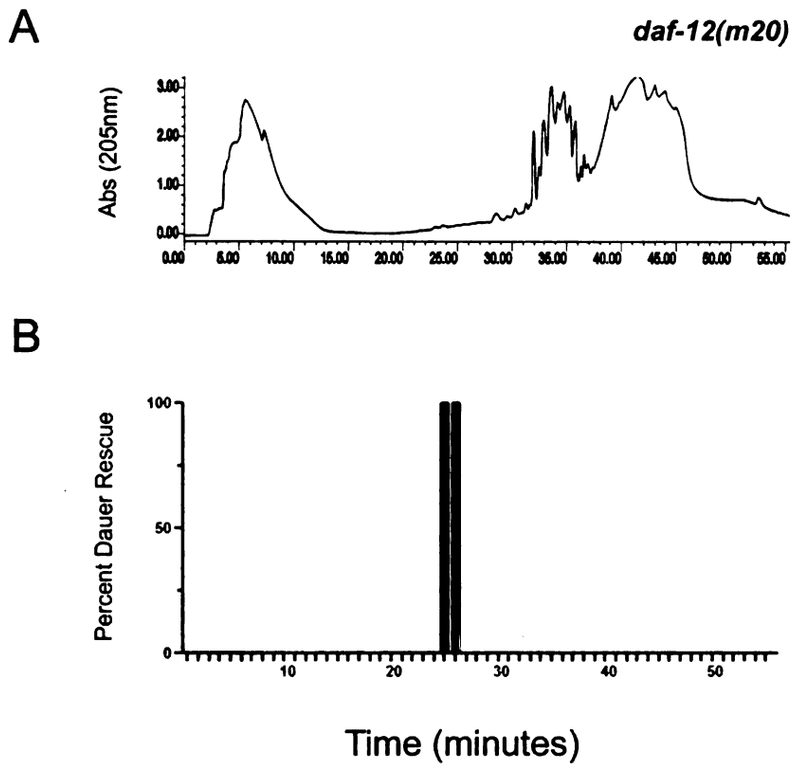

Figure 2.5 Diphenyl HPLC separation of extracts. (A) Chromatogram and (B) Bioassay of 1 minute HPLC fractions from *daf-12(m20)* extracts on *daf-2(e1368)* worms.

Normal phase HPLC

The extract was separated by normal phase HPLC using a silica column and a hexane-diethyl ether-isopropanol solvent system. Initially a hexane and diethyl ether solvent system was attempted, but the diethyl ether alone was not polar enough to elute the bioactive component off the column. Like reversed phase, the normal phase HPLC UV traces are very similar between *daf-12(m20)* and *daf-9(gk160) daf-12(m20)* extracts with detection at 254 nm (Figure 2.6 A and B). The 254 nm wavelength is a more selective wavelength than 205 and though there are several peaks, a single peak dominated the chromatogram with a retention time of 23 minutes. When one minute fractions were analyzed for bioactivity, the bioactivity corresponded to the fraction at 23 minutes (Figure 2.6 C).

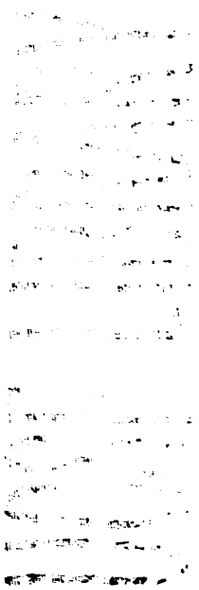

Gas chromatography–mass spectrometry

In order to evaluate the complexity of the HPLC fractions, each fraction was analyzed by gas chromatography-mass spectrometry (GC-MS) after trimethylsilyl derivatization in order to detect all potential analytes in each fraction. The HPLC fractions were found to contain hundreds to thousands of compounds (Figure 2.7). Searching a database of known compounds and their GC-MS spectra, it became clear that a wide variety of components were in the extract. Encouragingly, there were a tremendous number of differences between the bioactive HPLC fractions and nearby fractions suggesting that the HPLC was separating components very well. However, there were also many differences between fractions from the *daf-12(m20)* extracts and the *daf-9(gk160) daf-12(m20)* extracts making it difficult to pick out differential peaks for

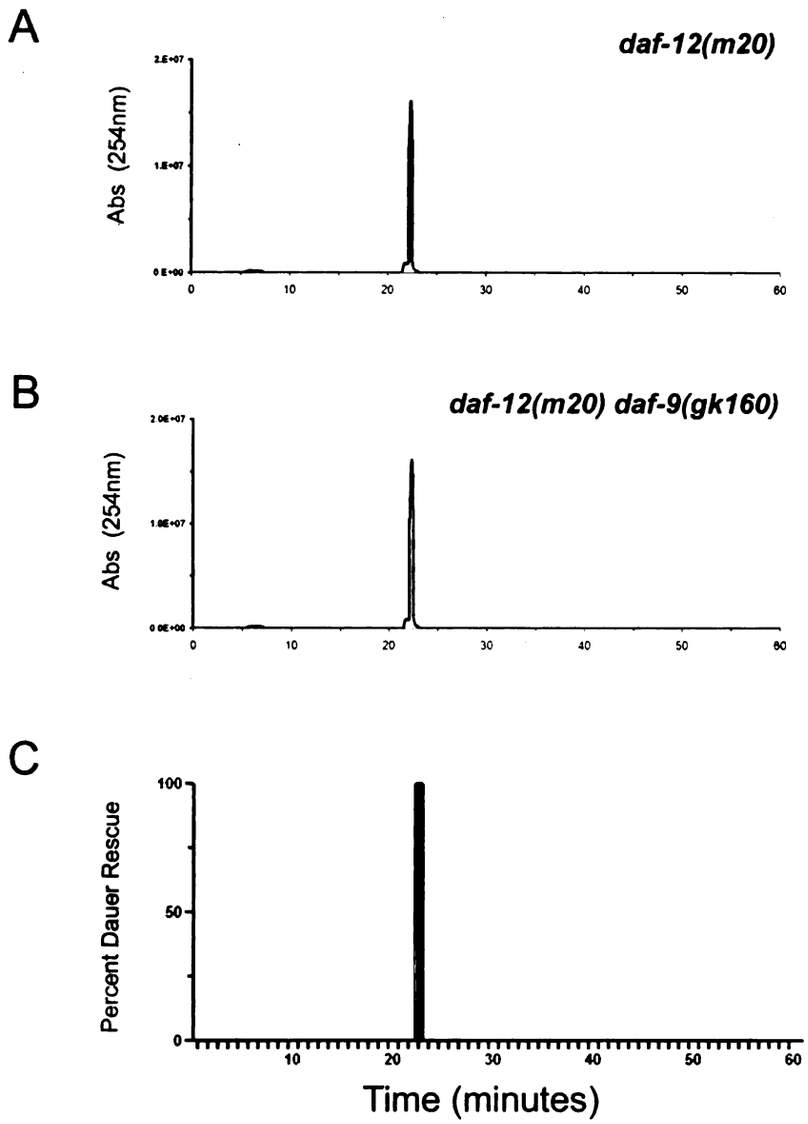

Figure 2.6 Normal phase HPLC of extracts. (A) *daf-12(m20)* chromatogram. (B) *daf-9(gk160) daf-12(m20)* chromatogram. (C) Bioassay of 1 minute HPLC fractions from *daf-12(m20)* extracts on *daf-2(e1368)* worms.

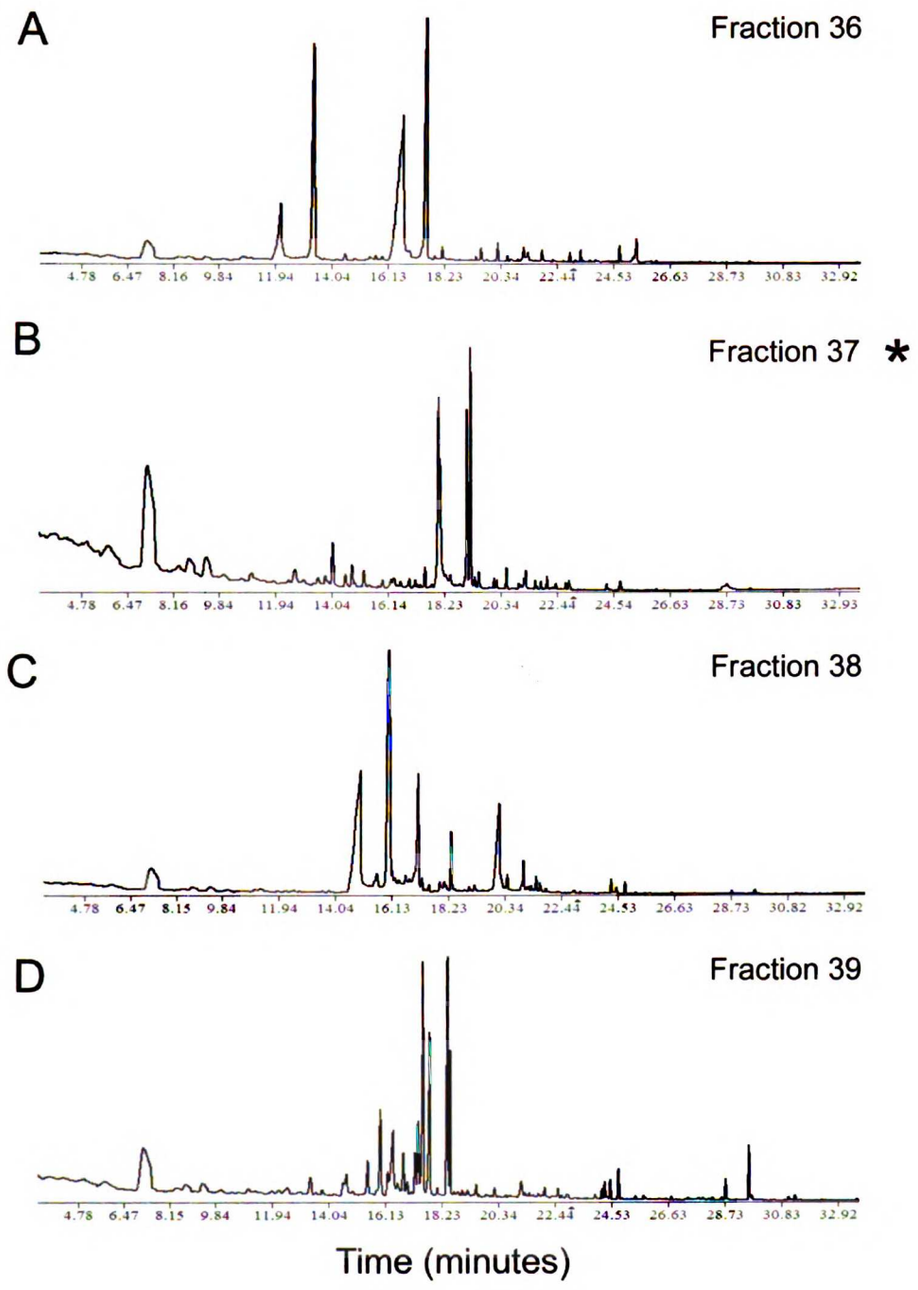

Figure 2.7 Initial HPLC fractions are complex. GC-MS total ion chromatograms of 1 minute *daf-12(m20)* extract fractions separated by reversed phase HPLC. (A) Fraction #36 (B) Fraction #37 (C) Fraction #38 and (D) Fraction #39. (*) Bioactive fraction(s) indicated by an asterisk.

more comprehensive analysis (data not shown). Furthermore, the GC-MS chromatograms had a high level of background and significant amount of peak tailing. Additionally, when the same sample was run several times we found that they were not sufficiently reproducible.

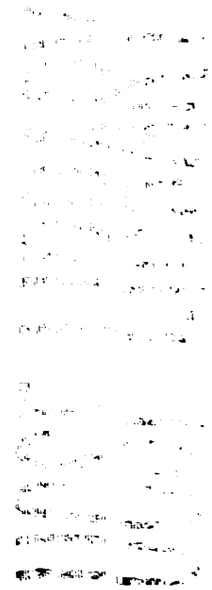

DISCUSSION

Normal phase versus reversed phase purification

Purification of the bioactive component is a key step to the identification of the DAF-12 ligand. Reversed phase and normal phase HPLC separation strategies were therefore developed in order to resolve the bioactive component and significantly reduce the number of components in downstream analysis. Reversed phase and normal phase HPLC, in general terms, are the opposite of each other, as suggested by the opposite retention of lipid classes in normal phase versus reversed phase. However, on a finer scale of analysis they are quite different modes of separation since they separate based on different characteristics of the molecule. Reversed phase separates based on hydrophobicity, which for lipids is typically the non-polar tail. Normal phase, on the other hand, separates based on the polar groups of the lipid by hydrogen bonding and dipole-dipole interactions. These are very different functional groups being selected for and the two phases can act in a complementary fashion as a two-step purification strategy. However, even using a significant amount of extract we were not able to detect bioactivity in normal phase HPLC fractions after we used it to chromatograph a bioactive reversed phase HPLC fraction (data not shown). Since the amount of extract generated is limited, the inefficiency of combining HPLC separations makes it unfeasible.

The bioactive component is both polar and hydrophobic

Small molecule hormones and nuclear receptor ligands are quite often characterized by a mix of hydrophobicity and polarity. The hydrophobic core allows the molecule to bind to the ligand binding pocket of the receptor with significant minimization of energy, and

specific localization of polarity on the ligand gives specificity for the receptor (Krumrine et al., 2003; Fradera and Mestres, 2004). The hydrophobic and hydrophilic nature of the bioactive component was first characterized using SPE cartridges (Figure 2.2 A and B). The improved resolution of these features by HPLC fractionation has further confirmed that the bioactive component has moderate polarity and has also elucidated that it is extremely hydrophobic. By eluting from a C18 column at the 100% acetonitrile portion of the run, bioactivity elutes well after cholesterol and even is several minutes later than palmitic acid (data not shown). Palmitic acid is a single polar carboxyl attached to a C16 carbon chain and would be expected to bind extremely tightly to the 18 carbon chains of the C18 HPLC column. For bioactivity to elute at this extreme hydrophobicity is unexpected since it is difficult to imagine a sterol much more hydrophobic than cholesterol. Simply based on retention, it is unlikely that any lipid class other than long-chain fatty acids should remain as potential bioactive candidates. However, the unexpected retention may potentially be explained by known but unusual interactions that can occur within a complex lipid-lipid mixture, especially those containing detergents (Hofmann and Small, 1967; Nasal et al., 2003). Therefore, we did not use reversed phase HPLC retention to rule lipid classes in or out.

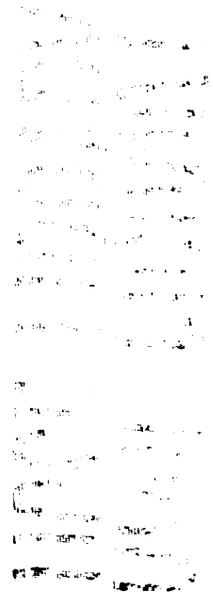

The bioactive component is not detected by UV

The bioactive component cannot be detected by UV in an HPLC run, either because it does not have a UV chromophore or because it is at levels lower than UV sensitivity. With reversed phase HPLC no peak at 205 nm, 240 nm, 254 nm, or 280 nm tracked with bioactivity nor were there consistent differences between *daf-12(m20)* and daf-*9(gk160)*

daf-12(m20) extracts. In normal phase HPLC, there was very little signal detected at all during the entire run at 205 nm. At 254 nm the dominant peak at 23 minutes did correspond to bioactivity but this peak is also present in *daf-9(gk160) daf-12(m20)* extracts and is not of significantly different abundance than in *daf-12(m20)* extracts (Figure 2.7 A and B).

GC-MS reveals HPLC fractions are still complex

C18 reversed phase HPLC likely resolves the bioactive component away from a large amount of material based on the fact that almost all of the 205 nm absorbing compounds elute much earlier than the fraction with bioactivity (Figure 2.4). Furthermore, though the dominant component at 254 nm in the normal phase HPLC chromatogram does contain bioactivity, there are a number of other less dominant peaks. Since varied lipid standards were tested and elute in a well resolved manner throughout the run, we believe that the normal phase is separating extracts well.

GC-MS analysis of reversed phase HPLC fractions found that there were hundreds to thousands of compounds of varied chemical nature in each fraction – many more than were initially expected (Figure 2.7). It was encouraging that there were significant differences between bioactive HPLC fractions and nearby non-bioactive fractions; however, many differences between the *daf-12(m20)* extracts and the *daf-9(gk160) daf-12(m20)* extracts were observed. The complexity of the extracts and the poor GC-MS results led us to decide to move forward with a strategy to chemically characterize the ligand further. This would allow for fine tuning of the separation to reduce the number of components in the extracts without the high cost of requiring

significantly more extract simply to find bioactivity, as we had with isocratic HPLC and the combination of normal and reversed HPLC phases. Furthermore, the GC-MS chromatograms had a high level of background and significant amount of peak tailing suggesting that we needed to optimize the derivatization strategy to achieve good GC-MS results. As an added benefit, chemical characterization could also potentially determine the lipid class to which the bioactive component(s) belongs, and most importantly allow improvement of the derivatization strategy so that it is more specific to the bioactive analyte(s) and more reproducible, leading to the ultimate goal of being able to identify a small number of differences between *daf-12(m20)* and *daf-9(gk160) daf-12(m20)* on a consistent basis using GC-MS.

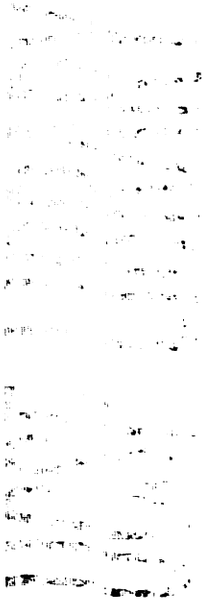

MATERIALS AND METHODS

Materials

Cholesterol (#C-8667) was purchased from Sigma (St. Lois, MO). Trifluoroacetic acid (#09653) was purchased from Fluka (Switzerland).

C. elegans strains

The following nematode strains used in this work were provided by the *Caenorhabditis* Genetics Center, which is funded by the NIH National Center for Research Resources (NCRR): Bristol N2 (wild-type), DR1572[*daf-2(e1368) III*], VC305[*+/szT1[lon-2(e678)] I; daf-9(gk160)/szT1 X*], DR20[*daf-12(m20) X*], and GL216[*daf-9(gk160) daf-12(m20) X*].

C. elegans ether extractions

For routine culture, *daf-20(m20)* worms were maintained at 20°C on 5 cm nematode growth medium (NGM) agar plates with a lawn of *E. coli* OP50. For generation of lipophilic extracts, worms were initially grown by mass culture on 10 cm plates at 25°C. Gravid 3 day old worms were washed off approximately 20 large plates and subjected to sodium hypochlorite treatment to generate eggs. The eggs were inoculated into 2 L glass flasks containing 90 mL S-medium (+ cholesterol, final concentration 5 µg/mL) and 10 mL of concentrated *E. coli*. The liquid cultures were then incubated in a shaking incubator at 25°C, 150 rpm for 2 d to generate L3/L4 worms. Worms were harvested by low speed centrifugation and washed 3 times with S-basal before the worm pellet was frozen.

Frozen worm pellets were thawed at room temperature (23°C) into an equal volume of TBS pH 7.5 (~5 g worms + 5 ml TBS) and then subjected to 4x1 min sonication on ice. Worm lysates were transferred to 50 mL glass centrifuge tubes. Worm lysate (10 mL) and ether (30 mL) were vortexed vigorously until the two phases became miscible and viscous. Following centrifugation for 10 min at 3000 rpm, the ether phase was transferred to a glass tube. This process was repeated once more and the ether extracts were then evaporated under N_2 and resuspended in hexane. The hexane was then transferred to a 1 mL reactivial, evaporated under N_2 and resuspended in dimethyl sulfoxide (DMSO).

Dauer rescue bioassay using extract

Our bioassay was developed by M. Gill. For routine culture, worms were maintained at 20°C on 5 cm nematode growth medium (NGM) agar plates with a lawn of *E. coli* OP50. Extract was added to a 3 cm NGM plate in 10 µL DMSO to the OP50 lawn. After 1 hr eggs from a temperature-sensitive Daf-c strain were added to the plates and then placed in an incubator at 25°C to generate dauers. Plates were scored for the number of dauer, L3/L4/young adult, and gravid adult worms after 72 hr. All worms that were scored as in the L3 stage or beyond were scored as rescued for the figures in this chapter.

Reversed phase HPLC

Analytical scale reversed phase HPLC was performed on a Waters Breeze HPLC system with dual UV detectors and a manual injector. The run started with a 50% H_20 and 50% acetonitrile equilibration for 10 min. The gradient changed linearly to 100% acetonitrile

over the next 25 min with a hold at 100% acetonitrile for 22 min. Unless specified, the solvents contained 0.1% trifluoroacetic acid. The sample loop was 5 mL and the flow rate was 1 mL per min. UV absorbance was detected at 205 nm and 254 nm. A Vydac C18 column (#218TP54) with 5 μm particle size, 4.6 mm inner diameter, and 250 mm length was used. A C18 guard column was also used (Vydac, #218GK54). The column was kept at 30°C for the duration of the run. A fraction collector automatically collected fractions at 1 min intervals.

Diphenyl HPLC

Analytical scale reversed phase HPLC was performed on a Waters Breeze HPLC system with dual UV detectors and a manual injector. The run started with a 50% H_20 and 50% acetonitrile equilibration for 10 min. The gradient changed linearly to 100% acetonitrile over the next 25 min with a hold at 100% acetonitrile for 22 min. The sample loop was 5 mL and the flow rate was 1 mL per minute. UV absorbance was detected at 205 nm and 254 nm. A Varian Pursuit diphenyl HPLC column (#A304025X046) with 5 μm particle size, 4.6 mm inner diameter, and 250 mm length was used. The column was kept at 30°C for the duration of the run. A fraction collector automatically collected fractions at 1 min intervals.

Normal phase HPLC

Analytical scale normal phase HPLC was performed with a Waters 600E system controller, a Waters 486 UV detector, and a PeakSimple chromatography data system. A manual injector was used. The run started with 1% isopropanol, 1% diethyl ether, and

98% hexane for 10 min. The gradient changed linearly to 15% isopropanol and 85% diethyl ether over the next 35 min and was held for 15 min. The sample loop was 2 mL and the flow rate was 1 mL per min. UV absorbance was detected at 254 nm. A Higgins Analytical silica column (#HS-2546-SIL5) with 5 μm pore size, 4.6 mm inner diameter, and 250 mm length was used. The column was kept at room temperature (23°C). A fraction collector automatically collected fractions at 1 min intervals.

GC-MS

An HP 5973 MSD with a 6890 GC was used for GC-MS analysis with a DB-1 column. The column was held at 80°C for 5 min, ramped to 300°C over 15 min, and held at 300°C for 20 min. Trimethylsilylation was achieved with 10 μL 99% [N, O-Bis(trimethylsilyl) trifluoroacetamide] (BSTFA) plus 1% trimethylchlorosilane (TMCS) (v:v) (Supelco, #33148) at 60°C for 1 hr. A 1 μL aliquot was injected into the GC-MS.

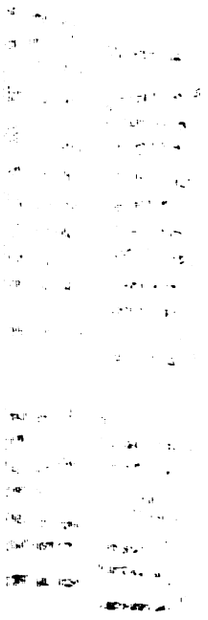

CHAPTER III

Chemical characterization of lipophilic activity in *C. elegans* extracts

ABSTRACT

In order to improve extract separation and GC-MS analysis the bioactivity in the extracts was chemically characterized. Carboxyl groups were shown to be important to bioactivity since their selective esterification prevented bioactivity of the extracts. The importance of carboxyls was confirmed after fractionation of the extract into neutral, carboxyl, and charged species demonstrated that bioactivity was only in the carboxyl-containing fraction. Since the DAF-12 ligand has been hypothesized to be sterol-derived, we made extracts from worms incubated with [4-^{14}C]-cholesterol and found that cholesterol-derived carboxylated species exist and that one of the bands has the same retention as the bioactive component. The bioactive component was found to be slightly more polar than cholesterol by thin-layer chromatography (TLC) which is consistent with a carboxyl addition to a sterol backbone. Chemical characterization of the bioactive extracts led to an excellent separation step that is orthogonal to HPLC, elucidated carboxyl groups as a target for analysis, and provided insight into the lipid class to which the DAF-12 ligand belongs.

INTRODUCTION

Common features of nuclear receptor ligands

Little is known about metabolism in *C. elegans* and none of its 284 putative nuclear receptors have an identified ligand. Therefore, rather than test known ligands or related structures we took a different approach that focused on understanding the fundamental chemical aspects of the bioactive component. Some properties of the DAF-12 ligand are likely predictable since nuclear receptor ligands share many chemical similarities including being small (250-350 $Å^3$) (Bogan et al., 1998), fairly rigid molecules with a high degree of hydrophobicity that enter cells by diffusion (Kralli et al., 1995). Polar groups capable of forming hydrogen bonds or electrostatic interactions are found at the ends of the molecules and provide interaction specificity with amino acids in the receptor. Generally, nuclear receptor ligands are classified as either steroidal or nonsteroidal based on whether or not they are derived from cholesterol. Examples of non-steroidal ligands include retinoic acids (derived from □-carotene) and 3,5,3'-triiodo-L-thyronine (T_3) (derived from thryoglobulin).

The DAF-12 ligand may be sterol-derived

There is evidence from *C. elegans* biology that the DAF-12 ligand might be sterol-derived. *C. elegans* requires exogenous cholesterol for proper development and sterol depletion enhances the Daf-c phenotype of *daf-9* mutants. This suggests that if the sterol pool is low not enough DAF-12 ligand can be produced. *C. elegans* has other enzymes involved in sterol metabolism such as *let-767*, a gene similar to 17□-hydroxysteroid dehydrogenases that are essential for growth, reproduction, and development (Kuervers et

al., 2003). However, *let-767* does not have a Daf phenotype (Kuervers et al., 2003). Therefore, it is unclear which sterols or sterol derivatives may specifically play a role in DAF-12.

Novel sterol metabolism in *C. elegans*

C. elegans has undergone a tremendous expansion in the number of putative nuclear receptor genes to 284 versus 48 in humans and 20 in *Drosophila*. It is not unlikely that *C. elegans* has also undergone an expansion in the number and variation of metabolic pathways that synthesize the ligands for the receptors. In fact, *C. elegans* has 83 putative P450s in its genome whereas humans have only 50 (Nelson, 1999). Furthermore, the complement of P450s in *C. elegans* differs significantly from that of humans. *C. elegans* has no mitochondrial P450s and 13 P450 families that are not present in mammals (Nelson, 1998). Biochemical evidence supports that novel biosynthetic pathways exist. First, the metabolism of sterols in *C. elegans* is in the opposite direction to mammalian cholesterol metabolism (Chitwood, 1999). In worms, cholesterol is dehydrogenated at the 7-position to form 7-dehydrocholesterol, whereas in mammals 7-dehydrocholeserol is reduced at the 7-position by □[7] reductase to form cholesterol (Figure 3.1) (Nwokoro et al., 2001). Secondly, mammals remove the 4-methyl groups from lanosterol to produce cholesterol which takes 20 enzymatic steps. *C. elegans* actually adds a methyl group to the 4-position of sterols (Figure 3.1), an enzymatic step that is unknown in any other organism (Chitwood et al., 1983).

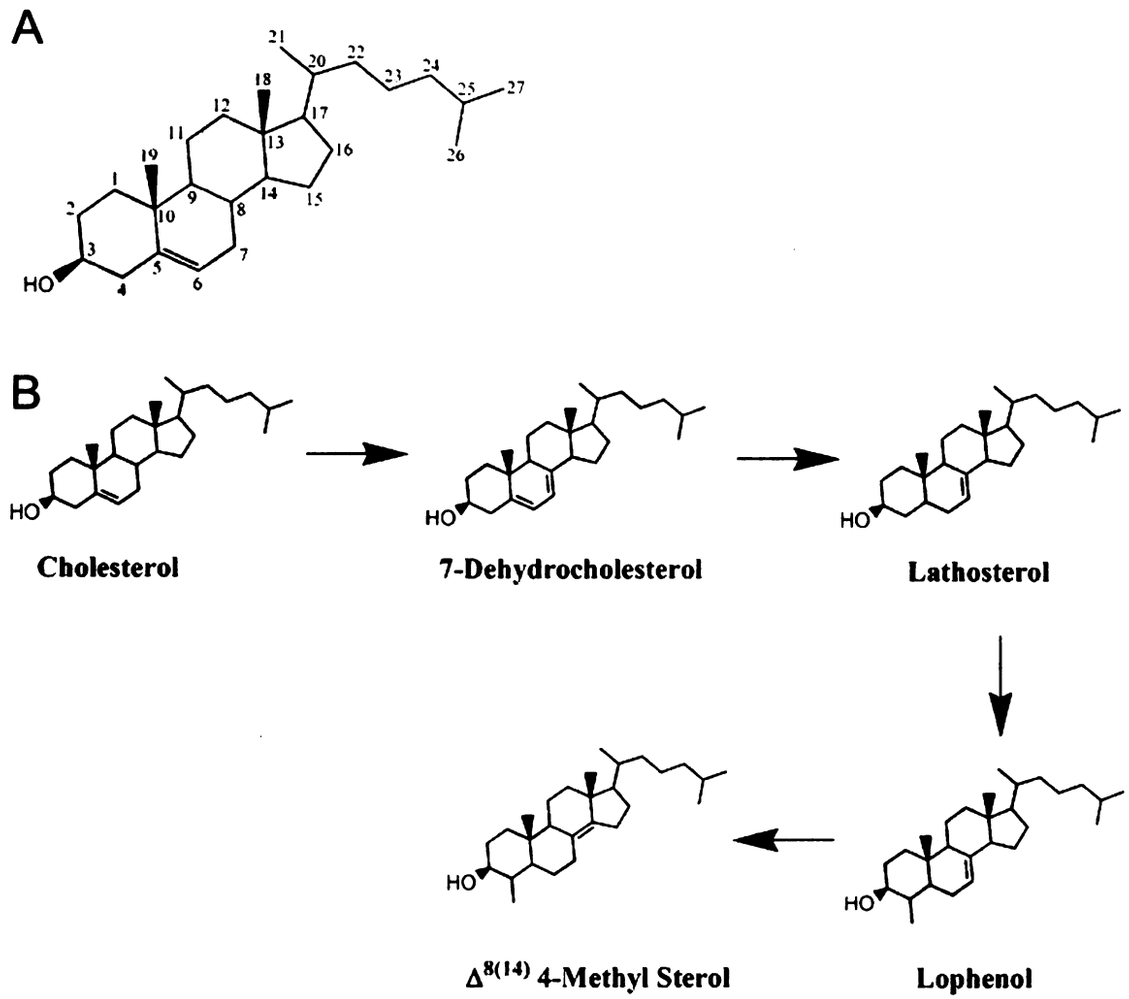

Figure 3.1 The known cholesterol metabolic pathway of *C. elegans*. (A) The cyclopentanoperhydrophenanthrene ring structure of cholesterol, a C27 alcohol. The designated carbon atom numbers are shown. (B) The *C. elegans* cholesterol biosynthetic pathway with cholesterol as the biosynthetic precursor.

Analysis of ligand chemical properties by combining chemical analysis with bioactivity

The evidence for a sterol or sterol product such as ecdysone, steroids, bile acids, and cholesterol esters as a potential DAF-12 ligand is substantial. Assays were designed that would help determine if the bioactive component belonged to a sterol-derived or alternate lipid class such as fatty acids, terpenoids, juvenile hormones, phospholipids, prostaglandins, or others (Figure 3.2). Diverse classes of compounds such as monomethyl branched-chain fatty acids (mmBCFAs) are known to play an essential role in *C. elegans* development suggesting that sterols are not the only important lipid in development since suppression of mmBCFA biosynthesis causes L1 arrest (Kniazeva et al., 2004). The chemical characterization was focused on two main goals: to find (1) which chemical class(es) the ligand might belong to and (2) what functional groups are present on the molecule. If pure material were available in large quantities several different analytical tools could be used, such as infrared spectroscopy to determine the functional groups present, or nuclear magnetic resonance spectroscopy (NMR) to determine the structure of the unknown ligand. However, the extract is complex and only trace levels of bioactive material are in the sample, making exact characterization of the chemical properties a much more complicated task. Our approach to understand more about the chemical nature of the DAF-12 ligand was to observe the effects of a variety of basic analytical techniques on bioactivity.

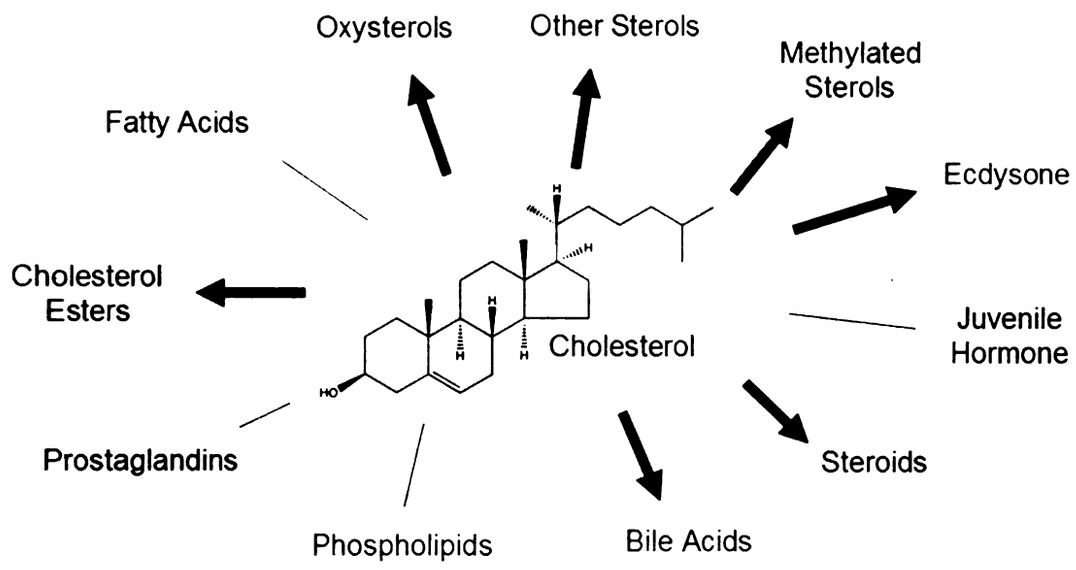

Figure 3.2 Potential steroidal and nonsteroidal DAF-12 ligands. Cholesterol is the metabolic origin of many bioactive lipids. An unbiased purification strategy is appropriate for bioactive lipids that are metabolites of cholesterol (thick arrows) or not cholesterol-derived (thin lines).

Chemical derivatization of bioactivity

One approach was selective derivatization of specific functional groups to see if modification prevented bioactivity. The rationale for this was that by modifying a functional group that is important for ligand binding and changing its chemical nature (charge, size, etc.), it should no longer be able to bind DAF-12 or function as a DAF-12 ligand. This is analogous to a site-directed mutagenesis approach to assess important amino acids for protein binding. Both the ligand and receptor have various functional groups such as hydroxyl, carboxyl, amino, and alkyl groups that are capable of forming non-covalent bonds with each other. Different ligands will have different spatial configurations of these functional groups which match to a specific configuration of amino acid functional groups on the protein. The specificity of binding is determined by the correct alignment of these functional groups. There are many ways to modify the common chemical groups; however, we used standard GC-MS derivatization reactions to make the modifications. This will facilitate the GC-MS analysis downstream for ligand identification. Derivatization reagents are also particularly useful since they are designed to be very specific to particular functional groups, proven to have minimal unwanted side reactions under most conditions, and modify most target functional groups even with differing steric or ionic circumstances. Using derivatization reagents also potentially requires less reaction optimization since reaction conditions are well characterized. This limits potential problems such as only a subset of the target functional group being modified in an experiment.

Lipid class characterization of bioactivity

Lipids were separated by class using aminopropyl columns that utilize weak anion exchange to separate neutral, carboxyl-containing, and charged lipid classes. Normal phase TLC was also used to separate based on the interaction of the polar functional groups with silica, a common technique which also provides lipid class separation. TLC allows for quick and easy comparison of relative polarity between compounds and can be used to characterize bioactive polarity relative to the retention of standards from several lipid classes.

RESULTS

Chemical derivatization bioassay

In order to test if particular functional groups are important for ligand binding, hydroxyls, amines, carboxyls, and ketones in 1 g of extract were selectively modified and tested for bioactivity. Hydroxyls and amines were acetylated with acetic anhydride/pyridine. Amines were crosslinked with disuccinimidyl suberate (DSS). Carboxyls were methyl esterified with either diazomethane or BF_3-methanol. Ketones were modified by either methoxyamine (MOX) or Girard's Reagent P. Since the reagents themselves are potentially toxic to the worm and may prevent dauer rescue even in the presence of unmodified, bioactive ligand, a control was used in which a blank reaction was freshly added to extract immediately before plating. If this control rescued worms it was assumed that the reaction products had minimal or no toxicity on their own.

Acetylating amines and hydroxyls with acetic anhydride/pyridine abolished bioactivity but crosslinking amines with DSS had no effect on bioactivity (Figure 3.3 A). Since nuclear receptor ligands are almost completely buried by H12 when properly bound, it is very unlikely that a crosslinked ligand would be functional. This suggests that a hydroxyl is important for the functionality of a DAF-12 ligand. When carboxyl groups were methyl esterified by either diazomethane or BF_3-methanol, bioactivity was prevented suggesting that a carboxyl is important for DAF-12 ligand activity (Figure 3.3 B). Finally, when ketones were modified using MOX or Girard's Reagent P there was no bioactivity in the extract (Figure 3.3 C). However, the control reaction with fresh extract also did not have bioactivity suggesting that these reagents alone prevent worm dauer rescue. Several reaction conditions and extractions were tested; however, it was not

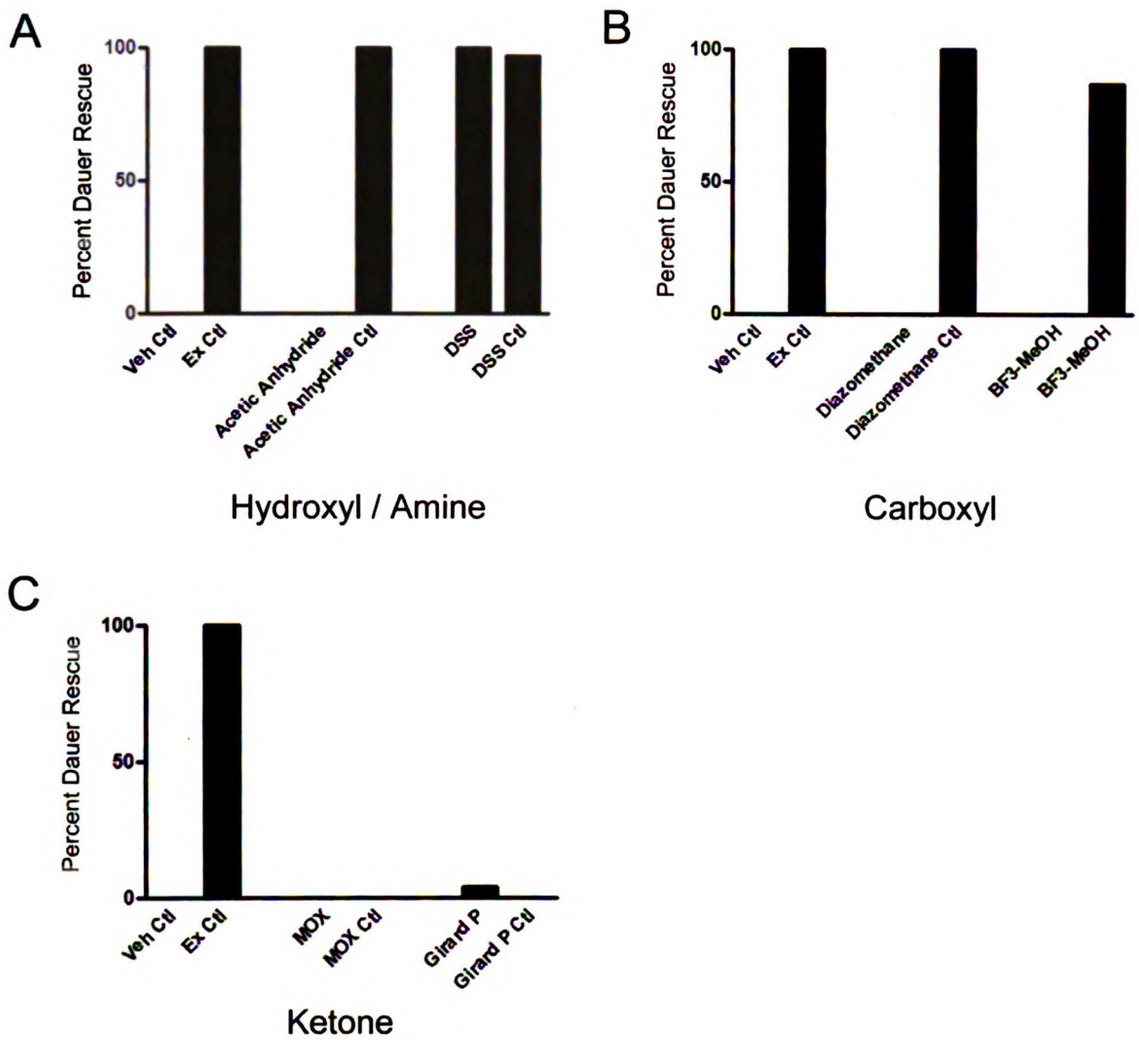

Figure 3.3 Modifying ligand functional groups by derivatization and assaying bioactivity on *daf-2(e1368)*. (A) Acetylation of hydroxyls and amines using acetic anhydride/pyridine and crosslinking of amines using DSS. (B) Esterification of carboxyl groups using diazomethane or BF_3-methanol. (C) Modification of ketones using MOX or Girard's Reagent P. In all cases the vehicle control (Veh Ctl) is DMSO and the extract control (Ex Ctl) is 1 g underivatized *daf-12(m20)* extract. The reagent column refers to 1 g extract derivatizated by the reagent and the reagent control is 1 g fresh extract added to a blank reaction to control for potential toxicity of the derivatization reagent itself.

possible to rescue worms exposed to these reagents leaving the question of whether a ketone is important to ligand binding of DAF-12 unanswered.

Aminopropyl SPE

To characterize the lipid classes in the extract, fractionation using an aminopropyl bonded SPE was carried out (Kaluzny et al., 1985). This separation scheme was chosen based on the suggestion by the chemical derivatization bioassay that the ligand has a carboxyl since it separates compounds into neutral, carboxyl-containing, and charged compounds. Aminopropyl fractionation allows both confirmation of the presence of a carboxyl as well as the ability to use it as a chromatographic handle for improved extract separation. Potential ligands such as sterols elute in the neutral lipid fraction, fatty acids and bile acids elute in the carboxyl fraction, and phospholipids elute in the polar lipid fraction. TLC of an aliquot of these fractions indicated good separation between the neutral lipids, fatty acids, and polar lipids with most compounds in the neutral fractions (Figure 3.4 A). When fractions were examined for dauer-rescuing activity of *daf-2(e1368)*, the bioactivity was found in only the fraction corresponding to carboxyl-containing compounds (Figure 3.4 B).

These retention data rule out many classes of lipids from Figure 3.2 such as most sterols, glycerides, cholesterol esters, phospholipids, ecdysones, juvenile hormones, and oxysterols as a potential DAF-12 ligand since they are either neutral or charged and would not elute in the carboxyl-containing fraction. This leaves prostaglandins, bile acids, and fatty acids as likely ligand candidates, in addition to the possibility that it is an unusual carboxylated version of one of the neutral lipid classes listed above.

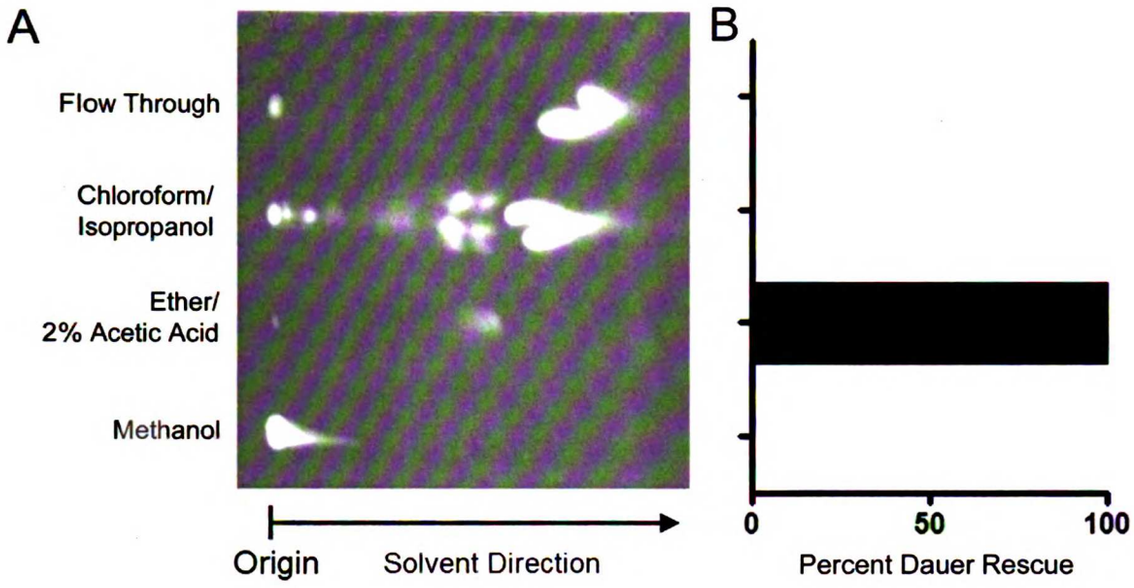

Figure 3.4 Aminopropyl SPE dramatically reduces extract complexity. (A) Normal phase TLC of a *daf-12(m20)* extract fractionated with an aminopropyl SPE column. Chloroform/isopropanol elutes neutral lipids, ether/2% acetic acid elutes carboxylated compounds, and methanol elutes polar lipids. TLC plate was visualized by primulin staining. (B) Bioactivity corresponding to aminopropyl fractions.

Normal phase TLC

A toluene:ethyl acetate:trimethyl borate 100:20:7.2 (v:v:v) solvent system was used for normal phase TLC since it is a solvent system that resolves most moderately polar lipids with improved resolution than the more traditional hexane-diethyl ether system. In order to compare the retention of bioactivity with standards, extract was added as a lane on the TLC plate along with other standards. Typical standards were monoolein, diolein, cholesterol, hexadecanoic acid, and triolein (in order from highest polarity to least polarity). After the TLC plate was run and visualized, the extract lane was divided into sections based on the retention of the standards. This made a distinction between lipid classes and polarities (Figure 3.5). When each section was bioassayed, the retention of bioactivity (Figure 3.5 B) was found to correspond to Section 2 of Figure 3.5 A. This section co-migrates with monoolein which is slightly more polar than cholesterol. Bioactivity would occasionally co-migrate with cholesterol as well. Monoolein has two polar groups whereas cholesterol has just one. The data from normal phase TLC likely rule out fatty acids as a lipid class since they consistently migrate farther than cholesterol to a more hydrophobic region of the TLC plate.

[4-^{14}C]-cholesterol

Due to the evidence that sterols play a role in dauer formation, we wanted to determine if the bioactivity in this carboxyl-containing fraction could be derived from a sterol.

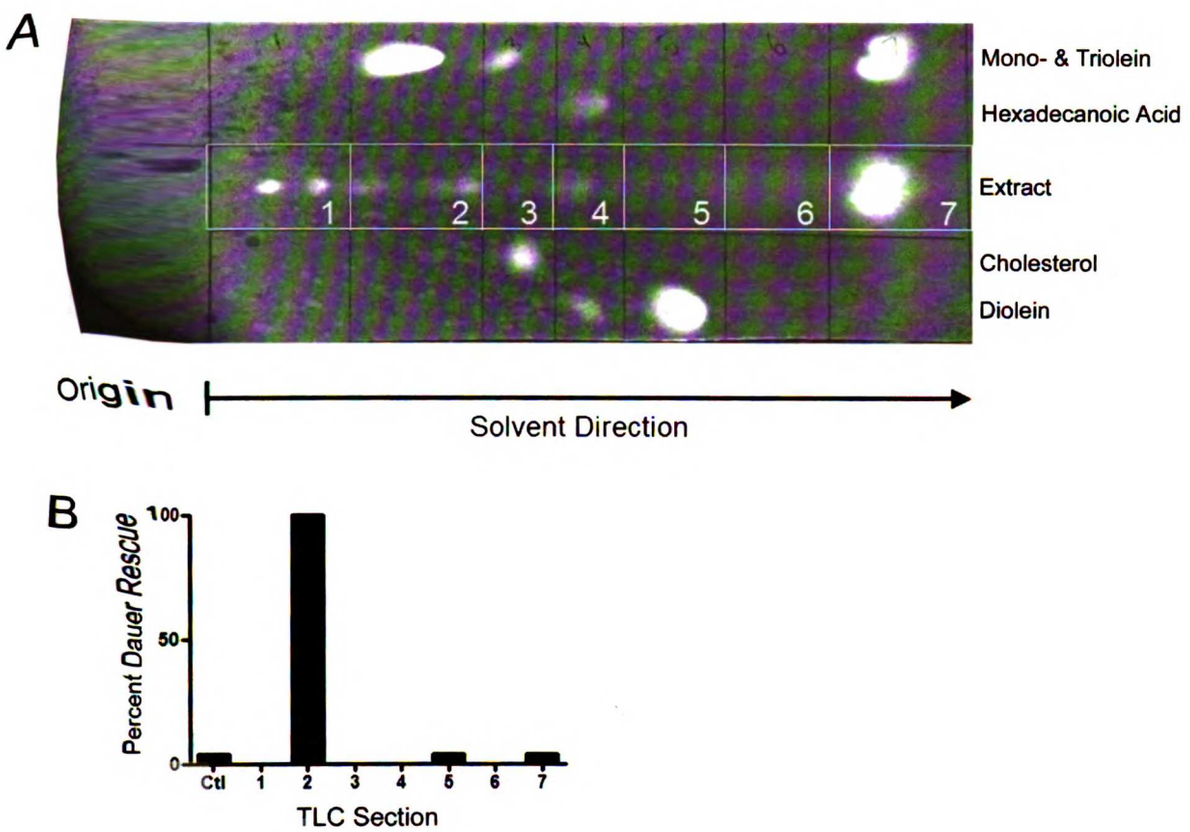

Figure 3.5 Normal phase TLC of extract demonstrates the bioactive component has moderate polarity. (A) Normal phase TLC fractionation of standards along with 1 g *daf-12(m20)* extract visualized by primulin staining. Sectioning of the extract portion of TLC plate is based on the retention of the standards. Each section of silica was scraped off the TLC plate individually and is labeled 1 through 7 with 1 being most polar and 7 being least polar. (B) Bioactivity corresponding to TLC sections in A.

Carboxylated sterols have not previously been identified in worms. *C. elegans* extracts derived from worms grown in the presence of [4-^{14}C]-cholesterol were fractionated using aminopropyl SPE. TLC of these radiolabeled fractions indicated that the majority of radioactivity eluted in the neutral lipid fraction ($CHCl_3$ lanes) as expected, with major bands corresponding to methylated and non-methylated sterols (Matyash et al., 2004) (Figure 3.6 A). Interestingly, the carboxyl-containing fraction (ether/2% acetic acid lane) does have several bands of radioactivity, suggesting that worms are capable of adding a carboxyl group to a cholesterol precursor (Figure 3.6 A). This confirms that the bioactive component of the dauer-rescuing extracts could be a modified sterol containing a carboxylic acid group. In order to determine the relative polarity of these compounds and to make an inference about their lipid classes, several standards were included on the TLC plate that was visualized with primulin (Figure 3.6 B). There are three distinct radioactive bands in the ether/acetic acid lane. When overlaid with the standards one radioactive band co-migrates with monoolein and thus has the same retention as bioactivity as well (Figure 3.6 C).

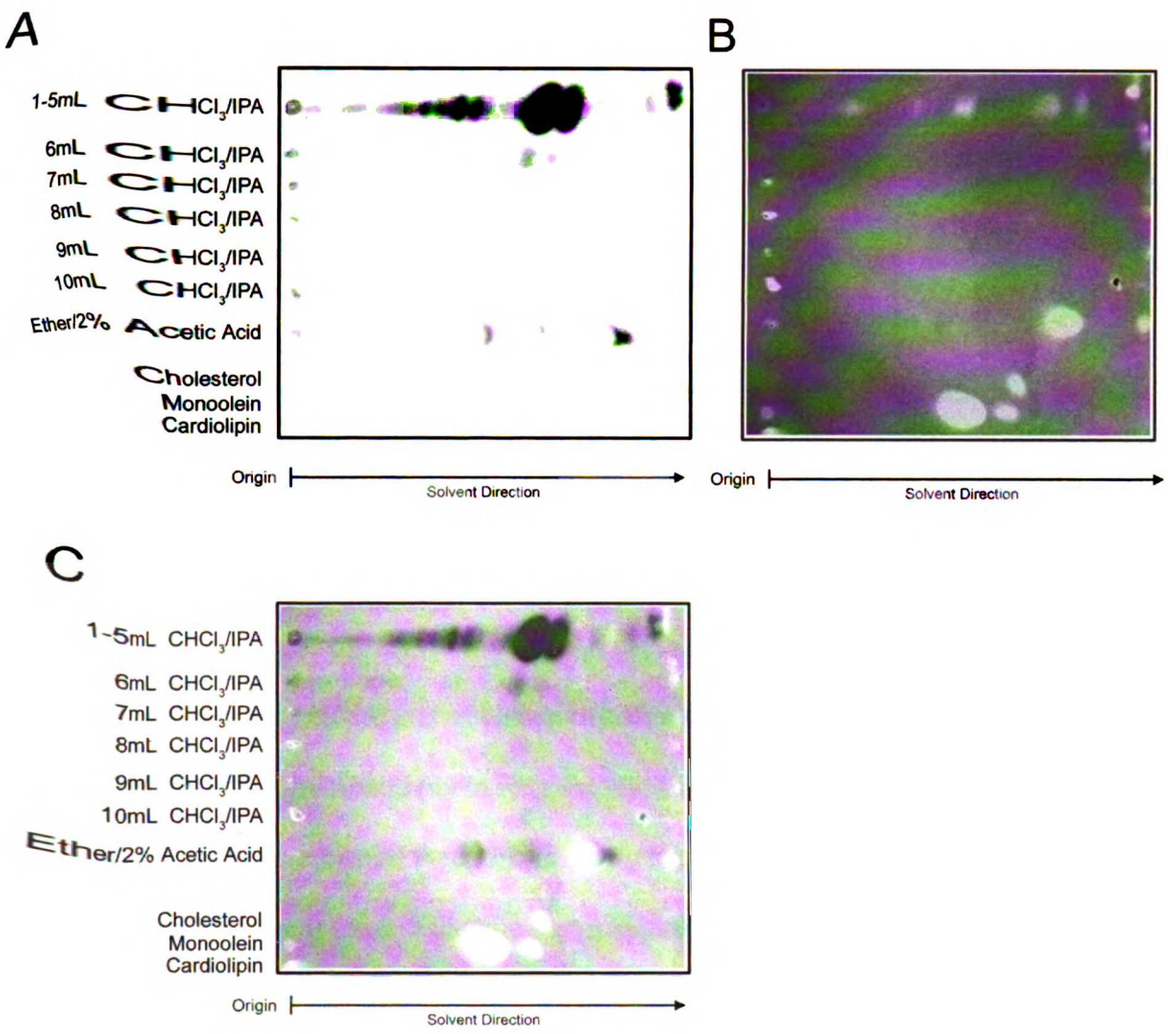

Figure 3.6 Cholesterol-derived carboxylated compounds exist in *C. elegans*. (A) Worms grown on [4-^{14}C]-cholesterol were extracted and fractionated by aminopropyl SPE. Chloroform/isopropanol ($CHCL_3$/IPA) elution (1-5 mL) and washes (6-10 mL) contain neutral lipids whereas ether/2% acetic acid elutes carboxylated compounds. An autoradiography film was placed over the TLC plate to detect radioactivity. (B) The same TLC plate as in A but stained with primulin to visualize the TLC standards as well as the abundant lipids in the extract. (C) Overlay of the TLC images in A and B to determine the relative retention and polarity of the cholesterol-derived carboxylated compounds.

DISCUSSION

We investigated the chemical nature of bioactivity in order to improve purification and derivatization. By examining the chemical properties of bioactivity such as its polarity and important functional groups, fractionating based upon carboxylation, and demonstrating the existence of sterol acids in *C. elegans*, we have achieved a much better understanding of how to target analytical techniques to identify the DAF-12 ligand.

The ligand is carboxylated and could be derived from a sterol

One of the most definitive results of the ligand chemical characterization was the determination of the carboxylated nature of the bioactive component. This was demonstrated by both the loss of bioactivity after targeted esterification of extract carboxyls as well as bioactivity in only the aminopropyl carboxyl-containing extract fraction. Sterols are neutral compounds and in mammalian systems are typically only known to be carboxylated in the bile acid metabolic pathway. The addition of a carboxyl to a sterol molecule fits with our normal phase TLC data in which bioactivity most often migrates to a point slightly more polar than cholesterol, near monoolein. Monoolein has two hydroxyl polar functional groups, which is the same number a putative carboxylated sterol would have. In addition, sterol acids are almost always hydroxylated which supports the data that bioactivity is lost after acetylation of hydroxyls. Since the biosynthesis of sterol acids has not been characterized in *C. elegans*, we added radiolabeled cholesterol to worms and determined the presence of carboxylated sterols. Furthermore, a subset of the sterol acids have the same retention on normal phase TLC as the bioactive component.

Derivatization helps optimize GC-MS sample preparation

The benefit of using standard chemical modifications in our derivatization bioassay is that they are all suitable as derivatization reagents for GC-MS. We were now in a position to be confident that our derivatization conditions will appropriately identify candidate bioactive components by GC-MS. TMS derivatization, which we have previously used, has several problems including sensitivity to moisture and lack of sensitivity from TMS-ester derivatives. Carboxyls modified by TMS become TMS-esters, therefore GC-MS analysis should be significantly improved when carboxyls are esterified rather than silylated.

One potential pitfall of the chemical derivatization approach is that although ligand modification that directly prevents ligand binding would prevent bioactivity, bioactivity may be affected by a non-specific effect such as preventing uptake or transport. In fact, derivatizing a small molecule to assay receptor binding is likely a novel approach to chemically characterizing an unknown compound in trace levels. Because of the above issues we were careful to corroborate our most interesting finding, that a carboxyl was required for bioactivity, by fractionating extracts and finding bioactivity in the carboxyl fraction as well as using [4-^{14}C]-cholesterol to identify sterol acids. Taken together, these data provide valuable insight for future analysis.

Chemical characterization will improve separation

Though SPE has limited resolution compared to HPLC, it is more reproducible and faster for the routine separation of complex extracts. It is clear that the aminopropyl SPE fractionation separates away a large amount of material in the neutral lipid fraction from

the carboxyl fraction, leaving it much cleaner (Figure 3.4). The primary components that are seen by TLC in the aminopropyl carboxyl-containing fraction are fatty acids (Figure 3.4). This makes aminopropyl SPE an excellent preparative step to reduce the complexity for downstream analysis, and it is an orthogonal separation to any of our HPLC strategies.

Bile acids are a likely candidate to be the DAF-12 ligand

The ligand characterization data strongly suggest that the bioactive component in the extracts is a bile acid. This information can now be used to screen known bile acids for dauer rescue bioactivity. Furthermore, our previously established purification strategies can be used downstream of an initial aminopropyl SPE fractionation as well as to optimize GC-MS analysis for detection of bile acids using updated derivatization methodology.

MATERIALS AND METHODS

Materials

Monoolein (#M-239), diolein (#D-236), and triolein (#T-235) were purchased from Nu-Check Prep (Elysian, MN). Hexadecanoic acid (#P-5585) was purchased from Sigma (St. Louis, MO). Cardiolipin (#710332) was purchased from Avanti Polar Lipids (Alabaster, AL).

C. elegans strains

As in Chapter 2.

Dauer rescue bioassay of extract

Performed as in Chapter 2.

Acetic anhydride/pyridine acetylation

A lgether extract was dried down and incubated with 1:1 0.5 mL acetic anhydride:pyridine (v:v) (Pyridine Plus kit, Alltech #18105) at 60°C overnight. H_20 (0.5 mL) was added and then extracted twice with 0.5 mL hexane. The hexane was then dried under N_2 and resuspended in 10 µL DMSO for bioassay.

Disuccinimidyl suberate crosslinking

A lgether extract was dried down and incubated with 30 µL 2.5 mM disuccinimidyl suberate (DSS) (Pierce #21658) in 1:1:1 (v:v:v) PBS (pH 7.5):DMSO:ethanol at room temperature (23°C) for 30 min. Reaction was quenched with 6 µL 1 M Tris (pH 8.0) for

15 min. The sample was then dried under N_2 and resuspended in 10 µL DMSO for bioassay.

Diazomethane esterification

A 3 mL quantity of diazomethane was freshly generated using an MNNG (1-methyl-3-nitro-1-nitrosoguanidide) diazomethane-generator (Aldrich #Z411736). Approximately 100 mg of MNNG reagent (TCI America #M0527) was placed into the interior tube of the generator along with 0.5 mL H_2O. Diethyl ether (3 mL) was then placed in the outer tube of the generator and the two tubes were assembled. The apparatus was then placed in an ice bath with a stir bar and placed behind a protective shield. NaOH (5N, 0.6 mL) (VWR #VWR3225-1) was then injected dropwise using a 22 gauge needle into the inner tube of the generator. After 1 hr, when the color of the ether stopped getting more yellow, the diazomethane was transferred to a 1 g extract already dried down. A 0.5 to 1 mL quantity of diazomethane (in ether) was added to 1 g dried extract and incubated for 1 min at room temperature (23°C). The diazomethane was then dried under N_2 and resuspended in 10 µL DMSO for bioassay.

Boron trifluoride (BF_3)-methanol esterification

A 1 g extract was dried down and incubated with 200 µL BF_3-10% methanol (w:w) (Supelco #33356) for 90 min at 100°C. H_20 (250 µL) was added and then extracted twice with 550 µL hexane. The hexane was then dried under N_2 and resuspended in 10 µL DMSO for bioassay.

Methoxyamine (MOX) derivatization

A 1 g extract was dried down and incubated with 500 µL MOX reagent (2% methoxyamine·HCl in pyridine, Pierce #45950) for 3 hr at 60°C. The sample was then dried under N_2 and resuspended in 10 µL DMSO for bioassay.

Girard's Reagent P derivatization

A 1 g extract was dried down and incubated with 10 mg Girard's Reagent P (Aldrich #124516) in 70% aqueous methanol containing 20% acetic acid for 30 min at 70°C (Khan et al., 2006). The sample was then dried under N_2 and resuspended in 10 µL DMSO for bioassay.

Normal phase TLC

Samples were spotted onto 20 cm x 10 cm high-performance Silica Gel 60 TLC plates (Alltech #811013) and dried with a hairdryer. Plates were resolved with toluene:ethyl acetate:trimethyl borate 100:20:7.2 (v:v:v) in order to separate lipid classes (Pollack et al., 1971). Plates were then dried with a hairdryer for 5 min.

Primulin dye (Sigma #206856) was used to visualize many lipid classes. Based on the method by Nudelman (White et al., 1998), dried TLC plates were sprayed with a 0.05% solution of primulin dye (a 1:100 dilution of a 5% aqueous stock into acetone:water, 8:2, v:v). All primulin stocks were wrapped in foil. Plates were sprayed with an atomizer in a uniform manner until just visibly moist and then dried with a hairdryer for 2 min. Lipid spots were visualized using a UV light box. Primulin did not show any signs of affecting bioactivity from the TLC plates.

Twenty percent phosphomolybdic acid (PMA) in ethanol (w:w) (Sigma #319279) was used as a charring reagent to detect all lipid classes. PMA was used since primulin does not detect bile acids well. The PMA solution was used without dilution and sprayed using an atomizer in a uniform manner onto the TLC plate until it was just visibly moist. The TLC plate was then dried with a hairdryer for 2 min using the cool setting only. The plates were then put into a 150°C oven for 5-30 min to char the plate and visualized by eye.

Preparative TLC for testing bioactivity

After running a TLC plate in which we desired to test for bioactivity, we would dry and spray the plate as if using primulin. However, if we wanted to use PMA, we would place a strip of tape over the extract lane on the TLC plate before spraying since PMA charring destroys bioactivity (data not shown). After spraying we would remove the tape and place the plate in the oven.

Bioactivity was extracted off the TLC plate by scraping off the silica and vortexing it extremely vigorously in a 3 mL reactivial with 1 mL 9:1 methanol:water (v:v). Vials were then centrifuged at 2000 rpm for 30 sec, supernatant was collected and the steps were repeated once more. The collected supernatant was dried down under N_2 and resuspended in DMSO for bioassay.

Aminopropyl fractionation

Extracts were dried under N_2 and resuspended in chloroform. Fractionation was performed by the method of Kaluzny on 500 mg aminopropyl cartridges (Supelco

#52637-U) (Kaluzny et al., 1985). The column was equilibrated with hexane and extracts were applied to the column in 5 mL chloroform. Neutral lipids were eluted in 10 mL 2:1 chloroform:isopropanol, carboxyl-containing groups eluted with 10 mL 2% acetic acid in diethyl ether, and polar lipids were eluted with 2 mL methanol.

[4-^{14}C]-cholesterol

We added 10 μCi (370kBq) [4-^{14}C]-cholesterol (PerkinElmer, #NEC018010UC) to *daf-12(m20)* eggs after hypochlorite treatment in 85 mL S-Media and 15 mL concentrated OP50. The amount of cholesterol was 160 μg, which is a little less than would normally be added (500 μg), but the normal amount of cholesterol is still in excess for normal growth. No additional cold cholesterol was added. Worms were shaken at 25°C at 150 rpm for 48 hr. Approximately 3 mL (3.3 g) of worm pellet was harvested. The frozen pellet was extracted as in Merris (Merris et al., 2004). Ethanol (5 mL) was added to the thawed pellet and put at 60°C for 1 hr. The samples were then cooled and 3 mL H_2O was added. Samples were extracted 3 times with 5 mL of hexane and allowed to dry overnight.

Aminopropyl fractionation was performed as above except that the neutral lipid fraction was collected slightly differently in order to demonstrate that all the neutral lipids had eluted off the column before carboxylated compounds were eluted. The first 5 mLs were collected and then each additional mL of elution was collected separately. TLC was performed as above on high-performance silica TLC plates with toluene:ethyl acetate:trimethyl borate 100:20:7.2 (v:v:v). An autoradiography film (Amersham

Hyperfilm MP #RPN1678K) was placed onto the extract and developed after 1 d, 3 d, and 30 d (30 d shown in Figure 3.6).

CHAPTER IV

Cholestenoic acid has dauer-rescuing bioactivity in *C. elegans* dauer mutants and acts as a DAF-12 ligand

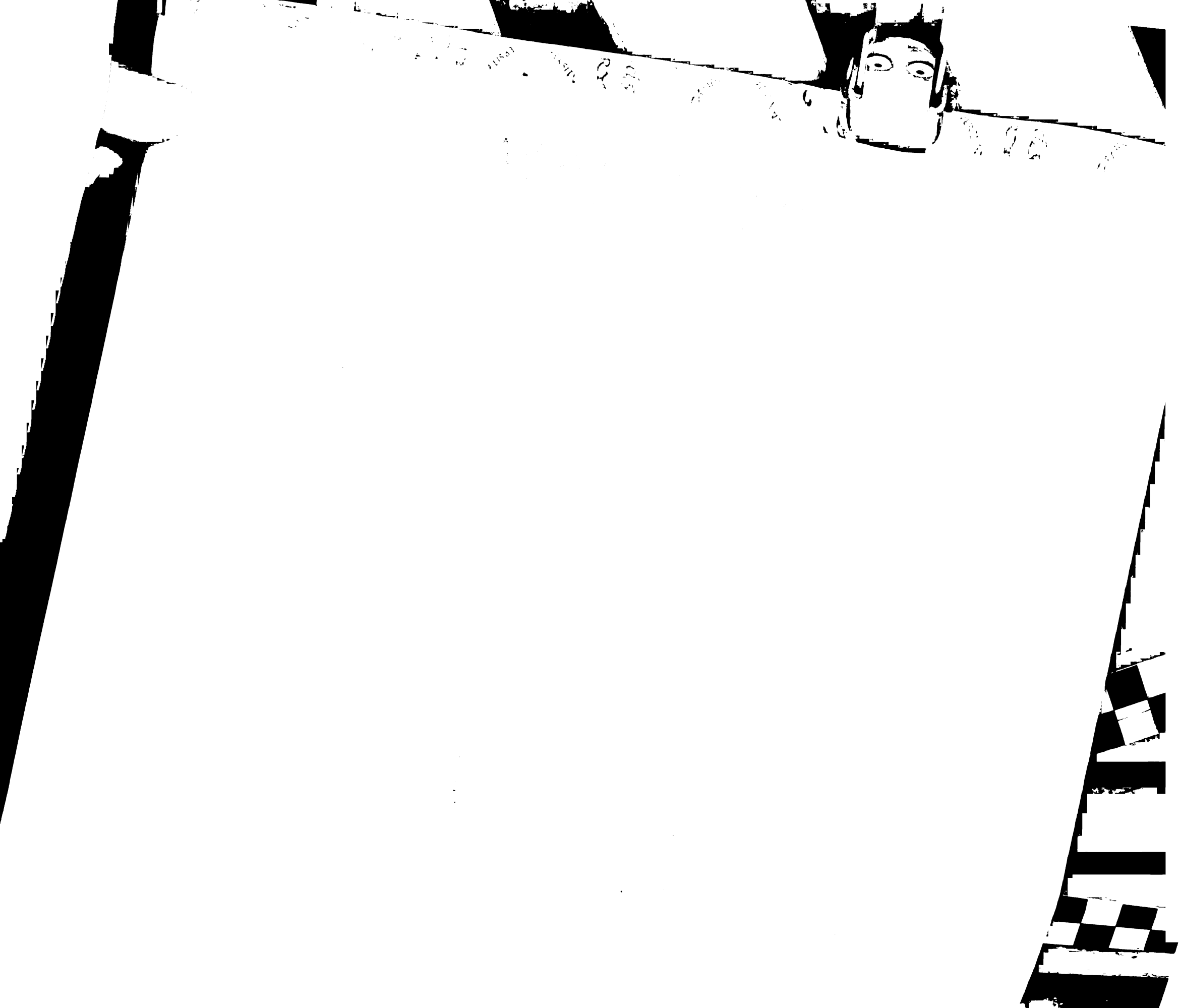

ABSTRACT

Based on the evidence that a sterol acid is the bioactive component in the extract, we screened for bile acids that rescue dauer formation. We found that (25S)-cholestenoic acid, like bioactive extracts, rescued the Daf-c phenotype of *daf-2(e1368)* and *daf-9(gk160)* mutants but not the ligand-insensitive *daf-12* mutant *daf-12(rh273)*. We also found that *daf-9(gk160)* worms treated with (25S)-cholestenoic acid had properly reflexed gonads whereas treated *daf-12(rh273)* mutants did not. The 25R form of cholestenoic acid competitively inhibits dauer rescue, suggesting that (25S)-cholestenoic acid is acting selectively to regulate dauer formation. TLC fractionation of the extract determined that only the section co-migrating with monohydroxylated bile acids has bioactivity, consistent with (25S)-cholestenoic acid as the bioactive component. Normal phase HPLC retention of (25S)-cholestenoic acid matches retention of bioactivity in the extracts as well. (25S)-cholestenoic acid was demonstrated to act as a ligand *in vitro* in a cell-based assay by M. Gill. We also demonstrated that (25S)-cholestenoic acid downregulates DAF-9 expression, suggesting that it activates DAF-12 *in vivo* and acts in a feedback loop with DAF-9.

INTRODUCTION

Bile acid metabolism

In mammals, one role of bile acids is to remove excess cholesterol from the body by conversion into bile acids. Bile acids are much more water soluble than cholesterol and are readily excreted. The complement of bile acids varies widely between different mammals, and this diversity is increased by anaerobic bacteria in the gut which convert the primary bile acids into dozens of secondary and tertiary bile acids (Russell, 2003). The variety of different bile acids in the gut is thought to ensure complete solubilization of hydrophobic vitamins and nutrients from food in the small intestine, a second role for bile acids in mammals (Hayakawa, 1982; Bortolini et al., 1997; Hofmann, 1999).

Bile acids are synthesized from cholesterol via 17 enzymes which modify its hydrophobic backbone by adding a carboxyl group at the end of the side chain and many different permutations of hydroxyl groups around the ring nucleus. Two classical routes have been established for mammalian bile acid synthesis, termed the neutral and acidic pathways (Figure 4.1; see Figure 3.1 for cholesterol numbering scheme). In the neutral pathway, which is the main metabolic pathway, cholesterol is initially hydroxylated at the 7-position by CYP7A1 followed by conversion of the □^{5} 3-hydroxy structure into a □^{4} 3-oxo form. An additional hydroxyl can be added at the 12-position; however, the next key step is removal of the □^{4} bond by a reductase. This is followed by reduction of the 3-oxo back to a 3-hydroxyl form. The side chain is oxidized next by a mitochondrial cytochrome P450, CYP27A1, that introduces a hydroxyl group at carbon 27, modifies it into an aldehyde, and then into a carboxylic acid (Dahlback and Holmberg, 1990; Cali and Russell, 1991; Pikuleva et al., 1998). The side chain of these C27 bile acids is then

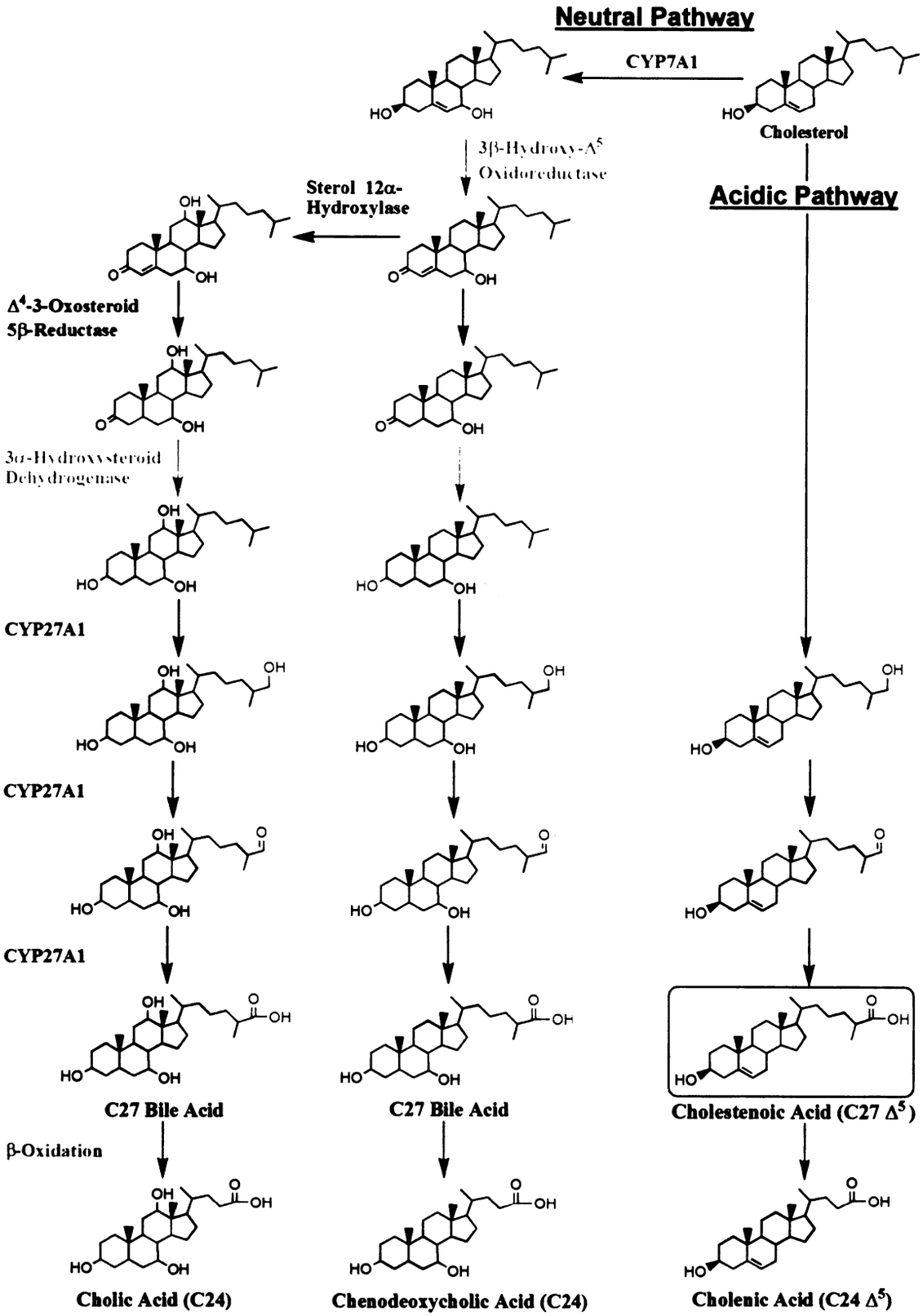
Neutral Pathway
CYP7A1
Cholesterol
3β-Hydroxy-Δ5 Oxidoreductase
Sterol 12α-Hydroxylase
Acidic Pathway
Δ4-3-Oxosteroid 5β-Reductase
3α-Hydroxysteroid Dehydrogenase
CYP27A1
CYP27A1
CYP27A1
C27 Bile Acid
C27 Bile Acid
Cholestenoic Acid (C27 Δ5)
β-Oxidation
Cholic Acid (C24)
Chenodeoxycholic Acid (C24)
Cholenic Acid (C24 Δ5)

Figure 4.1 Mammalian bile acid biosynthetic pathway. An acidic and a neutral pathway lead to formation of different bile acids in mammals. In the neutral pathway, cholesterol is initially metabolized by CYP7A1 and leads to saturated bile acids after modification by CYP27A1. In the acidic pathway, cholesterol is directly metabolized by CYP27A1 and leads to the formation of unsaturated bile acids including the C27 bile acid cholestenoic acid.

shortened by three carbon atoms in peroxisomes by enzymes similar to fatty acid β-oxidation enzymes.

An alternate acidic pathway, which accounts for 10 to 25% of bile acid generation in mice, is initiated when CYP27A1 directly carboxylates cholesterol to produce a C27 Δ^5 bile acid known as cholestenoic acid that has undergone no additional hydroxylation (Cooper, 1997; Schwarz et al., 1998; Duane and Javitt, 1999). The acidic pathway is distinguished from the neutral pathway because it produces unsaturated sterol acids that have a double bond at the Δ^5 position since CYP7A1 and the Δ^4 3-oxo ring structure modification is bypassed in this pathway (Javitt, 2000; Javitt, 2002b). Cholestenoic acid can then be further modified into the C24 mono-hydroxy bile acid cholenic acid which retains the Δ^5 bond, or the classical, saturated, polyhydroxylated C24 bile acids (Kulkarni and Javitt, 1982; Javitt et al., 1986; Javitt, 2000).

Bile acids act as nuclear receptor ligands

Regulation of the overall level and profile of bile acids is tightly regulated. This regulation occurs by bile acids acting as ligands for nuclear receptors which control the expression and activity of the upstream enzymes that produce bile acids (Russell, 1999). Cholesterol homeostasis is maintained via a network of lipid-sensing nuclear receptors that includes the liver X receptor (LXR), farnesoid X receptor (FXR), peroxisome proliferator-activated receptors (PPARs) and pregnane X receptor (PXR) (Chawla et al., 2001; Ory, 2004; Handschin and Meyer, 2005). FXR and LXR are the lipid receptors that bind bile acids, heterodimerizing with the retinoid X receptor (RXR) to establish a feed-forward autoregulatory loop coordinating the bile acid based signaling cascade. FXR

binds chenodeoxycholate and cholic acid which in turn suppresses transcription of CYP7A1, the rate-limiting enzyme of neutral bile acid biosynthesis, as well as IBABP, a protein that facilitates bile acid reuptake in the small intestine (Makishima et al., 1999; Parks et al., 1999; Dussault et al., 2003). At a lower affinity, FXR also binds the polyhydroxylated sterols that are bile acid precursors (Nishimaki-Mogami et al., 2004). LXR binds oxysterols including (22R)-hydroxycholesterol (Janowski et al., 1996) as well as the cholesterol-derived products of the acidic bile acid pathway 27-hydroxycholesterol and cholestenoic acid (Song and Liao, 2000; Fu et al., 2001). LXR activation decreases sterol transporters and CYP7A1, both of which downregulate bile acid production (Chawla et al., 2001). The possibility of DAF-12 as a lipid sensor that plays a role in *C. elegans* cholesterol homeostasis is intriguing, especially since sterols play an important role in dauer formation.

Bile acids in *C. elegans*

Almost nothing is known about bile acid synthesis in *C. elegans* and no bile acids have been identified. However, using the insight garnered from our ligand chemical characterization, specifically the knowledge that a carboxyl group is important for ligand binding and that sterol acids exist in worms, we screened many common C24 bile acids as well as the C27 sterol acid cholestenoic acid for rescue of the Daf-c phenotype of *daf-2(e1368)*, *daf-9(gk160)*, and *daf-12(rh273)*. We find that only (25S)-cholestenoic acid rescues dauer formation in a *daf-9* and *daf-12*-dependent manner. We then compare the analytical properties of (25S)-cholestenoic acid to the bioactive component in the

extract as well as examine the interaction of (25S)-cholestenoic acid with DAF-12 both *in vitro* and *in vivo*.

RESULTS

(25S)-cholestenoic acid rescues the Daf-c phenotype of *daf-2(e1368)*

We screened bile acid standards for rescue of dauer formation in worms and found that none of the common C24 bile acids (cholic acid, chenodeoxycholic acid, deoxycholic acid, lithocholic acid, and Δ^5 cholenic acid) were able to rescue the Daf-c phenotype of *daf-2(1368)* at 25°C (data not shown). However, when we tested the C27 sterol acid cholestenoic acid in the dauer assay, we found that (25S)-cholestenoic acid (5-cholesten-3β-ol-(25S)-carboxylic acid) (Figure 4.2 A) was able to completely rescue the Daf-c phenotype of *daf-2(e1368)* (Figure 4.2 B). A dose response curve determined that 50% rescue is achieved at approximately 100 nM (25S)-cholestenoic acid whereas the 25R stereoisomer had no effect even into the micromolar range (Figure 4.2 C). Co-incubation experiments in which *daf-2(e1368)* animals were treated with 1 μM or 5 μM (25S)-cholestenoic acid, a dose sufficient to completely rescue the Daf-c phenotype, determined that excess (25R)-cholestenoic acid could abolish the dauer rescue by the 25S diastereomer at 10 to 25 fold excess (Figure 4.2 D). This competition suggests that a high degree of selectivity is involved in the rescue by (25S)-cholestenoic acid.

(25S)-cholestenoic acid rescues the Daf-c phenotype of *daf-9(gk160)*

A DAF-12 ligand would be expected to rescue the Daf-c phenotype of a *daf-9* mutant, so we treated the *daf-9* knockout strain *daf-9(gk160)* with (25S)-cholestenoic acid. We found that (25S)-cholestenoic acid is able to rescue the Daf-c phenotype of *daf-9(gk160)* mutants treated from egg (Figure 4.3 A). Many *daf-9* mutants have a gonad migration defect in which the gonad fails to reflex properly. However, in *daf-9(gk160)* worms

A

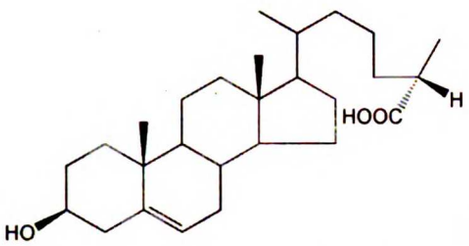

(25S)-Cholestenoic Acid

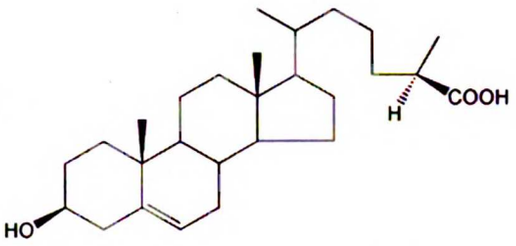

(25R)-Cholestenoic Acid

B

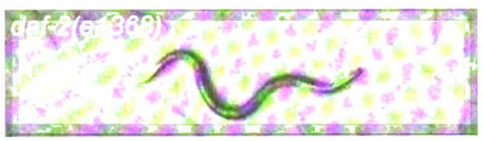

Control

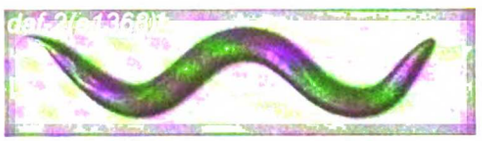

(25S)-Cholestenoic Acid

C

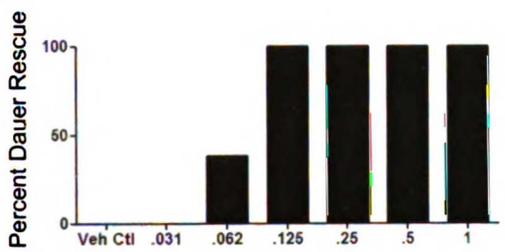

(25S)-Cholestenoic Acid (μM)

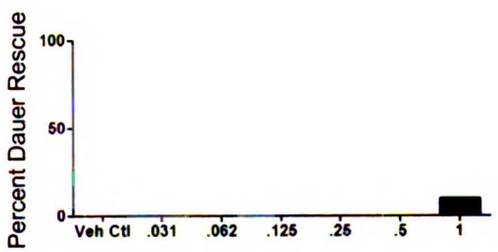

(25R)-Cholestenoic Acid (μM)

D

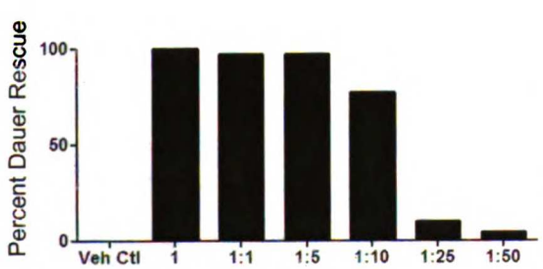

25S : 25R Ratio

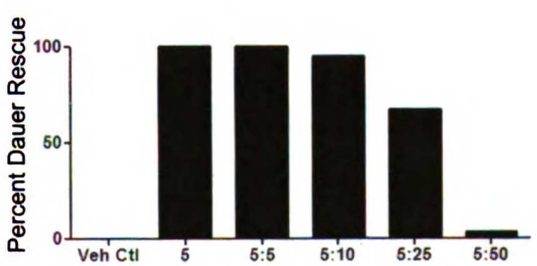

25S : 25R Ratio

Figure 4.2 (25S)-cholestenoic acid rescues the Daf-c phenotype of *daf-2(e1368)* but (25R)-cholestenoic acid does not. (A) Structure of (25S) and (25R)-cholestenoic acid. (B) Image of a *daf-2(e1368)* dauer control worm and a rescued *daf-2(e1368)* adult that was treated with 1 μM (25S)-cholestenoic acid from egg. (C) Dose response curves of (25S) and (25R)-cholestenoic acid rescue of *daf-2(e1328)* dauer formation. (D) Percent dauer rescue in *daf-2(e1368)* mutants in which increasing levels of the R stereoisomer are added to a set amount of (25S)-cholestenoic acid. Units correspond to μM and the ratios are in the form of S : R.

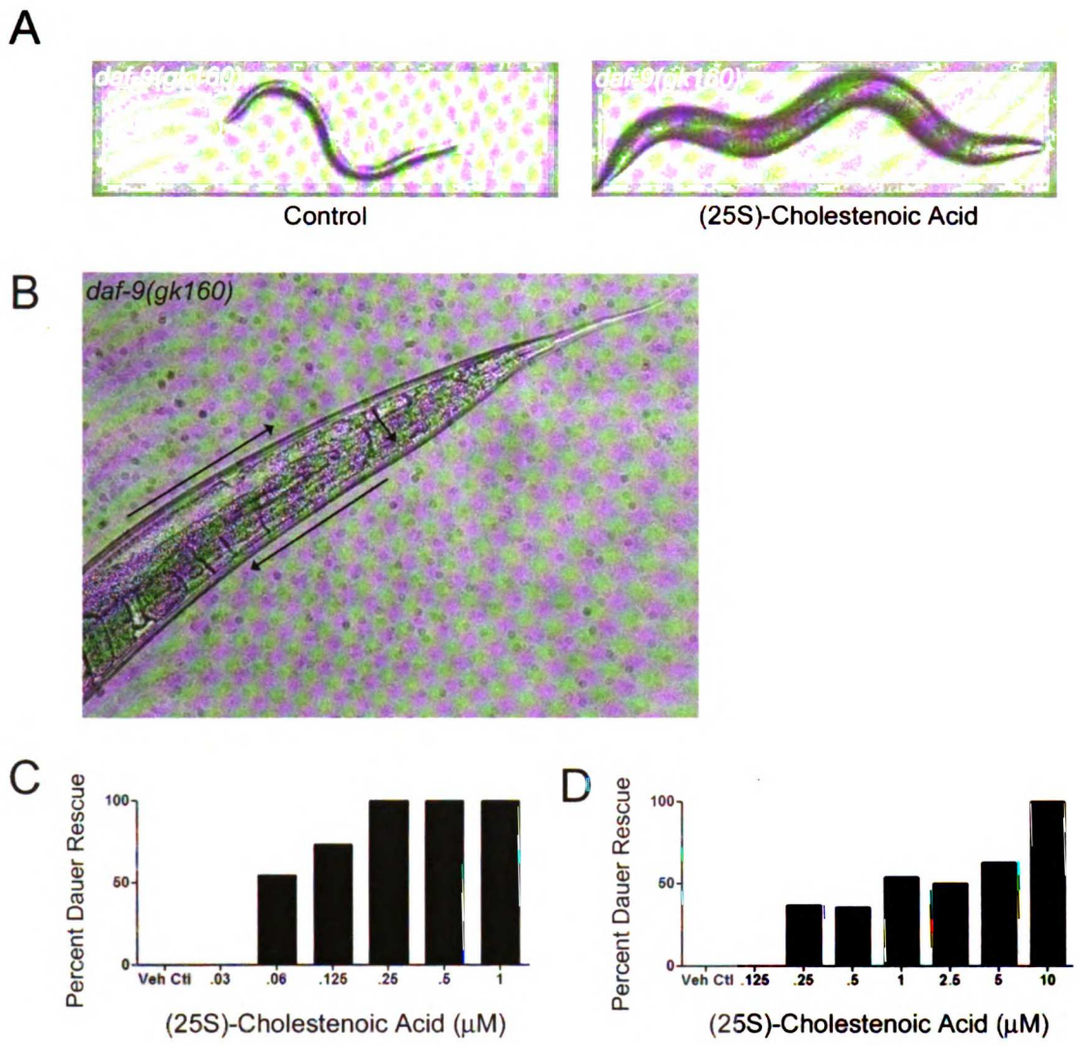

Figure 4.3 (25S)-cholestenoic acid rescues the Daf-c phenotype of *daf-9(gk160)*. (A) Image of a *daf-9(gk160)* control dauer and a treated *daf-9(gk160)* worm rescued to adult by 1 μM (25S)-cholestenoic acid from egg. (B) Reflexed gonad in a (25S)-cholestenoic acid-treated *daf-9(gk160)* worm. Arrows indicate the direction of cell migration during development. (C) Dose response curve of (25S)-cholestenoic acid rescue of the Daf-c phenotype of *daf-9(gk160)* mutants treated with (25S)-cholestenoic acid from egg and (D) after they arrest as partial dauers.

rescued to adult by (25S)-cholestenoic acid, the gonad was properly reflexed (Figure 4.3 B). A dose response curve determined that 50% of *daf-9(gk160)* dauers were rescued with approximately 100 nM (25S)-cholestenoic acid, about the same concentration that rescues *daf-2(e1368)* (Figure 4.3 C versus Figure 4.2 C). (25S)-cholestenoic acid even rescues *daf-9(gk160)* worms that have already become dauers, suggesting that DAF-12 is potentially involved in dauer exit as well (Figure 4.3 D). However, rescue from dauer is not as sensitive as treatment from egg.

(25S)-cholestenoic acid does not rescue the Daf-c phenotype of *daf-12(rh273)*

daf-12(rh273) is a mutation in H3 of the DAF-12 LBD that has been proposed to make the worm insensitive to the DAF-12 ligand. When *daf-12(rh273)* worms were treated with (25S)-cholestenoic acid doses up to 10 μM, rescue of dauer formation did not occur (Figure 4.4 A). Images of dauer *daf-12(rh273)* worms from control and (25S)-cholestenoic acid-treated conditions are shown in Figure 4.4 B. A portion of the *daf-12(rh273)* worms do spontaneously exit the dauer stage after several days, and when these worms become adults they have a gonadal migration defect (Antebi et al., 2000). Neither the control nor (25S)-cholestenoic acid-treated *daf-12(rh273)* adult worms have properly formed gonads (Figure 4.4 C). This is in contrast to the proper gonad formation in adult *daf-9(gk160)* worms treated with (25S)-cholestenoic mentioned previously (Figure 4.3 B).

A

B

C

Figure

migrati

2ES

2ES

2ES

he

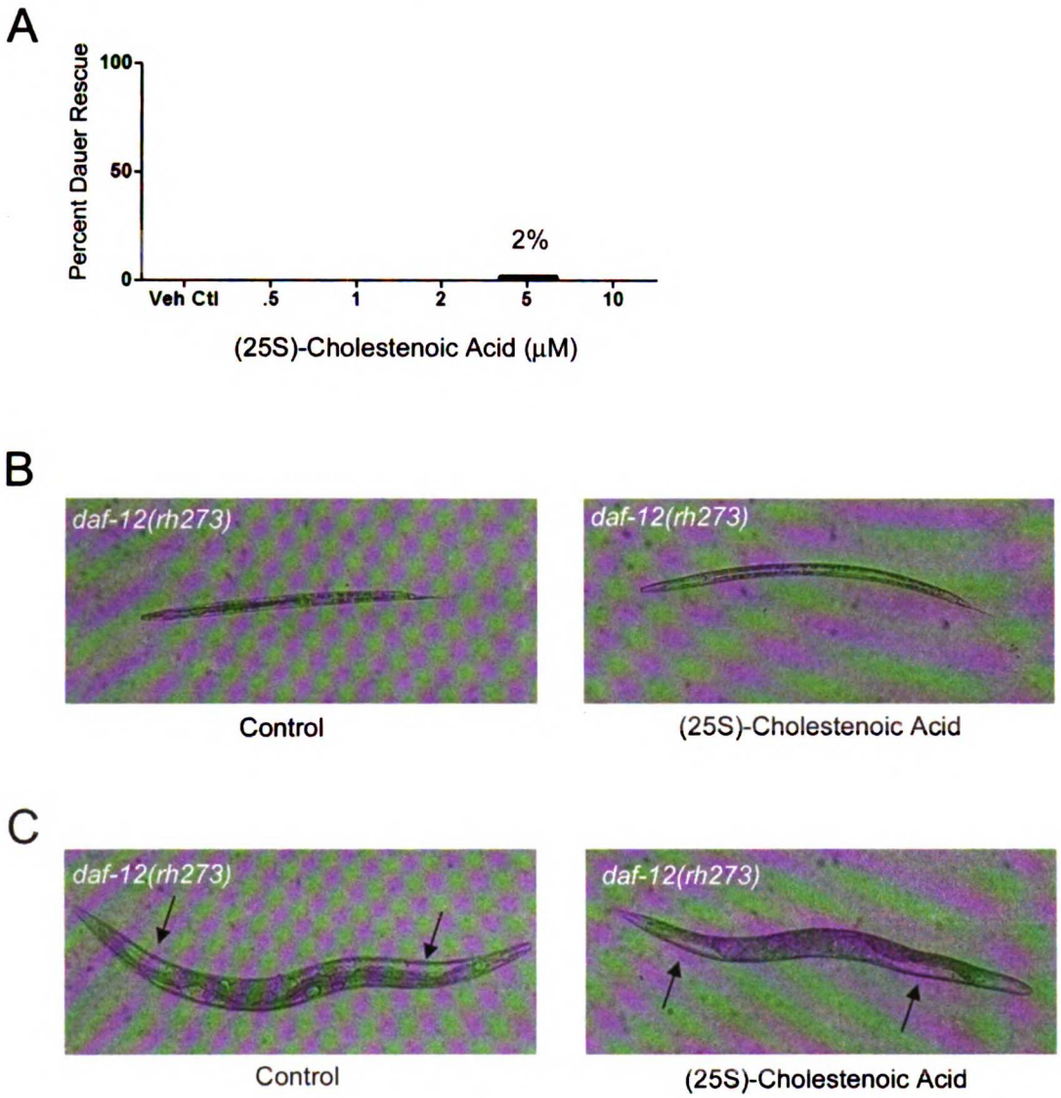

Figure 4.4 (25S)-cholestenoic acid does not rescue the Daf-c or gonad migration phenotype of *daf-12(rh273)* worms. (A) Dose response curve of (25S)-cholestenoic acid Daf-c rescue in *daf-12(rh273)*. (B) Images of control and (25S)-cholestenoic acid-treated *daf-12(rh273)* dauers. (C) Images of control and (25S)-cholestenoic acid-treated *daf-12(rh273)* adults. The arrows indicate where the gonad has failed to reflex and has migrated along the length of the body.

Bioactivity co-migrates with monohydroxylated bile acids in normal phase TLC

With a TLC methodology improved from that used in Figure 3.5, we tested if retention of bioactivity in the extract corresponded to a sterol acid with one, two, or three hydroxyl groups using normal phase TLC. Extract (2 g) was run in a lane alongside cholesterol, (25S)-cholestenoic acid (one hydroxyl), deoxycholic acid (two hydroxyls), and cholic acid (three hydroxyls) (Figure 4.5 A). *daf-2(e1368)* dauer-rescue bioactivity was found in the monohydroxylated bile acid section and supports cholestenoic acid as a bioactive component in worms (Figure 4.5 B, Section 3). Importantly, it also suggests that multiply hydroxylated bile acids are not bioactive since only the monohydroxylated section had bioactivity.

(25S)-cholestenoic acid elutes with the same retention as extract bioactivity in normal phase HPLC

The retention of (25S)-cholestenoic acid in normal phase HPLC was determined in order to see if it matched that of bioactivity from the extract. (25S)-cholestenoic acid elutes in normal phase HPLC at 22 minutes (Figure 4.6 A). This is also the point at which bioactivity comes off of the column when the (25S)-cholestenoic acid is run (Figure 4.6 B). Interestingly, this is also the same retention that extract bioactivity has using the same normal phase HPLC method, which further supports cholestenoic acid as a bioactive component in worms (Figure 2.6 C).

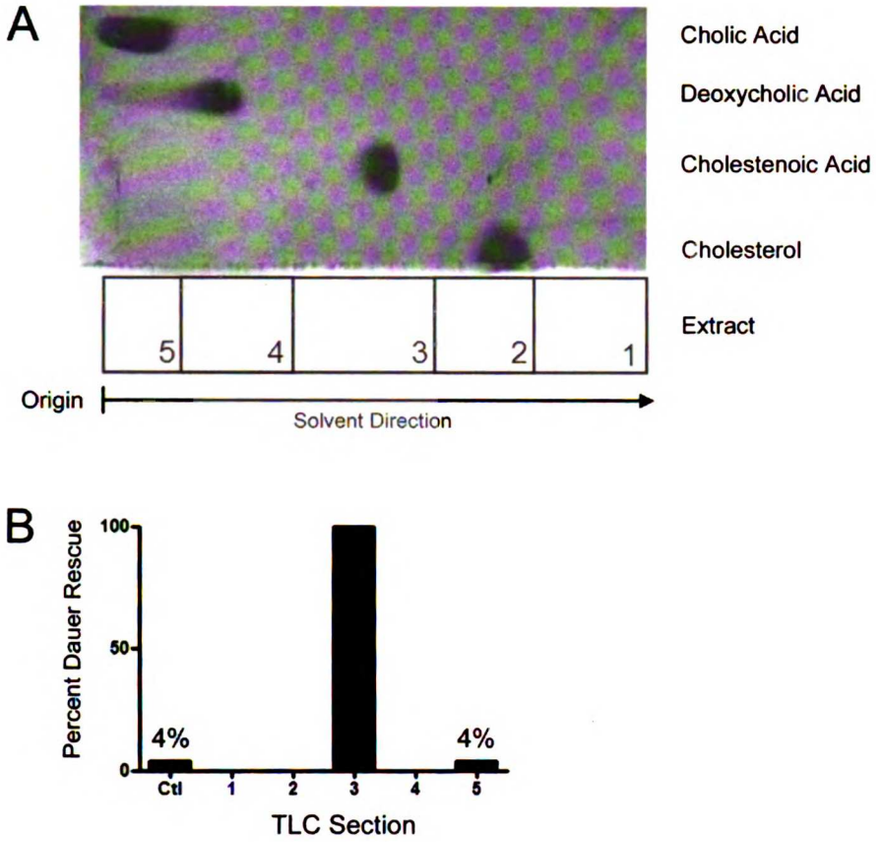

Figure 4.5 Normal phase TLC demonstrates that the bioactive component has a single hydroxyl. (A) Normal phase TLC fractionation of bile acid standards differing in the number of hydroxyls. Section 5 is the most polar and 1 is the least polar. A 2 g *daf-12(m20)* extract was run in a separate lane and sectioned based on the retention of standards. (B) Bioactivity corresponding to TLC sections in A.

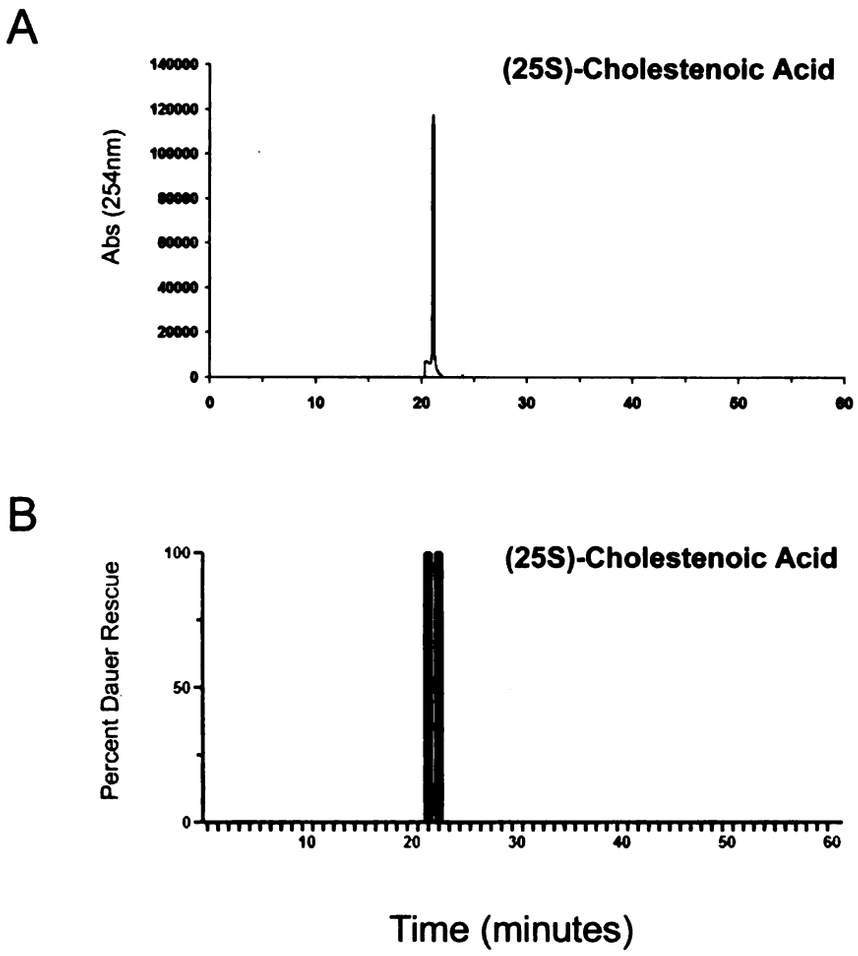

Figure 4.6 Normal phase HPLC of (25S)-cholestenoic acid standard.

(A) Chromatogram and (B) Bioassay of 1 minute normal phase HPLC fractions of 60 µg (25S)-cholestenoic acid.

(25S)-cholestenoic acid transactivates DAF-12 in a cell-based assay

In work by M. Gill, it was demonstrated that (25S)-cholestenoic acid can transactivate DAF-12 in a heterologous system using HEK293T cells. A DAF-12 LBD construct fused to the GAL4 DBD incubated with (25S)-cholestenoic acid resulted in a dose-dependent increase in luciferase expression via an upstream GAL4 response element (M. Gill). No change in luciferase was observed with the 25R stereoisomer (M. Gill). Co-incubation of the R and S isomers demonstrated that the (25S)-cholestenoic acid transactivation can be competed off by increasing levels of (25R)-cholestenoic acid much like what is seen *in vivo* in the dauer rescue bioassay (Figure 4.2 D) (M. Gill). Furthermore, no response was seen with either (25S) or (25R)-cholestenoic acid incubated with a mutant DAF-12 protein (R564H) from *daf-12(rh273)* which is predicted to be ligand-insensitive (M. Gill).

(25S)-cholestenoic acid reduces hypodermal DAF-9 expression

To determine if (25S)-cholestenoic acid can act *in vivo* to modulate the levels of DAF-9 via a feedback loop we treated N2 *dhIs64* worms with (25S)-cholestenoic acid. N2 dhIs64 is wild type strain with an integrated translational fusion of *daf-9* and *gfp* regulated by 7.16 kb of the genomic *daf-9* promoter (we will call this strain DAF-9::GFP) (Gerisch and Antebi, 2004). DAF-9 expression in the hypodermis, the syncitial epidermal tissue surrounding the worm, has been demonstrated to be regulated by environmental conditions and is highly expressed in L3 worms grown at 25°C (Gerisch and Antebi, 2004). We hypothesized that a DAF-12 ligand would act in a feedback loop to shut down DAF-9 hypodermal expression, so we grew DAF-9::GFP worms to L3 at 25°C with

different concentrations of (25S)-cholestenoic acid. Control worms had high hypodermal DAF-9 expression (Figure 4.7 A). DAF-9::GFP worms treated with a dose of 0.005 μM (25S)-cholestenoic acid, a dose that does not rescue the Daf-c phenotype of *daf-2(e1368)*, also had high hypodermal DAF-9 expression (Figure 4.7 B). Hypodermal DAF-9 expression is almost completely reduced with 0.5 μM (25S)-cholestenoic acid, a dose sufficient to rescue 100% of *daf-2(e1368)* dauers (Figure 4.7 C). Increasing the treatment of (25S)-cholestenoic acid to 5 μM completely reduces the level of DAF-9 hypodermal expression in DAF-9::GFP (Figure 4.7 D). In contrast to hypodermal expression, DAF-9 expression in the XXXL/R cells has been found to be insensitive to environmental changes (Gerisch and Antebi, 2004). Interestingly, we found that (25S)-cholestenoic acid also does not change the levels of DAF-9 expression in the XXXL/R cells (Figure 4.7 A-D). The exposure time in all pictures is the same.

(25S)-cholestenoic acid does not affect DAF-12 expression

DAF-12 is constitutively nuclear-localized except for during mitosis and, unlike DAF-9, no environmental factors have been demonstrated to modulate DAF-12 expression (Antebi et al., 1998). We wanted to test if (25S)-cholestenoic acid affected DAF-12 nuclear-localization, expression pattern, or abundance. We used the *daf-12(rh61rh411)* dhIs26 strain that is a DAF-12::GFP worm and expresses a translational fusion of *daf-12* and *gfp* with transcriptional regulation by the complete *daf-12* promoter (Antebi et al., 2000). Control L4 DAF-12::GFP worms have punctate, nuclear-localized DAF-12 that is expressed at fairly low levels throughout the body (Figure 4.8 A) (Antebi et al., 2000). Treatment with 5 μM (25S)-cholestenoic acid, a dose sufficient to rescue *daf-2(e1368)*

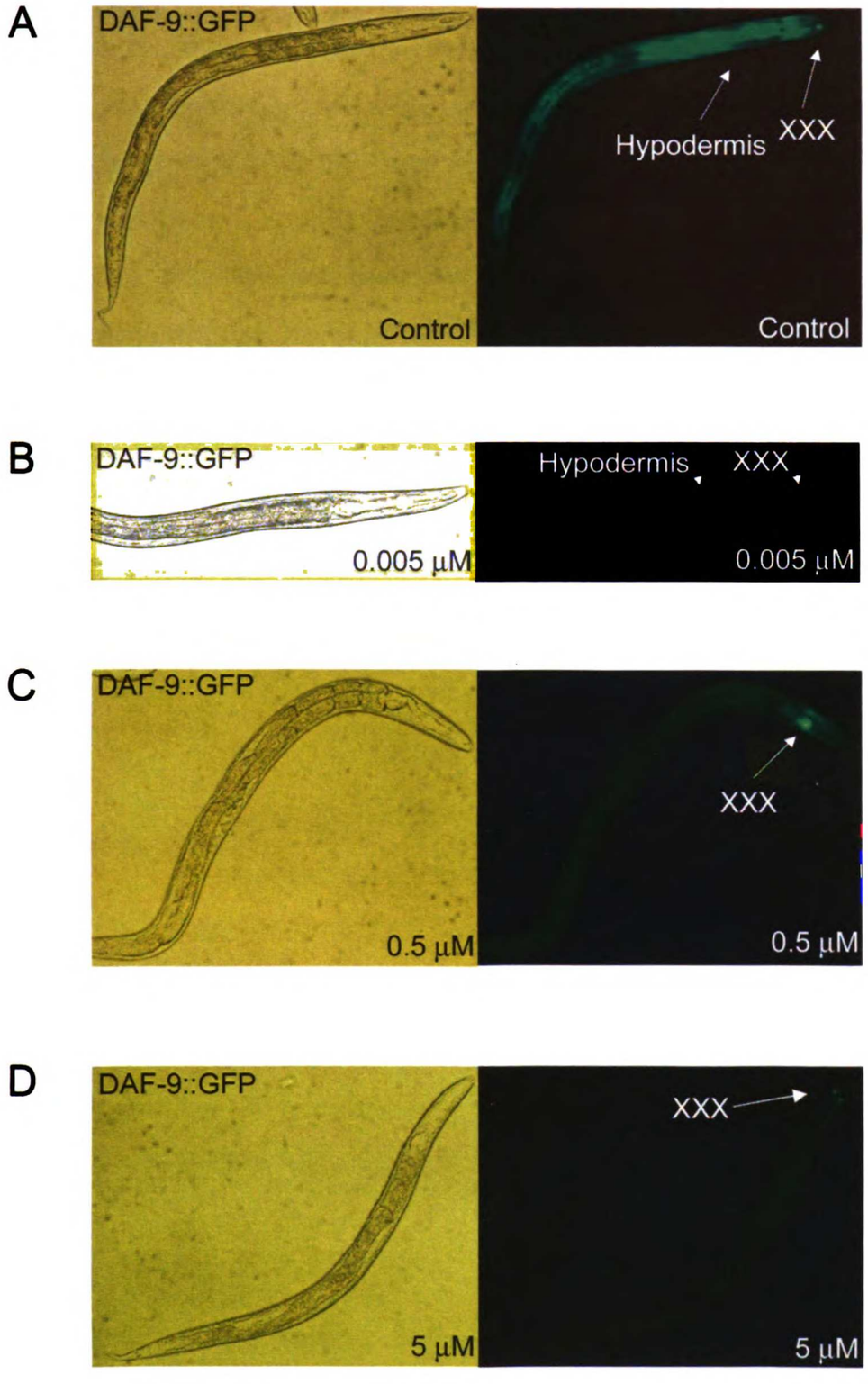
A
DAF-9::GFP
Control
Hypodermis
XXX
Control
B
DAF-9::GFP
0.005 µM
Hypodermis
XXX
0.005 µM
C
DAF-9::GFP
0.5 µM
XXX
0.5 µM
D
DAF-9::GFP
5 µM
XXX
5 µM

Figure 4.7 (25S)-cholestenoic acid reduces hypodermal expression of DAF-9. (A) Control L3 DAF-9::GFP worms at 25°C have high levels of expression of DAF-9. (B) L3 DAF-9::GFP worms exposed to 0.005 µM (25S)-cholestenoic acid, a sub dauer-rescuing dose, also have high levels of hypodermal DAF-9. (C) L3 DAF-9::GFP worms treated wth 0.5 µM (25S)-cholestenoic acid, a dauer-rescuing dose, have dramatically reduced hypodermal DAF-9 expression. (D) Increasing (25S)-cholestenoic acid levels to 5 µM reduces hypodermal DAF-9 expression completely. At all dose levels DAF-9 expression in XXXL/R cells is not affected in DAF-9::GFP worms (A-D).

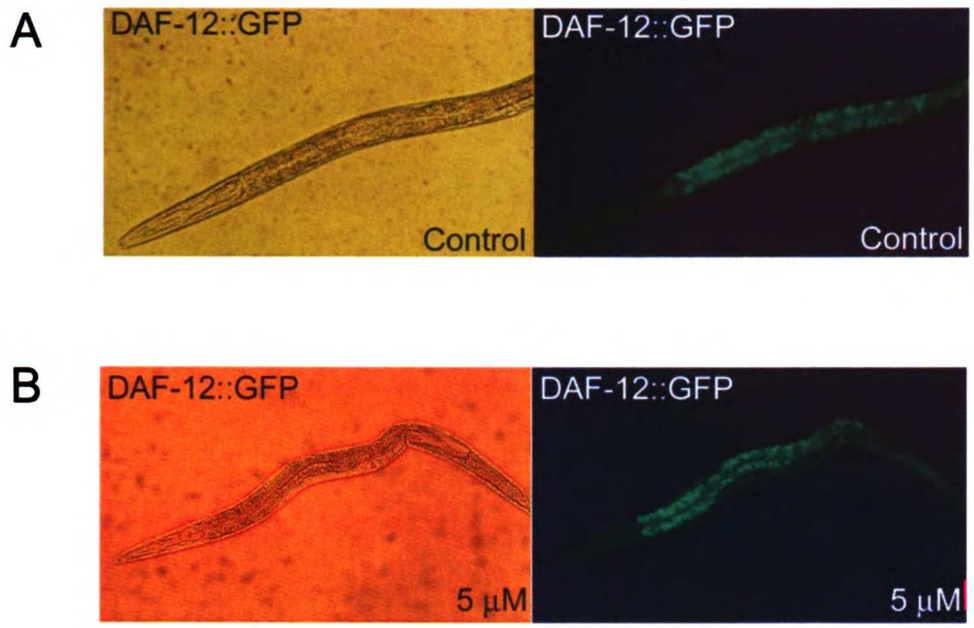

Figure 4.8 (25S)-cholestenoic acid does not affect DAF-12 expression. (A) A control L4 DAF-12::GFP worm with nuclear-localized DAF-12::GFP throughout the body. (B) A L4 DAF-12::GFP worm treated with 5 μM (25S)-cholestenoic acid also has nuclear-localized DAF-12 and has a similar DAF-12 expression pattern and abundance as control.

dauer formation, does not affect DAF-12 nuclear-localization, expression pattern, or abundance (Figure 4.8 B). Additionally, no change in DAF-12 expression was seen in L2 and L3 worms. The exposure time in all pictures is the same.

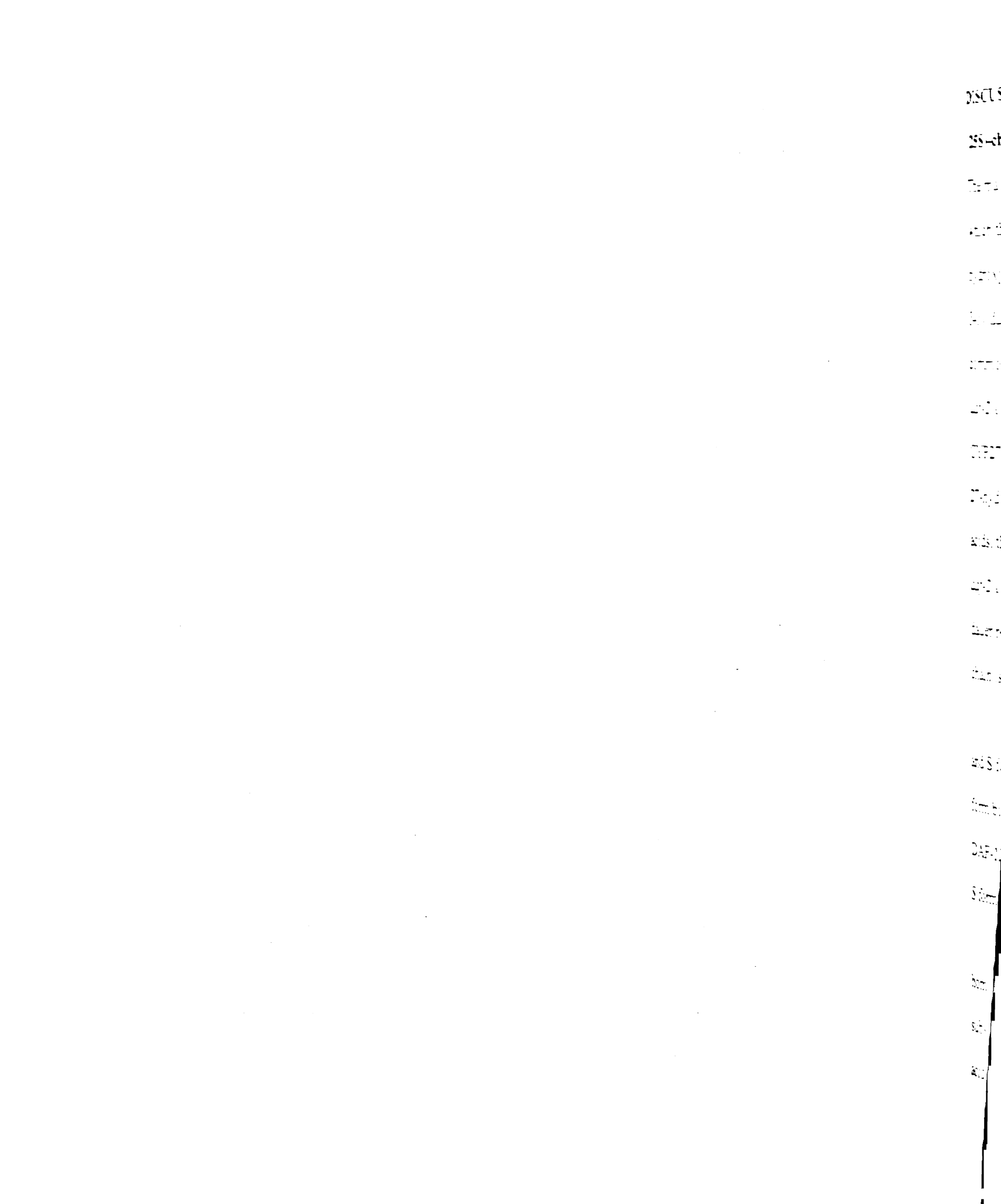

DISCUSSION

(25S)-cholestenoic acid rescues Daf-c phenotype of *daf-2(e1368)*

The major biosynthetic pathway of bile acids in mammals involves an acidic pathway in which the sterol backbone of cholesterol is initially modified into a saturated, multiply hydroxylated, C27 sterol acid. The side chain of most bile acids is then shortened via β-oxidation by three carbons to become a C24 bile acid (Chiang, 2002). We screened the common C24 bile acids and found that none were able to rescue dauer formation in *daf-2(e1368)* worms. A neutral mammalian bile acid biosynthetic pathway involves CYP27A1 directly converting cholesterol into Δ^5 cholestenoic acid with only 27-hydroxycholesterol as an intermediate (Chiang, 2002). In contrast to the C24 bile acids, the C27 bile acid (25S)-cholestenoic acid potently rescued dauer formation in *daf-2(e1368)* mutants. We found that the C24 bile acid Δ^5 cholenic acid had no effect on dauer rescue in *daf-2(e1368)* mutants (data not shown) suggesting that the extended alkyl chain is critical for DAF-12 binding.

The prevention of 25S dauer rescue by the 25R diastereomer suggests that the R and S form are both binding to the same location, likely DAF-12. Potentially when the R form binds DAF-12 it prevents the recruitment of the proper coactivators necessary for DAF-12 transactivation. In mammals the R diastereomer is much more prevalent than the S form (Javitt, 2002a).

Bile acid metabolism has not been investigated in *C. elegans* nor has a CYP27A1 homolog been identified. However, it is possible that *daf-9* might carboxylate a sterol substrate in worms in a manner similar to CYP27A1 to generate bioactive cholestenoic acid as a product. This would fit with the hypothesis that DAF-9 produces the DAF-12

ligand, and the direct conversion of a sterol to the DAF-12 ligand would explain why only a single cytochrome P450 has been found to play a role in dauer formation.

(25S)-cholestenoic acid rescues all non-*daf-12* Daf-c mutants

Based on dauer rescue, (25S)-cholestenoic acid fulfills the genetic criteria required for the activity of a DAF-12 ligand. Not only is (25S)-cholestenoic acid able to rescue *daf-2(e1368)* dauers, it can rescue the dauer phenotype of the homozygous *daf-9* knockout strain *daf-9(gk160)* that is predicted to not be able to produce the DAF-12 ligand. M. Gill extended the variety of Daf-c mutants that (25S)-cholestenoic acid is able to rescue and found that (25S)-cholestenoic acid prevents dauer formation in all non-*daf-12* Daf-c mutants tested. Furthermore, (25S)-cholestenoic acid is *daf-12*-dependent since it does not alter the phenotype of the *daf-12(rh273)* mutant that is predicted to be ligand-insensitive (Figure 4.5) (Antebi et al., 2000).

(25S)-cholestenoic acid acts *in vitro* and *in vivo* in a manner consistent with being a DAF-12 ligand

Biochemically, there are several interpretations of what defines a nuclear receptor ligand, including having a high binding affinity, generating ligand-dependent changes in coactivator recruitment, and transactivation of the nuclear receptor to modulate gene transcription in a cell-based reporter assay. Due to the difficulty in expressing recombinant DAF-12 protein for binding affinity or *in vitro* coactivator binding studies, M. Gill focused on a heterologous system to demonstrate (25S)-cholestenoic acid modulation of DAF-12 transactivation (M. Gill). Using a cell-based reporter assay,

M. Gill found that (25S)-cholestenoic acid is able to act as a DAF-12 ligand and transactivate DAF-12 to modulate gene expression.

One of the core regulatory elements of nuclear receptor signaling is feedback from the receptor to regulate the upstream enzymes involved in ligand metabolism. An increase in ligand levels usually causes a decrease in the expression or activity of the ligand metabolic enzymes. When DAF-9::GFP worms were treated with (25S)-cholestenoic acid, the level of DAF-9 in the hypodermis was dramatically suppressed suggesting that DAF-9 and DAF-12 are involved in a similar feedback loop (Figure 4.7). Levels of DAF-9 in the XXX cells did not change, however (Figure 4.7). These results parallel the modulation of hypodermal DAF-9 expression levels by environmental factors which, like (25S)-cholestenoic acid treatment, also fail to affect DAF-9 XXX expression (Gerisch and Antebi, 2004). It is unclear why DAF-9 is differentially regulated in these two regions; however, one potential hypothesis is that DAF-9 is metabolizing different substrates at the different locations. If DAF-9 is the worm equivalent of CYP27A1, a tonic level of bile acids may be produced in the XXX cells and thus DAF-9 needs to be expressed consistently. Under reproductive conditions in which the worm needs to maximize DAF-12 ligand production, DAF-9 is likely upregulated in the hypodermis in order to maximize metabolite output. This fits with mammalian data in which CYP27A1 uses different pools of cholesterol from different tissues (liver versus vascular endothelial cells and macrophages) as a regulatory mechanism (Javitt, 2000). The regulation of DAF-9 in different tissues will be an important avenue of future research, in particular how the three upstream dauer signaling pathways (insulin, TGFβ, and guanylate cyclase) are integrated at the level of DAF-9

(Figure 1.2). Understanding DAF-9 regulation should provide insight into why only one of these pathways, insulin signaling, plays a role in lifespan extension. *daf-9* itself plays a role in lifespan as well since *daf-9* mutants have extended longevity (Jia et al., 2002).

daf-9 C. elegans mutants may become a good model for the human disease cerebrotendinous xanthomatosis (CTX) which is caused by mutations in CYP27A1. CYP27A1 generates cholestenoic acid via the neutral pathway, and CTX patients have excessive cholesterol deposited in peripheral tissues (Setoguchi et al., 1974; Oftebro et al., 1980; Cali et al., 1991). Cholesterol localization and storage is easily studied in *C. elegans* and genetic screens could find additional genes regulating this disease (Matyash et al., 2001; Merris et al., 2003).

Comparison of ligand binding by DAF-12, LXR, and TR

Cholestenoic acid has been identified as one of several naturally occurring ligands for the mammalian LXR (Song and Liao, 2000), a nuclear receptor that is involved in cholesterol homeostasis. Based on sequence similarity, LXR is the closest mammalian homolog of DAF-12 (Mooijaart et al., 2005). Unlike LXR, which is known to bind several oxidized derivatives of cholesterol as well as carboxylated sterols (Janowski et al., 1996; Lehmann et al., 1997), DAF-12 likely only binds carboxylated molecules. This hypothesis is based on the fact that selective esterification of carboxyls in the extract completely abolished bioactivity. An oxysterol would not be modified by this procedure and should remain able to bind DAF-12 normally, retaining bioactivity after esterification. Additionally, though LXR and DAF-12 share cholestenoic acid as a ligand, the known LXR oxysterol ligands (22R), 25, and 27-hydroxycholesterol (Janowski et al., 1996) do not rescue dauer

formation in *daf-2(e1368)* (data not shown). Further support for the importance of a carboxyl to DAF-12 binding is that DAF-12 H5 residue R598 is a conserved residue in the bile acid receptor FXR (R328) that hydrogen bonds with the carboxyl group of bile acids (Mi et al., 2003). R598 is also conserved in TRβ (R316) which interacts with the carboxyl group of the TR ligand T_3 (Wagner et al., 1995). For an alignment of DAF-12 with other nuclear receptors based on Mooijaart *et al.* (2005), see Appendix A.

Specificity of DAF-12 for a carboxylated ligand is likely important to the Daf-c phenotype of *daf-12* mutants. The only two Daf-c *daf-12* mutants cloned have a single amino acid change in R564 to either a Cys [*daf-12(rh274)*] or a His [*daf-12(rh273)*] (Antebi et al., 2000). This DAF-12 residue in LBD H3 was shown to be conserved in the TR which utilizes the analogous Arg (R228 in rodent TRα and R282 in human TRβ) as a hydrogen bond donor to the carboxylate group of the TR ligand T_3 (Wagner et al., 1995). It is likely that this Arg, along with R598, makes critical hydrogen bonding contact with the carboxyl of (25S)-cholestenoic acid much like TR (Wagner et al., 1995). Modification of Arg to either a Cys or His, which do not hydrogen bond, likely prevents this interaction and makes DAF-12 ligand-insensitive. This explains why *daf-12(rh273)* is unresponsive to (25S)-cholestenoic acid. Notably, the DAF-12 R564 residue is spatially close to a conserved H5 Arg in LXR (R319 in LXRβ and R305 in LXRα) which hydrogen bonds with the 3-position hydroxyl of LXR ligands (Williams et al., 2003; Farnegardh et al., 2003; Hoerer et al., 2003; Svensson et al., 2003). This Arg is conserved in DAF-12 (R602) which supports the fact that (25S)-cholestenoic acid has a 3-position hydroxyl. This also fits with the data that acetylation of hydroxyls prevents the bioactivity of extracts.

Not only does DAF-12 have a similar ligand to LXR, it also likely shares the same mechanism of ligand activation. DAF-12 has an aromatic residue in H12 (F750) that is conserved in FXR (W469), LXRα (W442), LXRβ (W457), and the vitamin D receptor (F423). This aromatic residue has been shown to be involved in a π-cation interaction that acts as a ligand-dependent switch that is absolutely critical for H12 activation of the receptor. Homology of DAF-12 (F750) with these residues suggests that DAF-12 is also activated using a π-cation switch (Mi et al., 2003). Utilizing (25S)-cholestenoic acid will help further our biophysical understanding of DAF-12 activation.

How many DAF-12 ligands are there?

The importance of DAF-12 to the diverse phenotypes of dauer formation, gonad formation, and lifespan has made it unclear whether one ligand is sufficient to achieve appropriate DAF-12 regulation. Nuclear receptors often bind several ligands and it is possible that each ligand may selectively modulate different phenotypes suggesting that DAF-12 may require more than one ligand for complete regulation (Katzenellenbogen et al., 1996; Katzenellenbogen et al., 2000). Dauer formation regulation occurs at L2, gonad formation occurs at L3, and lifespan regulation most likely occurs in the young adult worm (Antebi et al., 1998; Antebi et al., 2000; Dillin et al., 2002). Since the developmental age at which DAF-12 plays a role in each phenotype is different, a different ligand could potentially be produced at each different developmental stage to drive transcription of phenotype specific target genes. For example, dauer related genes could be turned on at L2 and gonad migration genes at L3. We have, however,

demonstrated that (25S)-cholestenoic acid is at least sufficient to rescue both the dauer formation and gonad migration phenotypes suggesting that perhaps only a single ligand is necessary to activate DAF-12. However, additional experiments will be needed to determine the effect of (25S)-cholestenoic acid on lifespan determination.

Is (25S)-cholestenoic acid present in bioactive extracts?

The question that remains is whether (25S)-cholestenoic acid or related structures exist in *C. elegans*. We found cholestenoic acid in a screen of compounds and it may be of little to no relevance to *C. elegans* physiology. However, even if it is not present in worms, (25S)-cholestenoic acid will be a useful tool to understand DAF-12 biology. Support for (25S)-cholestenoic acid as a bioactive component in the extract comes from the similarity between its chemical traits and the bioactive component based on chemical analysis. For example, (25S)-cholestenoic acid has both a carboxyl and a hydroxyl group. We predicted that the bioactive component of the extract had a carboxyl and a hydroxyl moiety based on the loss of bioactivity after selective derivatization of these functional groups. Secondly, (25S)-cholestenoic acid has the same retention in both normal phase TLC and HPLC as the bioactive component. Pharmacological evidence supports (25S)-cholestenoic acid as a bioactive component as well since it transactivates DAF-12 *in vitro*. Furthermore, (25S)-cholestenoic acid modulates DAF-9 levels in the worm, suggesting that it activates DAF-12 *in vivo* and triggers a conserved nuclear receptor feedback loop regulating upstream metabolic enzymes. These pieces of evidence prompted us to focus on detecting (25S)-cholestenoic acid or related structures in bioactive *C. elegans* extracts using GC-MS.

MATERIALS AND METHODS

Materials

Sodium azide (#S8032), cholic acid (#C-1129), chenodeoxycholic acid (#C-9377), deoxycholic acid (#D-2510), and lithocholic acid (#L-6250) were purchased from Sigma (St. Louis, MO). 22R-hydroxycholesterol (#1114-3), 25-hydroxycholesterol (#1116-3), and 27-hydroxycholesterol (11160-3) were purchased from Research Plus (Manasquan, NJ). (25S)-cholestenoic acid (#C6787-000), (25R)-cholestenoic acid (#C6786-000), and Δ^5 cholenic acid (#C2450-000) were purchased from Steraloids (Newport, RI).

C. elegans strains

The following nematode strains used in this work were provided by the *Caenorhabditis* Genetics Center, which is funded by the NIH National Center for Research Resources (NCRR): Bristol N2 (wild type), DR1572[*daf-2(e1368) III*], VC305*[+/szT1[lon-2(e678)] I; daf-9(gk160)/szT1 X*], DR20[*daf-12(m20) X*], AA87[*daf-12(rh273) X*]. GL216[*daf-9(gk160) daf-12(m20) X*]. AA277, *dhIs64*[*daf-9::gfp lin15(+)) I*], AA120, *dhIs26*[*daf-12::gfp lin15(+)) I*].

Dauer rescue bioassay using bile acids and oxysterols

Our bioassay was developed by M. Gill. For routine culture worms were maintained at 20°C on 5 cm nematode growth medium (NGM) agar plates with a lawn of *E. coli* OP50. Bile acids and oxysterols were resuspended in ethanol. For dauer assays, 15 µL of a stock solution was added to 185 µL S-basal before being spotted onto a 3 cm petri dish containing 3 mL NGM and 50 µL *E. coli*. The S-basal was allowed to cover the whole

surface of the plate and was left for 1 hr prior to adding worms. The plates were then placed in an incubator at 25°C to generate dauers. Plates were scored for the number of dauer, L3/L4/young adult, and gravid adult worms after 72 hr. All worms that were scored as in the L3 stage or beyond were scored as rescued for the figures in this chapter.

Normal phase TLC of bile acids

The procedure is the same as described in Chapter 3 except that the TLC plate was heated to 150°C for at least 1 hr prior to chromatography in order to completely dry it out. Secondly plates were resolved with toluene:acetic acid:water 5:5:1.2 (v:v:v) in order to separate bile acids (Cazon Narvaez and Suhring, 1999). Plates were visualized with phosphomolybdic acid and bioactivity was extracted as in Chapter 3.

Normal phase HPLC

Performed as in Chapter 2.

DAF-9::GFP analysis

A synchronous population of AA277 DAF-9::GFP worms was generated by leaving several gravid DAF-9::GFP adults to lay eggs on a 3 cm NGM plate for 3 hr. The plates were then placed in a 25°C incubator. Cholestenoic acid treatment was the same as used for the dauer rescue bioassay described above. Worms were removed after approximately 30 hr when all the worms were L3. Worms were picked onto a microscope slide into 15 μL of S-basal plus 10 mM sodium azide and imaged. GFP exposure time for all images was 200 msec.

DAF-12::GFP analysis

A synchronous population of AA120 DAF-12::GFP worms was generated by leaving several gravid DAF-9::GFP adults to lay eggs on a 3 cm NGM plate for 3 hr. The plates were then placed in a 20°C incubator. Cholestenoic acid treatment was the same as used for the dauer rescue bioassay described above. Worms were removed after approximately 35 hr after the worms were L2, 48 hr when the worms were L3, and 60 hr when all the worms were L4. Worms were picked onto a microscope slide into 15 μL of S-basal plus 10 mM sodium azide and imaged. GFP exposure time for all images was 200 msec.

DAF-12 alignment

We attempted to reproduce the alignment of DAF-12 with other nuclear receptors by Mooijaart *et al.* (2005) (Appendix A). The protein sequences were the same as listed in their publication. We used the default ClustalW parameters (www.ebi.ac.uk/clustalw) except that we selected the blosum matrix, a gap open penalty of 10, and a gap extension penalty of 2.5.

CHAPTER V

Identification of cholestenoic acid regioisomers in *C. elegans* extracts

ABSTRACT

Since (25S)-cholestenoic acid was characterized as a DAF-12 ligand that also rescues dauer formation, we used GC-MS to find cholestenoic acid and cholestenoic acid-like molecules in bioactive *C. elegans* extracts. Methyl-ester TMS-ether derivatives of several regioisomers of cholestenoic acid were detected in L3/4 *daf-12(m20)* bioactive extracts. These isomers all share the major fragmentation ions characteristic of monohydroxylated, monounsaturated C27 bile acids; however, they likely differ in the position of their double bond. Extracts from L3/4 *daf-9(gk160) daf-12(m20)* worms had no trace of these cholestenoic acids, supporting the role of DAF-9 in carboxylating sterols into cholestenoic acids. We quantified the levels of the cholestenoic acids in bioactive extracts and found that they range from 50 to 650 pg per gram of worm starting material and have significant extract to extract variability. We also used HPLC fractionation to determine which cholestenoic acid regioisomer likely has the most potent bioactivity. Finally, a preliminary analysis of extracts from N2 worms reveals that N2 also contains cholestenoic acid regioisomers.

INTRODUCTION

Bile acids in insects

Little is known about bile acid metabolism in *C. elegans*; however, other insects are known to have bile acid systems (Lafont et al., 1983). For example, although the common mammalian bile acids have not been identified in *Drosophila*, carboxylated metabolites of ecdysone at the 27-position have been identified and are known as ecdysonoic and 20-hydroxyecdysonoic acid (Grau and Lafont, 1994). These compounds have also been identified in the desert locust *Schistocera gregaria* (Isaac et al., 1983; Isaac and Rees, 1984) and the freshwater prawn *Macrobrachium rosenbergii*, and ecdysonoic acid has been found in the nematode *Ascaris suum* (O'Hanlon et al., 1991). Other ecdysteroid 27-oic acids have also been identified in insects, including 25-deoxy-20-hydroxyecdysonoic acid in the crab *Carcinus maenas* (Lachaise and Lafont, 1984) and 3-epi-20-hydroxyecdysonoic acid in the tobacco hornworm *Manduca sexta* (Thompson et al., 1988). Interestingly, these ecdysteroid 27-oic acids have been found to be induced by both ecdysone and an ecdysteroid agonist in the cotton leafworm *Spodoptera littoralis* establishing that an inactivation pathway for ecdysones parallels the role of bile acids in mammals in removing excess cholesterol (Chen et al., 1994).

There is little evidence that *C. elegans* uses bile acids. Since *C. elegans* does not have an ecdysteroid system, it is unlikely that it produces ecdysonoic acids. Furthermore, neither bile acids nor the hydroxy sterols that are mammalian bile acid precursors have been identified in worms. Furthermore, of the 83 putative P450 genes in the genome of *C. elegans*, none are predicted to be homologs of the key mammalian bile acid synthesizing enzymes CYP7A1 or CYP27A1 (Nelson, 1998; Nelson, 1999). The key

enzyme to carboxylate sterols into bile acids, CYP27A1, is a mitochondrial P450 in mammals yet worms are thought to have no mitochondrial P450s (Nelson, 1998).

One piece of evidence that does support bile acids in *C. elegans* is that a Type II 3-oxoacyl-CoA thiolase has been identified in *C. elegans* that is similar to the mammalian SCPx (Bun-Ya et al., 1997). 3-oxoacyl-CoA thiolases are the final enzyme in the bile acid β-oxidation pathway and shortens the bile acid side chain by 3 carbons (Hashimoto, 1999). Termed P-44, this protein is expressed in *C. elegans* in all developmental stages and is in many tissues, with the highest expression in the intestine (Bun-Ya et al., 2000). P-44 lacks the SCP2 domain which targets its mammalian homolog to the peroxisome; however, *in vitro* experiments did demonstrate that P-44 has thiolase activity and shortens the carbon chain of a bile acid precursor (Bun-Ya et al., 1997; Maebuchi et al., 1999).

Bile acid analysis

There are three cholestenoic acids present in human circulation at significant concentrations (40-80 ng/mL): 3β-hydroxy-5-cholestenoic acid ("cholestenoic acid"), 3β,7α-dihydroxy-5-cholestenoic acid, and 7α-hydroxy-3-oxo-4-cholestenoic acid (Meaney et al., 2003). We want to be able to detect these and any potential novel forms of cholestenoic acids that might be present in *C. elegans* such as a 4-methyl cholestenoic acid. Existing analytical methods for identification and quantification of bile acids have their advantages and disadvantages. HPLC with UV or fluorescence detection does not permit conclusive identification because of the complexity of the matrix and poor sensitivity (Scalia, 1995). HPLC coupled with radioimmunoassay, while very sensitive

and specific, is limited to a subset of bile acids that bind to currently available antisera (Street et al., 1983). Although nuclear magnetic resonance (NMR) spectroscopy can provide definitive structural data, it lacks sufficient sensitivity and requires isolation and purification of large amounts of starting material, making it impractical as a trace analytical technique.

Bile acids are routinely analyzed by GC-MS since the high resolution of gas chromatography resolves complex mixtures well and the sensitivity of electron impact ionization mass spectrometry is typically in the nanogram to sub nanogram range. Thus it is a technique uniquely suited to trace level analysis in complex mixtures. Other mass spectrometric options for the analysis of bile acids include matrix-assisted laser desorption ionization (MALDI) (Mims and Hercules, 2003; Mims and Hercules, 2004), electrospray ionization (ESI) (Yang et al., 1997; Perwaiz et al., 2001) including MS/MS (Eckers et al., 1990; Lemonde et al., 1999; Griffiths, 2003), and atmospheric pressure chemical ionization (APCI) (Goto et al., 1998). GC-MS is the most commonly used of these mass spectrometry techniques and is unique since it is both extremely sensitive and provides some structural information about the compounds that are analyzed.

Derivatization for GC-MS analysis

In order to use GC-MS to detect polar compounds such as cholestenoic acid, the analytes must initially be derivatized in order to make them volatile. Active hydrogens on polar heteroatoms cause strong intermolecular interactions, usually caused by hydrogen bonding, which makes the analytes involatile. We initially used trimethylsilylation (TMS) alone as a derivatization strategy since it technically derivatizes all potential polar

hydrogens. However, TMS derivatization is not ideal for some functional groups such as carboxyls and often does not allow for the sensitivity required to find trace level analytes (Batta and Salen, 1999). By previously characterizing derivatization procedures that affect the extract in Chapter 3 we have a variety of potential derivatization strategies already established. Secondly, unlike when we were screening HPLC fractions in Chapter 2, we now have (25S)-cholestenoic acid as a target analyte. Cholestenoic acid is commercially available as a standard so we can optimize its sample preparation and detection to push the limits of sensitivity for detection of cholestenoic acid and cholestenoic acid-like molecules in extracts from *C. elegans*. GC-MS of most bile acids, including previous analysis of cholestenoic acid in the literature, uses a double derivatization protocol. First carboxyls are methyl-esterified and then the hydroxyls are silylated (Eneroth et al., 1966; Szczepanik et al., 1976; Setchell et al., 1983; Axelson et al., 1988; Ichimiya et al., 1991; Axelson et al., 1991; Toll et al., 1992; Shoda et al., 1993; Pikuleva et al., 1998).

GC-MS ionization and fragmentation

An advantage of the electron impact (EI) ionization of GC-MS is that it provides a fragmentation fingerprint that is often unique to a particular analyte and can be searched against a database of known EI spectra (Ryhage and stenhagen, 1960). We used the NIST 2002 and Wiley 7.0 databases with 440,000 reference spectra. EI ionization and fragmentation occur when an electron at 70 electron volts strikes a neutral analyte, knocking out a second electron. This creates what is known as a molecular ion ($M^{+\cdot}$): the ion that corresponds to the entire compound. Additional energy from the electron impact

is internalized via a series of vibrations, rotations, and molecular rearrangements which results in fragmentation. The mass analyzer, in our case an ion trap, distinguishes analytes by measuring the mass-to-charge ratio (*m/z*). The spectrum is a readout of the number of ions (counts) at each *m/z* in the mass analyzer at a given time. Two types of chromatograms can be generated from this data: a total ion current (TIC) chromatogram is the total number of counts detected over time and corresponds to the overall level of material being analyzed at a given time; an extracted ion current (XIC) chromatogram is the number of counts for a selected *m/z* over time.

Bile acid fragmentation

The fragmentation of the methyl-ester TMS-ether cholestenoic acid derivative is published and its levels have been analyzed in several bile acid metabolic disorders (Parmentier et al., 1979; Axelson et al., 1988; Axelson et al., 1989a; Axelson et al., 1989b; Setchell et al., 1998). The mechanisms for the formation of fragment ions are quite well defined, largely by the work of Carl Djerassi (Diekman and Djerassi, 1967; Eadon et al., 1972; Popov et al., 1976; Partridge and Djerassi, 1977; Partridge et al., 1977), Arnis Kuksis (Child and Kuksis, 1979; Child et al., 1979a; Child et al., 1979b; Kuksis and Child, 1980), and others (Galli and Maroni, 1967; Mammato and Eadon, 1975; Knapp, Jr. and Schroepfer, Jr., 1976; Knapp et al., 1976; Wyllie et al., 1977; Pelillo et al., 2000). Understanding the mechanism that generates fragment ions should help to understand related unknown structures if found. For example, worms may have a 4-methylated version of cholestenoic acid, or one that is hydroxylated in an unusual position.

Sample preparation

For analysis of *C. elegans* extracts, ether extracts were made which was followed by aminopropyl SPE. The aminopropyl SPE carboxyl-containing fraction was collected and a portion was bioassayed to determine bioactivity level. The rest of the sample was then derivatized and analyzed by GC-MS. In a few cases as noted, normal phase HPLC was used to provide an additional level of separation after aminopropyl SPE.

RESULTS

GC-MS analysis of different (25S)-cholestenoic acid derivatives

To find the best derivatization protocol for (25S)-cholestenoic acid, we tested three different derivatization protocols including TMS-ester TMS-ether, methyl-ester acetate, and methyl-ester TMS-ether. All three generated analytes with easily interpretable spectra (Figure 5.1 A-C). TMS alone was tried (Figure 5.1 A), which has the advantage that it does not require an extraction step which should minimize sample loss. However, the signal from 100 ng silylated cholestenoic acid was barely detectable (data not shown). This is likely due to the poor GC-MS response of the TMS-ester formed by the silylation of the carboxyl group (Batta and Salen, 1999). Esterifying the carboxyl of cholestenoic acid and then acetylating the hydroxyl (Figure 5.1 B) has the advantage that the derivatized product is very stable relative to silylation derivatives, and is often the preferred derivatization method for analysis of synthetic derivatives of bile acids (Child et al., 1979a; Kuksis and Child, 1980). This method easily detected 5 ng or more of cholestenoic acid (data not shown). However, when the methyl-ester acetate derivative was compared to signal from the same amount of methyl-ester TMS-ether cholestenoic acid derivative (Figure 5.1 C), it was clear that the methyl-ester TMS-ether signal was at least five times as sensitive (data not shown). Since cholestenoic acid will be at trace levels, sensitivity is of paramount importance and our data confirm that the previously published protocol analyzing a methyl-ester TMS-ether cholestenoic acid derivative is best. In addition, the confirmation of the molecular weight of an unknown by the presence of the molecular ion in the spectra is an important piece of evidence. This also supports using the methyl-ester TMS-ether derivatization procedure since this derivative

A **Cholestenoic Acid - TMS-ester TMS-ether**

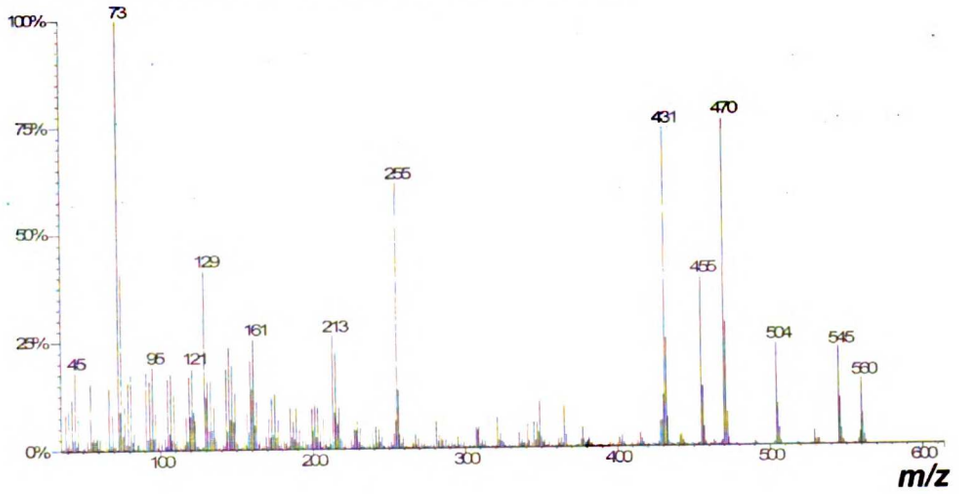

B **Cholestenoic Acid - Methyl-ester Acetate**

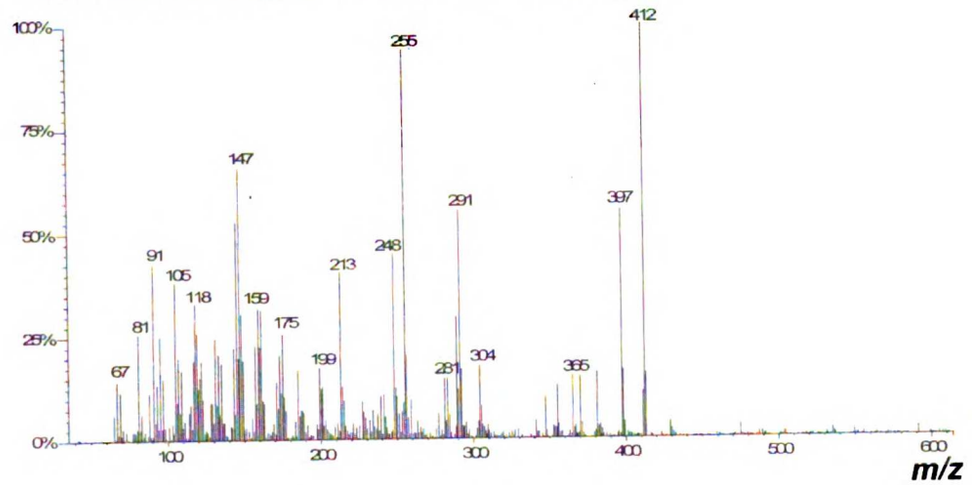

C **Cholestenoic Acid - Methyl-ester TMS-ether**

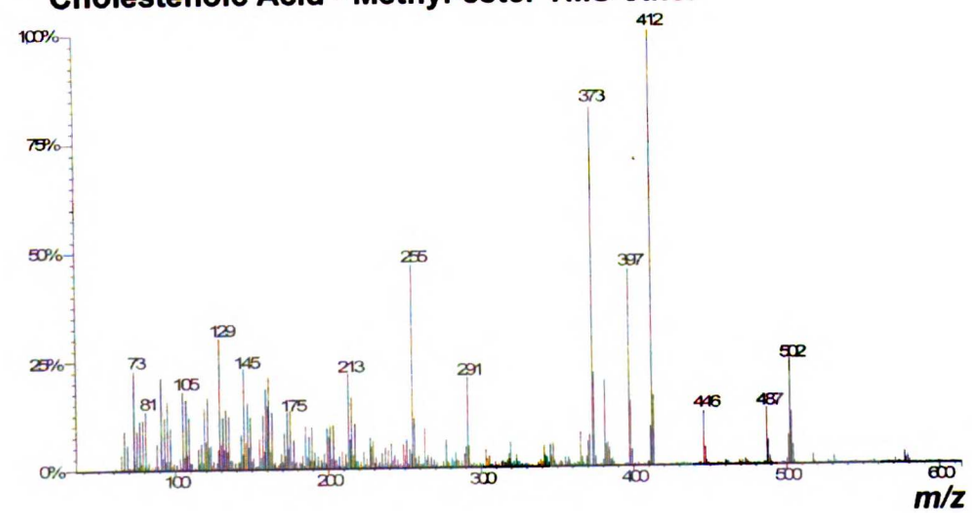

Figure 5.1 GC-MS spectra of different (25S)-cholestenoic acid derivatives. Spectrum of a (A) TMS-ester TMS-ether cholestenoic acid derivative, (B) Methyl-ester acetate cholestenoic acid derivative, and (C) Methyl-ester TMS-ether cholestenoic acid derivative.

has a significant abundance of the molecular ion (*m/z* 502, Figure 5.1 C) whereas the methyl-ester acetate has very little molecular ion (*m/z* 472, Figure 5.1 B).

Interpretation of methyl-ester TMS-ether (25S)-cholestenoic acid derivative spectrum

Examining the spectrum of the methyl-ester TMS-ether cholestenoic acid derivative revealed that the spectrum was very similar to the published spectra (Figure 5.2 A) (Setchell et al., 1998). The major fragment ions correspond to the molecular ion at *m/z* 502, loss of a trimethylsilanol (TMSO) group leading to *m/z* 412, and major ions at *m/z* 446, *m/z* 373, and *m/z* 129 which are characteristic of a 3-trimethylsiloxy-Δ^5 structure (Figure 5.2 B). The ion at *m/z* 255 represents the monounsaturated nuclear ring structure remaining after loss of both the TMSO and side chain and the *m/z* 291 ion is a fragment that contains the side chain along with the C and D rings (Figure 5.2 B). Additional structures representing more minor fragments are shown in Figure 5.2 B.

GC-MS of aminopropyl fractionated extracts

The carboxyl-containing fraction of bioactive *daf-12(m20)* extracts was analyzed by GC-MS after esterification/silylation and compared to extracts from *daf-9(gk160) daf-12(m20).* The TIC of three separate extracts is compared in Figure 5.3; panels A-C correspond to *daf-12(m20)* extracts and panels D-F correspond to *daf-9(gk160) daf-12(m20)* extracts. A and D are extracts made in parallel, as were B and E, and C and F. The extracts are poorly reproducible between biological replicates, which is likely related to the known variability of sterol content in worms (Merris et al., 2004). However, there

A

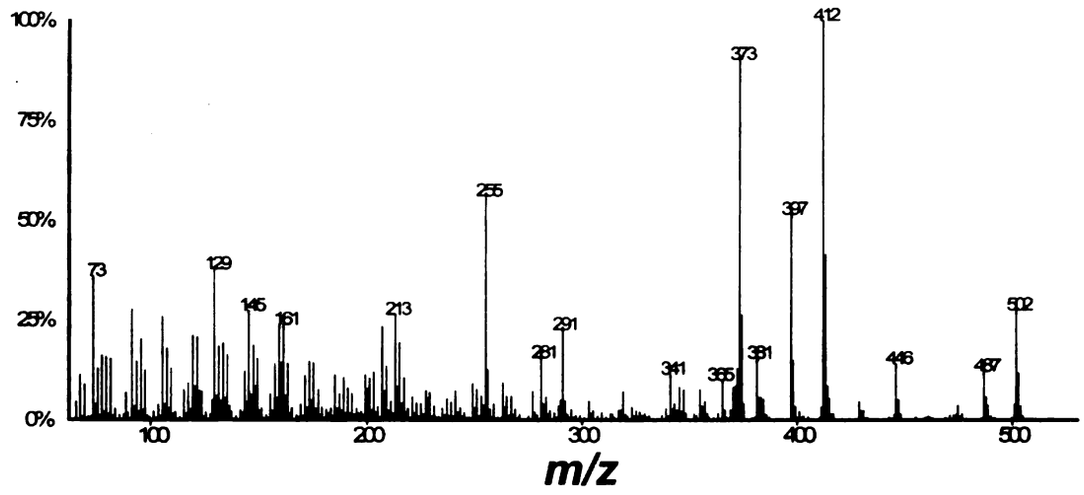

B

m/z	Fragment	Description	Structure
502	M ($M^{+\cdot}$)	Molecular ion	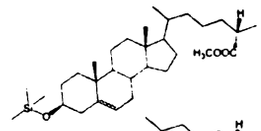
487	M - 15	M - CH_3	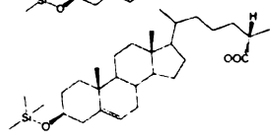
446*	M - 56	M - C2,C3 w/ TMS to C6	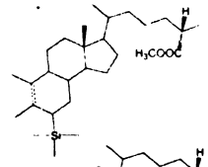
412	M - 90	M - TMSOH	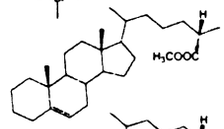
397	M - 90 - 15	M - TMSOH - CH_3	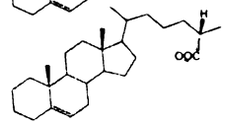
373*	M - 129	M - C1,C2,C3 - TMSOH	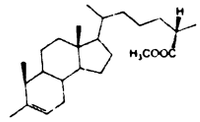
291*	M - 211	Ring C/D + Side Chain	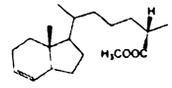
255	M - 90 - 157	ABCD Ring Nucleus	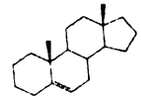
129*		C1,C2,C3 + TMSO	

Figure 5.2 Interpretation of the methyl-ester TMS-ether (25S)-cholestenoic acid spectrum. (A) GC-MS electron impact spectrum of methyl-ester TMS-ether (25S)-cholestenoic acid derivative. (B) Fragmentation analysis of (25S)-cholestenoic acid spectrum. (✱) Fragment ions corresponding to specific fragments produced by a Δ^5 double bond are marked with an asterisk.

daf-12(m20)

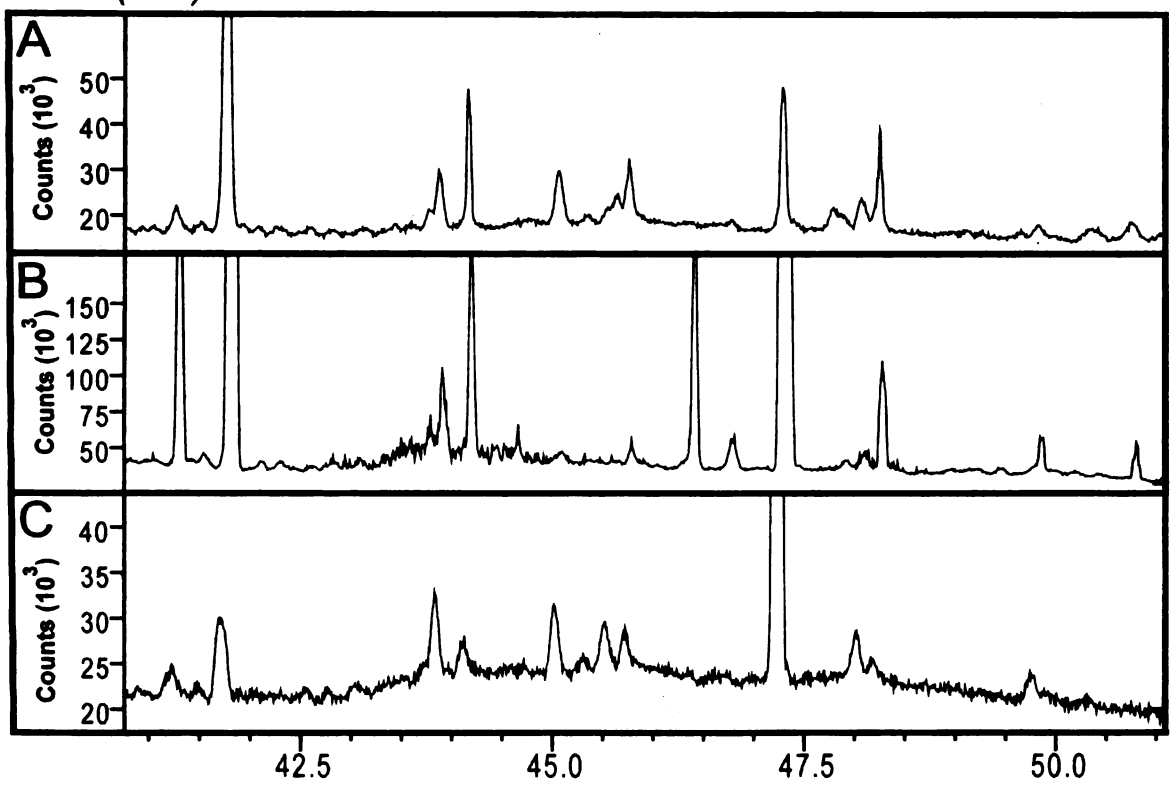

daf-9(gk160) daf-12(m20)

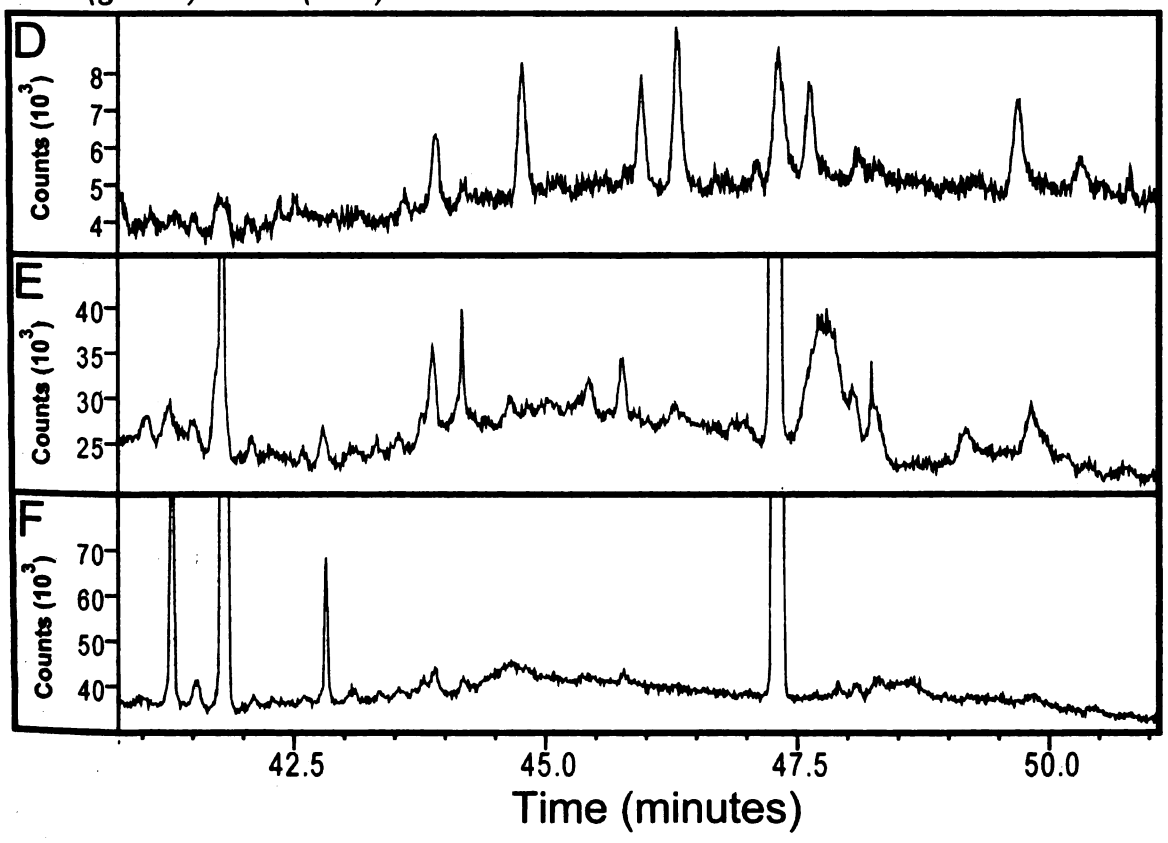

Figure 5.3 GC-MS TICs from *daf-12(m20)* and *daf-9(gk160) daf-12(m20)* aminopropyl fractionated extracts. (A), (B), and (C) represent GC-MS TICs from independent *daf-12(m20)* aminopropyl fractionated extracts. (D), (E), and (F) represent GC-MS TICs from independent *daf-9(gk160) daf-12(m20)* aminopropyl fractionated extracts.

are very few differences between *daf-12(m20)* and *daf-9(gk160) daf-12(m20)* extracts which is encouraging. In fact, there is only one peak that is consistently in the *daf-12(m20)* extracts that is not in any of the *daf-9(gk160) daf-12(m20)* extracts and has a retention of 45.0 minutes. Notably, this is the same retention as the methyl-ester TMS-ether cholestenoic acid derivative. To examine if peaks corresponding to cholestenoic acid or related molecules are in these extracts we examined an XIC of its base peak, *m/z* 412. The *m/z* 412 ion is a unique ion not found in the EI spectrum of many other compounds and is likely shared between related cholestenoic acid-like ions (Figure 5.4, with A-E as in Figure 5.3). Each of the three *daf-12(m20)* extracts has a peak at 45.0 minutes, and none of the *daf-9(gk160) daf-12(m20)* extracts do. Remarkably, this is the only peak that we identified in extracts that is consistently in bioactive extracts and not present in *daf-9(gk160) daf-12(m20)* extracts.

Examination of extract peak at 45.0 minutes

Closer inspection of the bioactive component at 45.0 minutes reveals that although it has the same retention time as the methyl-ester TMS-ether cholestenoic acid standard (Figure 5.5 A) it has a slightly different mass spectrum (Figure 5.5 B). These spectra share the major ions of *m/z* 502, 412, and 255 which are typical of C27 monohydroxylated, monounsaturated bile acids; however, the endogenous spectra is missing all of the cholestenoic acid fragments at *m/z* 373, 291, and 129 which are characteristic of a Δ^5 double bond (Setchell et al., 1998). The endogenous component spectrum also has an additional *m/z* 345 ion. Since we did not detect any *m/z* 373 ion, which is a major ion in the methyl-ester TMS-ether cholestenoic acid spectrum, in the *daf-12(m20)* extract it

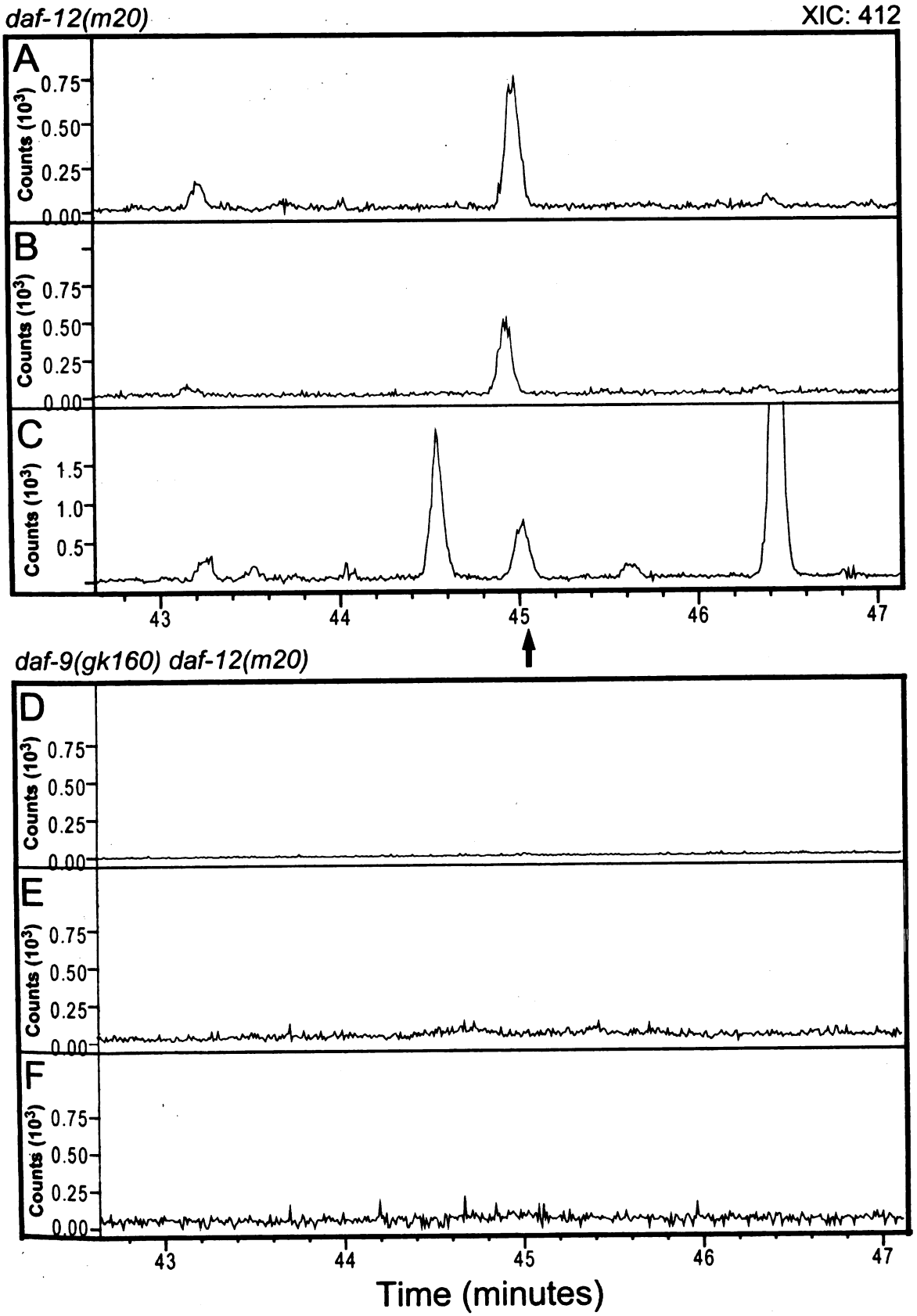
daf-12(m20)
XIC: 412
A
B
C
Counts (10³)
0.75
0.50
0.25
0.00
1.5
1.0
0.5
43
44
45
46
47
daf-9(gk160) daf-12(m20)
D
E
F
Time (minutes)

Figure 5.4 GC-MS XICs (*m/z* 412) from *daf-12(m20)* and *daf-9(gk160) daf-12(m20)* aminopropyl fractionated extracts.

(A), (B), and (C) represent GC-MS *m/z* 412 XICs from independent *daf-12(m20)* aminopropyl fractionated extracts. (D), (E), and (F) represent GC-MS *m/z* 412 XICs from independent *daf-9(gk160) daf-12(m20)* aminopropyl fractionated extracts. The arrow represents the retention time of authentic Δ^5 cholestenoic acid standard.

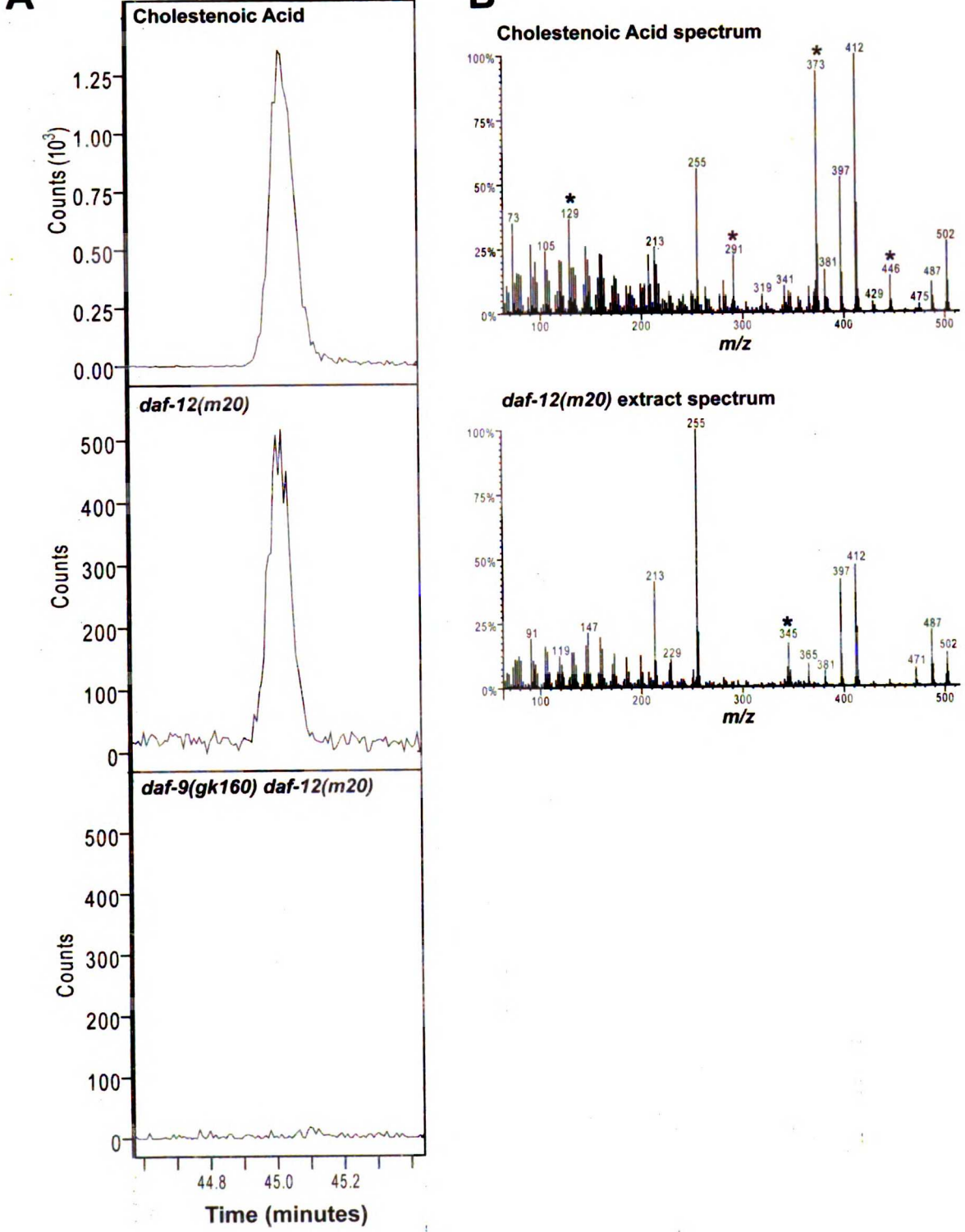
A
XIC: 412
Cholestenoic Acid
Counts (10^3)
daf-12(m20)
Counts
daf-9(gk160) daf-12(m20)
Counts
Time (minutes)
B
Cholestenoic Acid spectrum
m/z
daf-12(m20) extract spectrum
m/z

Figure 5.5 Comparison of cholestenoic acid and cholestenoic acid-like compounds in *daf-12(m20)* aminopropyl fractionated extracts. (A) XIC of *m/z* 412 demonstrating that *daf-12(m20)* extracts have a peak with the same retention time as (25S)-cholestenoic acid but *daf-9(gk160) daf-12(m20)* extracts do not. (B) Comparison of the spectra of the methyl-ester TMS-ether derivatives of cholestenoic acid and *daf-12(m20)* extract. (✱) Unique fragment ions in each spectrum are marked with an asterisk.

suggests that perhaps Δ^5 cholestenoic acid is absent in worm extracts or is at least significantly less abundant than the compound with the *m/z* 345 ion. Examination of the other peaks in the *daf-12(m20) m/z* 412 XIC (Figure 5.4 A-C) revealed that many of the peaks have similar, but not identical, spectra to cholestenoic acid though none contain the *m/z* 373 ion (data not shown). These data are consistent with detection of regioisomers of cholestenoic acid which have positional changes in the location of the double bond in the ABCD ring. We therefore propose that *C. elegans* makes a variety of monohydroxylated, monounsaturated C27 bile acids.

We wanted to examine the retention time of the extract peak at 45.0 minutes more closely so we co-injected 3 g equivalents of methyl-ester TMS-ether extract along with 8 ng cholestenoic acid (Figure 5.6 A). By examining the XIC ions specific to cholestenoic acid (*m/z* 373) and the extract peak (*m/z* 345) we can look closely at whether these peaks exactly overlap or are only slightly resolved (Figure 5.6 A). Co-injection revealed that the extract peak and cholestenoic acid do not completely overlap, with the peak maximum of the *m/z* 345 ion of the extract eluting a few seconds earlier than the cholestenoic acid peak. As expected, the spectrum for the co-injected analytes is a hybrid of the two individual components with detectable, but less than usual, *m/z* 373 and 345 ions characteristic of each component (Figure 5.6 B). Note that these peaks no longer elute at 45.0 minutes since they were run a significant period of time after the data for Figure 5.3 and 5.4 were collected. During routine maintenance the column is shortened and therefore analytes elute earlier.

A

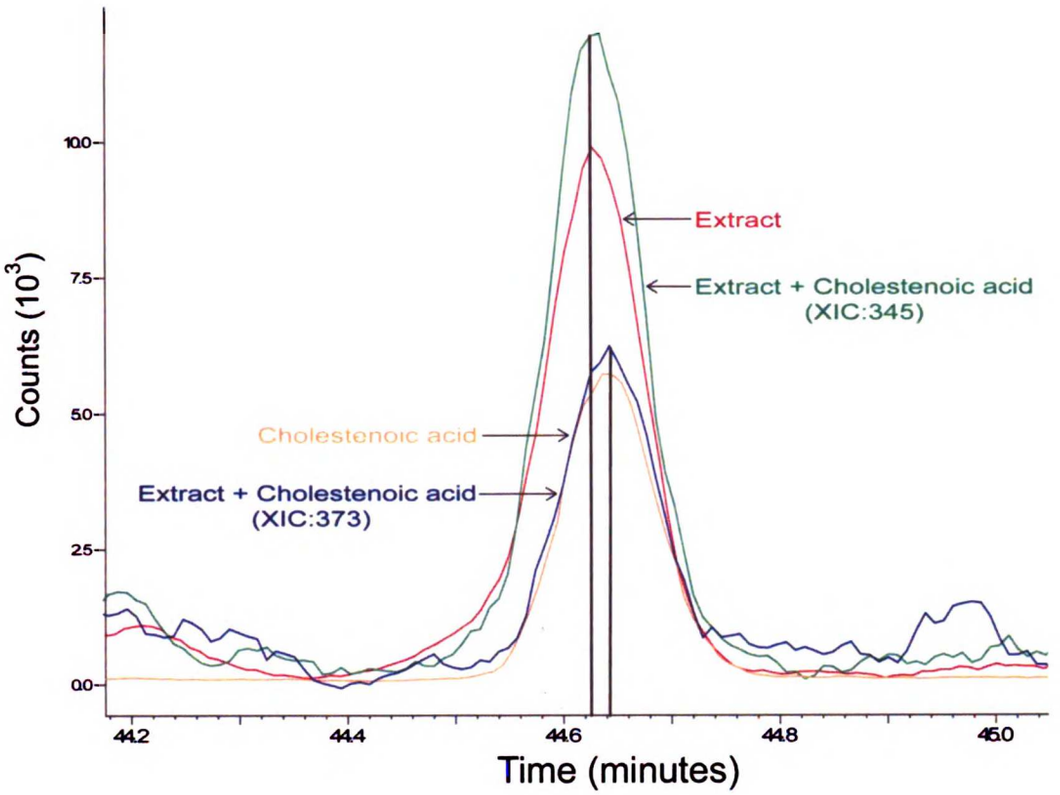
Counts (10^3)
10.0
7.5
5.0
2.5
0.0
Extract
Extract + Cholestenoic acid
(XIC:345)
Cholestenoic acid
Extract + Cholestenoic acid
(XIC:373)
44.2
44.4
44.6
44.8
45.0
Time (minutes)

B

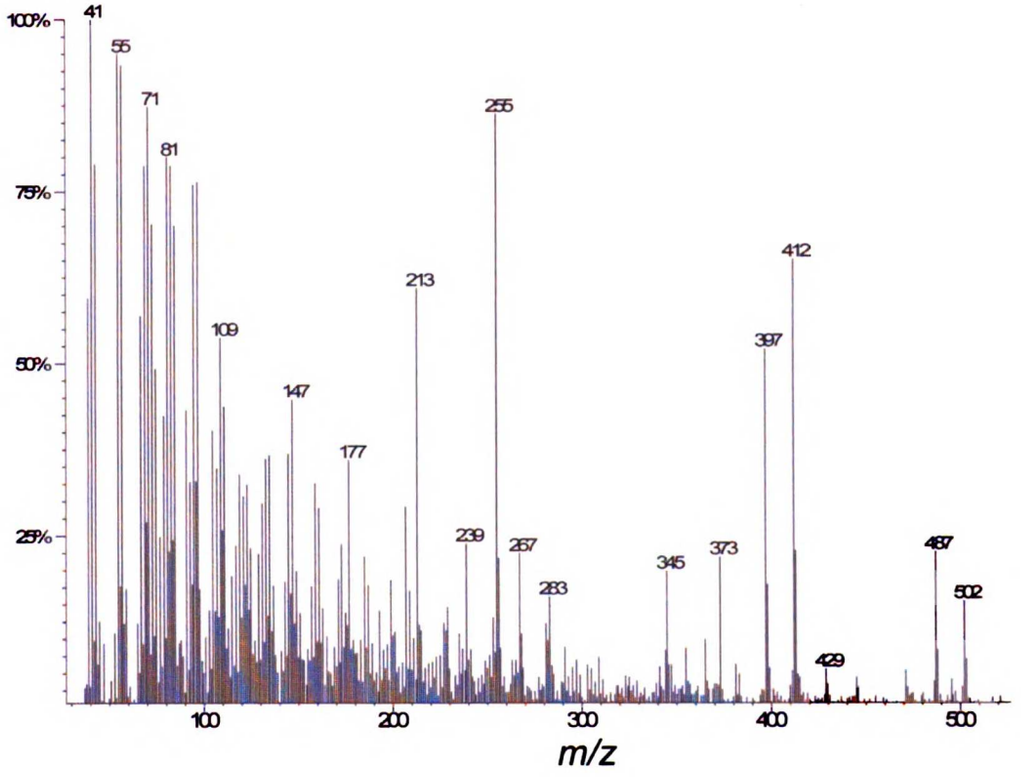
100%
75%
50%
25%
41
55
71
81
109
147
177
213
239
255
257
283
345
373
397
412
429
467
502
100
200
300
400
500
m/z

Figure 5.6 Co-injection of cholestenoic acid and *daf-12(m20)* aminopropyl fractionated extract. (A) GC-MS chromatograms of extract (red) and cholestenoic acid (orange) alone. Two XIC chromatograms are shown for the co-injected sample. XIC of *m/z* 345 (green) corresponds to a unique fragment ion from the extract and *m/z* 373 XIC (blue) corresponds to a unique fragment ion from cholestenoic acid. (B) Spectrum of co-injected Δ^5 cholestenoic acid and the *daf-12(m20)* extract.

GC-MS concentration curve of cholestenoic acid regioisomers

To quantify the levels of the cholestenoic acid regioisomers in the extracts we generated a standard curve of methyl-ester TMS-ether cholestenoic acid based on the *m/z* 412 ion (Figure 5.7 A). The chromatograms near the detection limit are shown in Figure 5.7 B. We then integrated the peak areas of the *m/z* 412 XICs from the three *daf-12(m20)* extracts in Figure 5.4. We chose to quantitate based on the *m/z* 412 ion since the regioisomers were near the detection limit and XIC was more sensitive than TIC (0.5 ng versus 1 ng) (Figure 5.7 C). Interestingly, we determined that selected ion scanning (SIS), the ion trap equivalent of selected ion monitoring (SIM) in which the ion trap only analyzes a single ion, had much better sensitivity than XIC (Figure 5.7 C).

Since we do not have standards corresponding to each regioisomer, we cannot be completely certain that the quantitation of the unknown compounds is accurate. However, it is generally assumed that very closely related structures such as cholestenoic acid regioisomers should have a similar signal for the same amount of material analyzed. We found that, per gram of worm starting material, the abundance of the peak with a retention of 44.6 minutes was 0.16 ± 0.16 ng, the abundance of the peak at 45.0 minutes was 0.47 ± 0.09 ng, the abundance of the peak at 45.7 minutes was 0.06 ± 0.06 ng, and the abundance of the peak at 46.4 minutes was 0.62 ± 0.47 ng. The levels are quite variable, with the most abundant peak (46.4 minutes) not detectable in one of the extracts and extremely high in another. On the other hand, the peak consistently seen at 45.0 minutes has a fairly small standard of deviation.

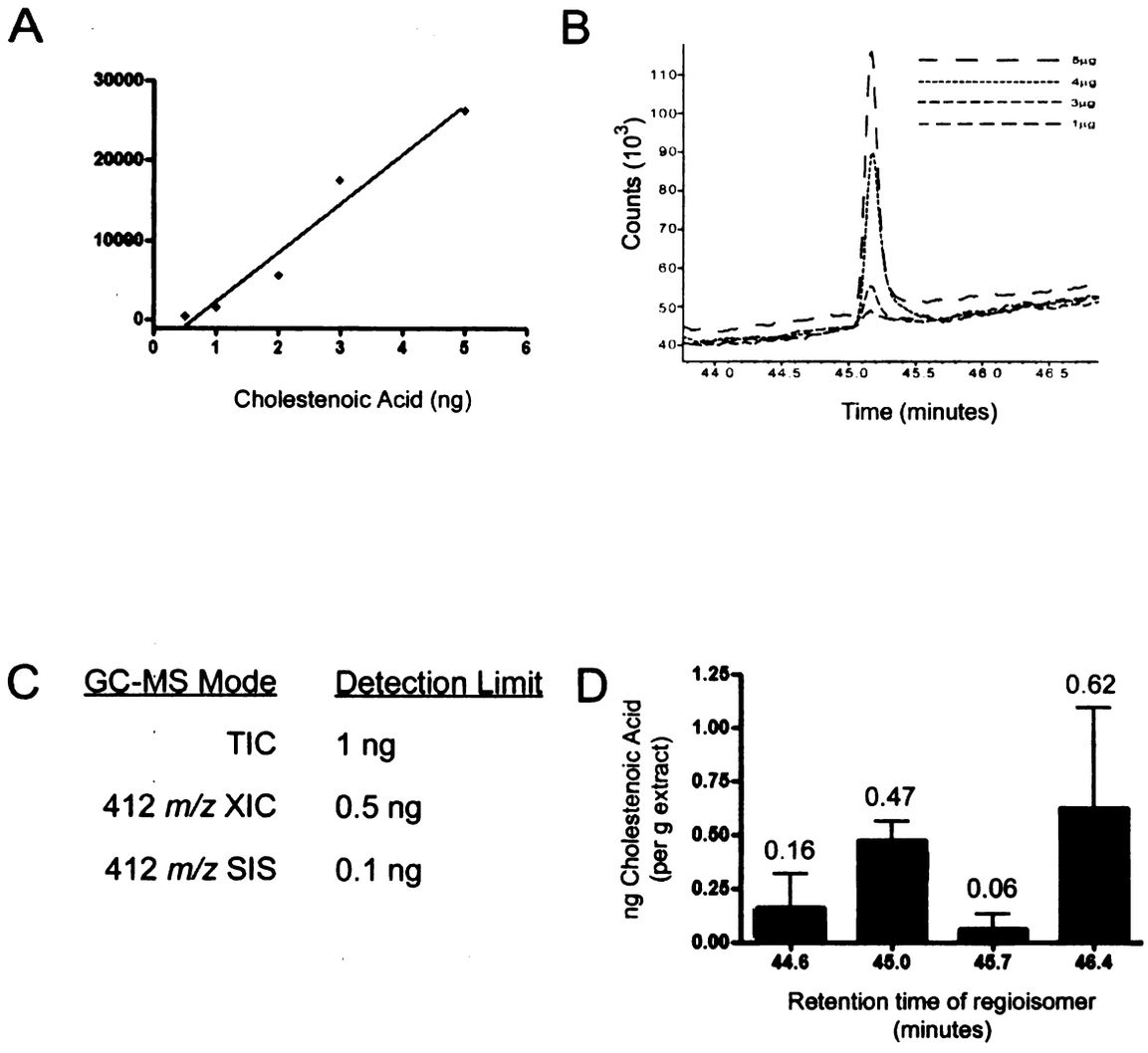

Figure 5.7 Cholestenoic acid quantitation in *daf-12(m20)* extracts.

(A) Standard curve of the methyl-ester TMS-ether cholestenoic acid derivative.

(B) Chromatograms of cholestenoic acid dilution series of 5, 4, 3, and 1 µg.

(C) Detection limit of cholestenoic acid in different GC-MS modes.

(D) Quantitation of cholestenoic acid regioisomers (retention times of 44.6, 45.0, 45.7 and 46.4 minutes) in *daf-12(m20)* extracts.

GC-MS of normal phase HPLC fractions

To examine which of these cholestenoic acid regioisomers is the most potent for dauer-rescue, we further fractionated a *daf-12(m20)* aminopropyl extract using normal phase HPLC and analyzed each fraction by GC-MS (Figure 5.8 A). To determine which fractions rescued dauer formation most potently, we tested a dilution series of each fraction for bioactivity (1 g, 0.5 g, and 0.25 g) on *daf-2(e1368)* (Figure 5.8 B). When scoring this bioassay we counted the number of worms that were not arrested as dauers but only were rescued to L3, L4, or young adult separately from those that became gravid adults. The rationale for this is that rescuing worms to gravid adult likely requires more bioactive potency than simply rescuing the Daf-c phenotype. Fraction #21 was the most potent, with almost complete rescue of dauer formation to gravid adulthood with 0.5 g and 1 g added as well as significant rescue from 0.25 g (Figure 5.8 B). Fraction #23 was also bioactive, but much less so, with 1 g rescuing about 80% of the worms from dauer, but only 50% of these as gravid adults. Fraction #23 also had significantly less rescue than Fraction #22 at both the 0.5 g and 0.25 g levels (Figure 5.8 B).

Examination of the most potent fraction, Fraction #21, revealed a regioisomer of cholestenoic acid that we had not previously detected in the aminopropyl fractions, likely due to its low abundance. The retention time of this isomer is 43.0 minutes and is the only cholestenoic acid regioisomer in this HPLC fraction, suggesting that the more abundant cholestenoic acids identified by examining aminopropyl fractions are not the most potent ligands. However, the previously identified regioisomers primarily eluted in Fraction #23, which is the only fraction other than #21 to have significant bioactivity.

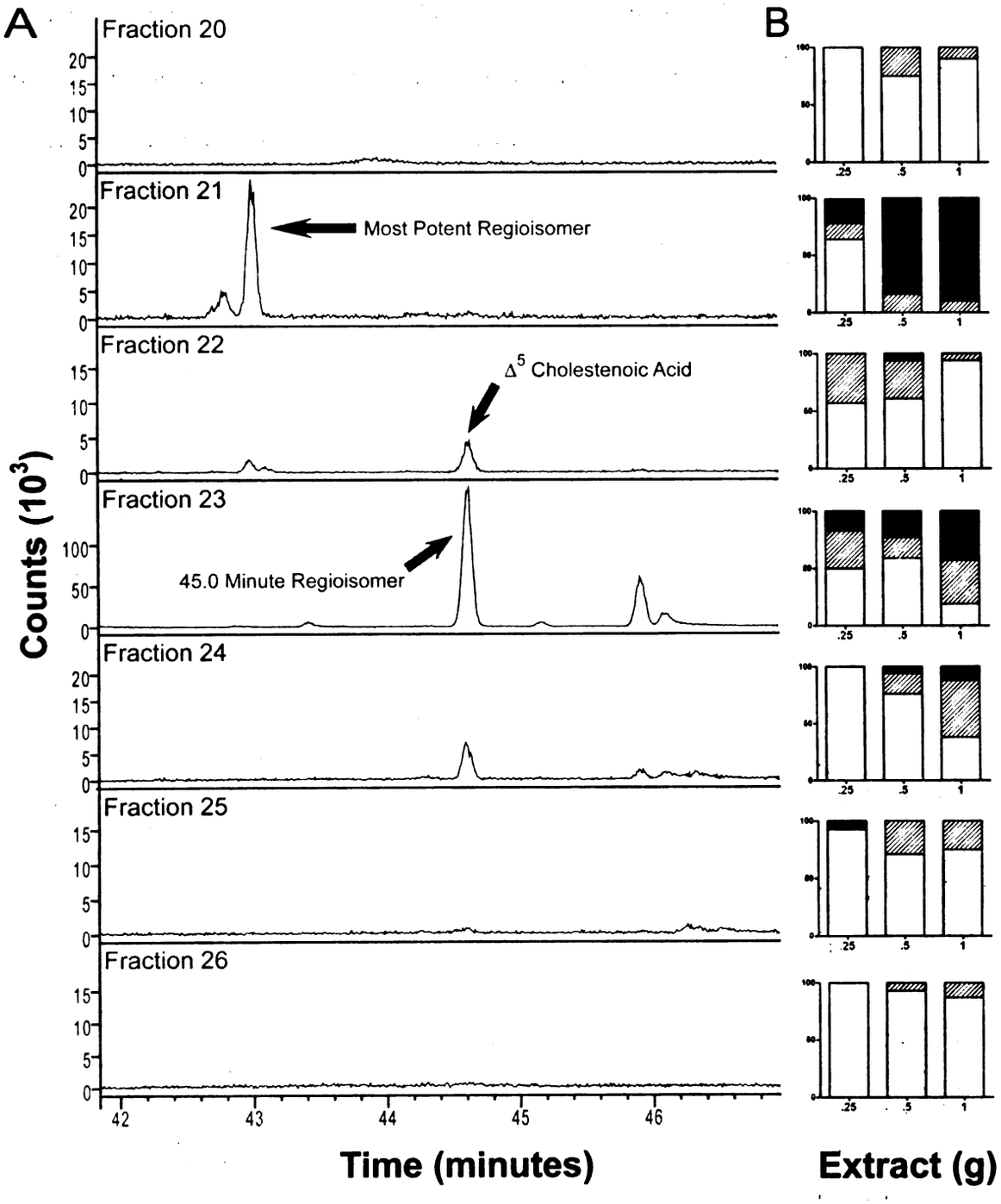
A
B
Fraction 20
Fraction 21
Most Potent Regioisomer
Fraction 22
Δ5 Cholestenoic Acid
Fraction 23
45.0 Minute Regioisomer
Fraction 24
Fraction 25
Fraction 26
Counts (10^3)
Time (minutes)
Extract (g)

Figure 5.8 GC-MS of normal phase HPLC separated extracts. (A) XIC of *m/z* 412 of 1 minute normal phase HPLC fractions (#20 to #26). (B) Bioactivity from a dilution series of each fraction to determine dauer rescue potency. 1 g, 0.5 g, and 0.25 g of each fraction were bioassayed on *daf-2(e1368)* worms. The percent of worms that became dauers is shown in white (▭ Dauer), the percent that were rescued to L3, L4, or young adult worms is shown with a diagonal box (▰ L3/YA), and the percent rescued to gravid adult is shown in black (■ Gravid Adult).

Examining the spectra of the regioisomers present in each fraction revealed that Δ^5 cholestenoic acid is actually present in the extracts (Fraction #22) and has the characteristic *m/z* 373 ion in typical abundance (data not shown). This peak is over 20 fold smaller than the extract peak in Fraction #23 at the same retention time, which likely prevents detection of the *m/z* 373 ion when the extract is only aminopropyl SPE fractionated. The fraction with Δ^5 cholestenoic acid had very little bioactivity suggesting that there are more potent regioisomers that exist in worms.

GC-MS of other larval extracts

Since the extracts are made from a *daf-12* mutant worm, and not wild type, we profiled the cholestenoic acid regioisomers in N2 at different larval stages. This was a preliminary profile and we analyzed only a single extract for each condition. We analyzed aminopropyl fractionated extracts from N2 L1/2 as well as L3/4 worms, *daf-12(m20)* L1/L2 worms, and *daf-9(gk160) daf-12(m20)* L1/2 worms (Figure 5.9 A). Since these extracts were chromatographed at different times, we overlaid the chromatograms by aligning the retention of the cholestenoic acid standard under the conditions in which each extract was run.

Analysis of the larval data strongly supports DAF-9 as the enzyme that synthesizes cholestenoic acid since *daf-9(gk160) daf-12(m20)* L1/L2 extracts do not have any trace of cholestenoic acids nor do L3/4 extracts. Furthermore, we previously demonstrated that extracts from *daf-12(m20)* L1/2 worms have a low level of dauer-rescuing bioactivity (Figure 2.1 C) and we found that these *daf-12(m20)* L1/2 worms

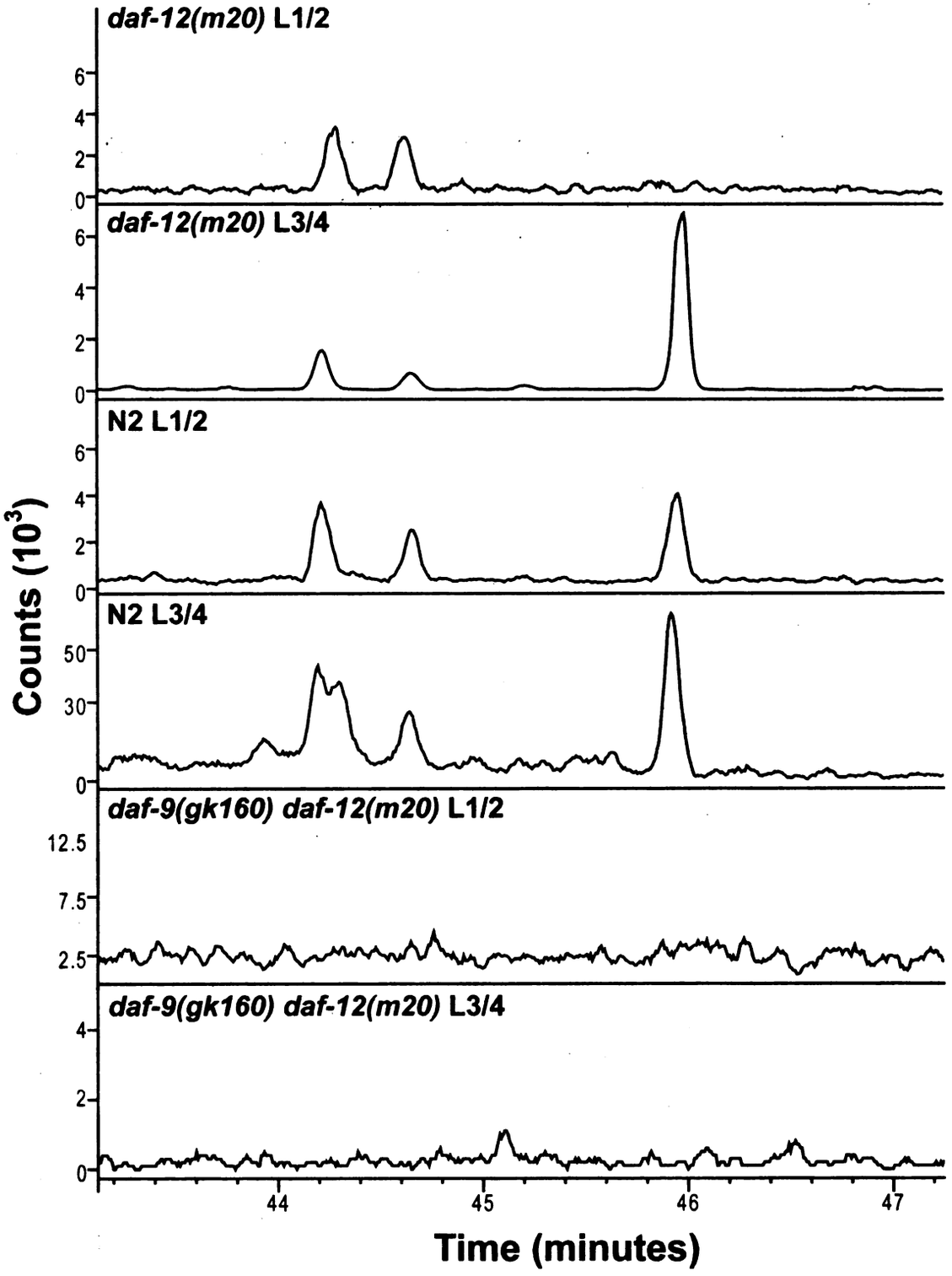
daf-12(m20) L1/2
daf-12(m20) L3/4
N2 L1/2
N2 L3/4
daf-9(gk160) daf-12(m20) L1/2
daf-9(gk160) daf-12(m20) L3/4
Counts (10^3)
Time (minutes)
44
45
46
47

Figure 5.9 Cholestenoic acid regioisomers are present in extracts from L1/2 and L3/4 N2 and *daf-12(m20)* worms but not *daf-9(gk160) daf-12(m20)*. XIC of *m/z* 412 for L1/2 and L3/4 extracts from *daf-12(m20)*, N2, and *daf-9(gk160) daf-12(m20)* worms. Cholestenoic acid regioisomers are found in each extract from *daf-12(m20)* and N2 but not in *daf-9(gk160) daf-12(m20)* extracts.

have some cholestenoic acid regioisomers. We also found previously that N2 L1/2 worms have a similar level of dauer-rescuing bioactivity (Figure 2.1 C), which accounts for the presence of cholestenoic acid regioisomers in the N2 L1/2 extract. However, we were surprised to see that there are a number of cholestenoic acid regioisomers with significant abundance in the N2 L3/L4 extract that does not have dauer-rescuing bioactivity (Figure 2.1 C). Since we were not able to detect the putative potent cholestenoic acid regioisomer in these aminopropyl fractions without the HPLC fractionation step (data not shown), the significance that N2 L3/4 worms produce other cholestenoic acids is unclear.

DISCUSSION

Cholestenoic acid regioisomers exist in worms

Data from worm extracts support that cholestenoic acids may act as a DAF-12 ligand since GC-MS data suggest the presence of several cholestenoic acid regioisomers in bioactive *daf-12(m20)* extracts. These compounds are not present in *daf-9(gk160) daf-12(m20)* extracts that do not have bioactivity. The magnitude and presence of particular peaks vary from extract to extract, which is not surprising given the significant variability in concentration of worm sterols from synchronous cultures (Merris et al., 2004); however, as a group they are consistently present in bioactive extracts. The most consistent peak is at almost the exact same retention time as the (25S)-cholestenoic acid standard with the spectra shown in Figure 5.5. Correlation of bioactivity with GC-MS data from an HPLC fractionated extract suggests that although this may have some bioactivity, the most bioactive cholestenoic acid regioisomer likely elutes at 43.0 minutes and is undetectable in extracts fractionated by aminopropyl SPE alone (Figure 5.8).

Different GC retention times of compounds that have similar MS spectra are characteristic of sterols and bile acids with different locations of unsaturation (Child et al., 1979a; Child et al., 1979b; Gerst et al., 1997). The spectra from the endogenous compounds contain major ions of *m/z* 502, 412, and 255 which are also major ions in the methyl-ester TMS-ether cholestenoic acid spectra from a standard. These ions correspond to the molecular ion, the loss of a trimethylsilanol group (TMSO) from the parent, and the subsequent loss of the carboxylic acid side chain. These ions are characteristic of a monohydroxylated, monounsaturated bile acid, especially the *m/z* 255 ion which is a

monounsaturated ABCD sterol backbone (Setchell et al., 1998). All but one of the endogenous spectra are missing the major fragments at *m/z* 373, 291, and 129 which, as interpreted in Setchell *et al.* (1998), are characteristic for a Δ^5 double bond. Worms are known to produce sterols with a wide variety of double bond locations (Chitwood and Lusby, 1991) and potentially generate cholestenoic acids with a wide variety of double bond locations as well.

Rigorous identification and complete chemical characterization of these cholestenoic acids is difficult since no chemical standards other than Δ^5 cholestenoic acid are available. Modifying the extract by ozonolysis (Pulfer and Murphy, 2004) or catalytic hydrogenation with deuterium incorporation may provide some insight into the position of the double bonds. However, they would likely create a complex number of products and be extremely difficult to interpret. We have looked exhaustively in the literature in an attempt to correlate the effects of double bond locations on the retention and fragmentation patterns within related sterol and C24 bile acid regioisomers. However, the effect of a particular double bond location to the relative retention of the compound is not consistent between bile acids and sterols. Additionally, very little GC-MS data of unsaturated bile acid isomers is published since they are extremely uncommon mammalian metabolites.

The fragmentation data of published bile acids do not match our own, potentially since the published data are from a quadropole mass analyzer and our instrument is an ion trap (Child and Kuksis, 1979; Child et al., 1979a; Child et al., 1979b; Kuksis and Child, 1980). The analyte internal energy and the time in the gas phase are key parameters that determine the fragmentation pattern, but are different between these two

types of instruments. For example, the published spectrum for methyl-ester acetate Δ^5 cholenic acid has a fragment ion at *m/z* 262 which distinguishes it from the Δ^6 cholenic acid (Kuksis and Child, 1980); however, the spectrum our instrument generates from Δ^5 cholenic acid does not have this fragment (data not shown). Furthermore, the relative abundance of the fragment ion at *m/z* 249 is used to distinguish between Δ^5 and Δ^7 cholenic acids since Δ^5 cholenic acid has a relatively high level of this ion and Δ^7 cholenic acid does not (Kuksis and Child, 1980). However the spectrum we have for Δ^5 cholenic acid has low levels of *m/z* 249 making this key determination not possible (data not shown). Furthermore, Child and Kuksis (1979) suggest that only the extensive use of argentation chromatography along with retention analysis using a series of different GC columns with wide-ranging polarities can determine where the double bond exists with a sufficient degree of certainty (Child and Kuksis, 1979; Child et al., 1979b). Therefore we cannot make any significant predictions about where the double bond is in our C27 methyl-ester TMS-ether derivatives based on GC-MS data. In the future, synthesis of these cholestenoic acid regioisomers will be required in order to conclusively determine the position of the double bond of each component by matching their retention and fragmentation to components in the extract. Furthermore, having synthetic cholestenoic acids standards will allow for definitive determination of which regioisomer is the most potent in the dauer rescue bioassay.

Why are there so many cholestenoic acid regioisomers?

C. elegans has a diverse sterol profile which includes a variety of monounsaturated forms including Δ^7, $\Delta^{8(9)}$, and $\Delta^{8(14)}$ as well as polyunsaturated sterols with double bonds at the

$\Delta^{9(11)}$, Δ^{22}, Δ^{23}, and Δ^{24} positions (Chitwood and Lusby, 1991; Chitwood, 1999). Furthermore, worms have the ability to utilize a number of different dietary sterols other than cholesterol for proper development. One feature of CYP27A1 is that it is known to catalyze the carboxylation of several diverse sterol substrates (Pikuleva and Javitt, 2003). Potentially DAF-9 carboxylates a variety of these unsaturated sterols, which would explain the GC-MS evidence that many isomers or closely related structures to cholestenoic acid exist in worms. DAF-9's role as a CYP27A1 is in contrast to the prediction based on homology that *daf-9* is most similar to human CYP17 and CYP21 which are 17α- and 21-hydroxylases, respectively (Nelson, 1998; Jia et al., 2002). Our data that cholestenoic acids are not present in L1/2 or L3/4 *daf-9(gk160) daf-12(m20)* worms support the role of DAF-9 as a CYP27A1.

Why do N2 L3/4 worms contain cholestenoic acid regioisomers?

Cholestenoic acids may play many roles in *C. elegans*. Different regioisomers may act as phenotype-specific DAF-12 ligands during dauer, gonad, and lifespan regulation since specific *daf-12* mutants affect dauer regulation and gonad regulation separately (Antebi et al., 2000). Synthetic cholestenoic acid regioisomers could be tested to see if they have differential dauer, gonad, and lifespan effects. Secondly, the large variety of cholestenoic acids may be due to their role in an inactivation pathway to remove excess sterols from worms much like the ecdysonoic acids in *Drosophila* and bile acid in humans. Alternatively, they may help solubilize nutrients from the soil. Therefore, it is not surprising that N2 L3/4 extracts have cholestenoic acids even though they are not bioactive. Future experiments examining the putative potent bioactive cholestenoic acid

regioisomer at 43.0 minutes and its presence in N2 L3/4 and other mutants will be interesting. We hypothesize this particular regioisomer is not present in N2 L3/4 extracts which leads to their lack of bioactivity.

Δ^7 cholestenoic acid is likely the most potent dauer-rescuing cholestenoic acid

In worms, the sterol metabolic pathway begins at cholesterol and moves to 7-dehydrocholesterol, lathosterol, and finally lophenol, a sterol which contains a novel worm sterol modification of 4-methylation (Figure 3.1) (Chitwood, 1999). Lophenol has been implicated in dauer formation since worms grown on lophenol instead of cholesterol arrest as dauers. Since this methylation step does not support rescue from dauer, it is likely lophenol is too far down the metabolic pathway to be metabolized by DAF-9 into a cholestenoic acid-like molecule that contains bioactivity. This could either be because it is not a good DAF-9 substrate or because it is not a good DAF-12 ligand. We have found, however, that the sterol immediately upstream of lophenol, the Δ^7 sterol lathosterol, is able to rescue dauer formation in *daf-2(e1368)* but not *daf-9* mutants (Figure 5.10 A) though it requires a very high dose – 200 μM lathosterol rescues only 60% of *daf-2(e1368)* worms (Figure 5.10 B). However, lathosterol is the only sterol tested that can rescue dauer formation since neither cholesterol, 7-dehydrocholesterol, $\Delta^{8(14)}$ cholesterol, nor lophenol is able to rescue the Daf-c phenotype of *daf-2(e1368)* (Figure 5.10 A). This suggests that lathosterol may be the point of divergence to generate the bioactive regioisomer of cholestenoic acid. We therefore hypothesize that the Δ^7 version of cholestenoic acid may be the regioisomer that elutes at 43.0 minutes. The fact that a

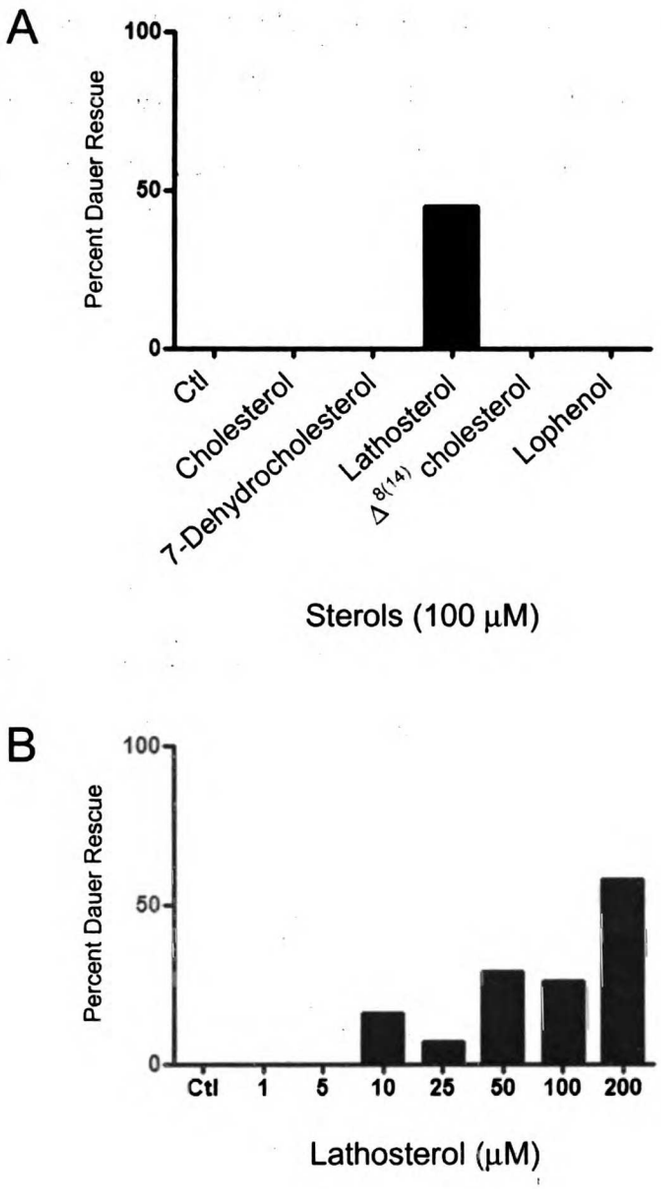

Figure 5.10 The Δ^7 sterol lathosterol rescues the Daf-c phenotype of *daf-2(e1368)*. (A) *daf-2(e1368)* dauer rescue assay with 100 μM of different members of the known sterol pathway in *C. elegans*. (B) Concentration curve of lathosterol rescue of *daf-2(e1368)* dauer formation.

sterol can rescue the Daf-c phenotype of *daf-2(e1368)* and not *daf-9(gk160)* also suggests that the mechanism for the dauer-rescuing ability of *gamravali* was likely replacement of lathosterol or a lathosterol derivative that is upstream of DAF-9 metabolism (Matyash et al., 2004).

Bile acid metabolism in *C. elegans*

Examination of the GC-MS data for aminopropyl fractionated extracts did not detect any additional bile acids beyond cholestenoic acid in worm extracts. Nothing in the extracts had the same retention and fragmentation as the common C24 bile acid standards cholic acid, deoxycholic acid, chenodeoxycholic acid, lithocholic acid, and Δ^5 cholenic acid (data not shown). To be certain that novel C24 bile acids were not missed, we examined the spectra of peaks detected in XIC chromatograms of ions that correspond to major fragment ions from C24 bile acids with 3 hydroxyls (*m/z* 368 and 253), 2 hydroxyls (*m/z* 370 and 255), and 1 hydroxyl (*m/z* 372 and 257) and detected no spectra that resemble bile acid fragmentation. The lack of C24 bile acids was unexpected since the only piece of evidence for the presence of bile acids in *C. elegans* before our findings was that worms have a 3-oxoacyl-CoA thiolase β-oxidation enzyme that can shorten the side chain of C27 bile acid precursors to C24 (Bun-Ya et al., 1997; Maebuchi et al., 1999).

Furthermore, although the doubly hydroxylated 3β,7α-dihydroxy-5-cholestenoic acid is important in mammals, we saw no spectra that were similar to cholestenoic acid that had a molecular ion of *m/z* 590. 7α-hydroxy-3-oxo-4-cholestenoic acid is also important in mammals and would be predicted to have a molecular ion at *m/z* 516 and a major fragment at *m/z* 426 due to loss of a TMSO group, which also was not detected.

The lack of bile acid variety in *C. elegans* suggests that the worm may only have a primitive bile acid pathway, much like *Drosophila*. The *C. elegans* pathway may resemble the neutral bile acid pathway in mammals.

An avenue of future research will be the examination of the oxysterol precursors of cholestenoic acid in *C. elegans*. In mammals oxysterols are known nuclear receptor ligands and may function to activate other *C. elegans* nuclear receptors. The presence of cholestenoic acids in worms suggests that these metabolic intermediates of CYP27A1 conversion of sterols to sterol acids are likely present. These were not detected in a global analysis of sterols in *C. elegans*; however, they may be at low levels or missed in the chromatographic separation which primarily detected non-polar sterol variants (Chitwood and Lusby, 1991). Worms may generate novel 27-hydroxysterol variants with double bond locations other than Δ^5.

Bile acid quantitation

Quantitation of the four cholestenoic acid regioisomers in extracts revealed that they are present at levels between 50 and 650 pg per gram of starting material. The limit of detection of our current GC-MS methodology is 500 pg for the cholestenoic acid standard, but realistically about 1 μg is needed for detection in the complex background matrix of the extracts that increases the level of noise (Figure 5.7 C). Therefore, detection of cholestenoic acids in worms requires at least several grams of starting material for reliable detection, an amount which requires considerable effort to obtain. Furthermore, the *daf-12(m20)* worms analyzed are predicted to be producing the maximum amount of DAF-12 ligand based on their bioactive potency. This may make it challenging to

quantify cholestenoic acid levels in worms that would be predicted to have lowered cholestenoic acid levels, such as worms entering the dauer stage. A potential solution to this problem is using SIS to collect only the *m/z* 412 ion in the ion trap. This is analogous to selected ion monitoring with a quadropole instrument that is the standard method for quantifying trace level material. SIS increases the sensitivity for the methyl-ester TMS-ether cholestenoic acid standard approximately fivefold and should reduce the levels of extract needed for detection by a similar amount. A second approach to improve the detection limit is making HPLC purification of the extracts a routine fractionation step. This will significantly reduce the background level in the sample by reducing the very high levels of fatty acids found in the aminopropyl fraction (Figure 3.4).

Quantitation of cholestenoic acid regioisomers in worms should provide valuable insight into the mechanism of DAF-12 in dauer formation. For example, quantifying cholestenoic acids in *daf-2*;*daf-12* double mutants that have either synergistic or antagonistic effects on lifespan could provide insight into this complicated interaction. An analysis of cholestenoic levels in wild type and long-lived worms throughout the worm lifetime would be interesting as well. Understanding how the levels of cholestenoic acid are regulated in N2 under dauer formation conditions and Daf-c or Daf-d mutants will help understand how dauer formation is regulated, especially if temporal expression of cholestenoic acids is punctuated throughout development like ecdysone signaling. Furthermore, cholestenoic acid levels are essentially a measure of the output of DAF-9. By quantitating cholestenoic acid levels we can determine how different levels of input from the different upstream dauer signaling pathways (insulin, TGFβ, and guanylate cyclase) are integrated to drive the worm into dauer or reproductive growth.

Quantitation of cholestenoic acid regioisomers should also provide valuable insight into the mechanism of DAF-12 in gonad formation and lifespan extension. Cholestenoic acids are likely involved in the intercellular *daf-12* and *daf-16* interaction that extends the lifespan of gonad ablated animals. Getting significant numbers of gonad ablated animals is impossible; however, genetic mutants are available that have defective gonads and examining levels of cholestenoic acid in them may help provide insight into the mechanism of this type of lifespan extension. Finally, the role of *daf-12* in dauer recovery is still unclear. By examining a time course of cholestenoic acid levels in dauers after they are placed in conditions of recovery it may become clear if a spike of cholestenoic acid triggers DAF-12 into activating the worm to move towards reproductive growth.

More speculative conditions in which quantifying cholestenoic acid levels would be interesting are during starvation, heat shock, or other stressful conditions. Cholestenoic acid quantitation could also be included in a metabolomic profile of *C. elegans* mutants with homology to sterol/steroid modifying enzymes. One such enzyme is *let-767* which has homology to a 17β-hydroxysteroid dehydrogenase and effects *C. elegans* growth, development, and reproduction but the mechanistic role it plays is completely unknown (Kuervers et al., 2003).

MATERIALS AND METHODS

Materials

Lathosterol (#C-3652), 7-dehydrocholesterol (#D-4429), and cholesterol (#C-8667) were purchased from Sigma (St. Louis, MO). (25R)-cholestenoic acid (#C6786-000) and (25S)-cholestenoic acid (#C6787-000) were purchased from Steraloids (Newport, RI). Δ^7 3-keto sterol (#1218-3), Δ^5 3-keto sterol (#1214-3), $\Delta^{8(14)}$ cholesterol (#1222-3), and lophenol (#12160-3) were purchased from Research Plus (Manasquan, NJ). Dotriacontane (C32, #620320) was purchased from Alltech (Columbia, MD).

Derivatization

TMS-ester TMS-ether derivatization: Sample was dried completely under N_2 and silylated with 200 µL of 99% [N, O-Bis(trimethylsilyl)trifluoroacetamide] (BSTFA) plus 1% trimethylchlorosilane (TMCS) (v:v) (Supelco, #33148) at 75°C for 3 hr. Sample was then dried under N_2, resuspended in 400 µL hexane, and dried under N_2 again. The sample was then resuspended in 1 µL hexane and immediately injected into the GC-MS.

Methyl-ester acetate derivatization: The sample was esterified by incubating it with 250 µL BF_3-10% methanol (w:w) (Supelco #33356) for 90 min at 100°C. H_20 (200 µL) was added and then extracted twice with 550 µL hexane. The hexane was then dried under N_2. The sample was then acetylated by incubation with 1:1 0.5 mL acetic anhydride:pyridine (v:v) (Pyridine Plus kit, Alltech #18105) at 60°C overnight. H_20 (0.5 mL) was added and then extracted twice with 0.5 mL hexane. The hexane was dried under N_2 and the sample was then resuspended in 1 µL hexane and injected into the GC-MS.

Methyl-ester TMS-ether derivatization: The sample was esterified by incubating it with 250 µL BF_3-10% methanol (w:w) (Supelco #33356) for 90 min at 100°C. H_20 (200 µL) was added and then extracted twice with 550 µL hexane. The hexane was dried completely under N_2. The sample was then silylated with 200 µL of 99:1 BSTFA+TMCS (v:v) (Supelco, #33148) at 75°C for 3 hr. Sample was then dried under N_2, resuspended in 400 µL hexane, and dried under N_2 again. The sample was then resuspended in 1 µL hexane and immediately injected into the GC-MS.

GC-MS analysis

GC-MS analysis was on a Varian 2100T ion-trap GC/MS/MS with a 3900 GC (Varian Inc., Walnut Creek, CA) operating in splitless mode with a VF-5ms capillary column (30 m X 0.25 mm i.d., 5% phenyl-95% methyl polysiloxane, 0.25 µm film thickness; Varian, Inc., Walnut Creek, CA). *GC conditions:* Injector was at 300°C and pressurized to 40 psi for 0.8 min at the time of injection. Initial column temperature was 180°C for 3 min and then ramped linearly at 2.8°C per min to 300°C and held for 18 min. *MS conditions:* Positive-ion mode, electron impact ionization, scan time 0.53 sec, and mass range 30-650 *m/z*.

Database searching was performed using NIST MS Search 2.0 and the databases used were the NIST 2002 and Wiley 7.0 mass spectral libraries.

Bioassay scoring for dauer, L3/L4/young adults, and gravid adults

Bioassay was performed as described in Chapter 4 in which the plates were left for 72 hr at 25°C. Worms were scored as dauer or gravid adult and worms that had broken out of dauer but not become gravid were scored as L3/L4/young adult.

Sterol bioassay

*daf-2(e1368) w*orms were maintained at 20°C on 5 cm nematode growth medium (NGM) agar plates with a lawn of *E. coli* OP50. Lathosterol and other sterols were resuspended in ethanol. For dauer assays, 15 µL of a stock solution was added to 185 µL S-basal before being spotted onto a 3 cm petri dish containing 3 mL NGM and 50 µL *E. coli*. The S-basal was allowed to cover the whole surface of the plate and was left for 1 hr prior to adding worms. The plates were then placed in an incubator at 25°C to generate dauers. Plates were scored for the number of dauer, L3/L4/young adult, and gravid adult worms after 72 hr. All worms that were scored as in the L3 stage or beyond were scored as rescued for the figures in this chapter.

Miscellaneous

Worm strains, ether extraction, aminopropyl SPE, normal phase HPLC, and worm growth were all performed as described in other chapters.

CHAPTER VI

Discussion

DAF-12 and *C. elegans* physiology

Nuclear receptor signaling pathways often coordinate many diverse aspects of organismal physiology. DAF-12 is no different, playing a role in dauer formation, gonad formation, developmental timing, lipid metabolism (Larsen et al., 1995), fertility (Gems et al., 1998), and adult lifespan (Larsen et al., 1995). In particular, there has been much interest in DAF-12's role in the determination of lifespan in *C. elegans*. This interest has placed an emphasis on understanding how downstream endocrine effectors such as the DAF-12 ligand are modulated by longevity genes to bring about lifespan extension (Tatar et al., 2003). The identification of (25S)-cholestenoic acid as a ligand for the nuclear receptor DAF-12 prompts new approaches to delineating the role of this receptor and its mammalian counterparts in the regulation of life history and the determination of lifespan. The biochemistry of worms has only recently begun to be explored, and the identification of cholestenoic acids in worms is a key step in understanding how complex processes such as aging and development are regulated by small molecule endocrine effectors.

DAF-12 as a potential sterol sensor

We have focused our research primarily on the role of DAF-12 in the dauer phenotype. Sterols are important to dauer formation and suggest that DAF-12 may act as a sterol sensor. This is supported by the identification of (25S)-cholestenoic as a DAF-12 ligand and the presence of cholestenoic acids in extracts from *C. elegans*. LXR acts as a cholesterol sensor by binding oxidized derivatives of cholesterol (Janowski et al., 1996; Lehmann et al., 1997) and LXR has been implicated in cholesterol homeostasis in

mammals (Handschin and Meyer, 2005). The functions of LXR and DAF-12 are likely linked since bioinformatic evidence suggests that DAF-12 is homologous to LXR (Mooijaart et al., 2005) and our data suggest that LXR and DAF-12 share cholestenoic acid as a ligand. Sensing of levels of a sterol metabolite such as cholestenoic acid by DAF-12 could be evidence of a lipid homeostatic mechanism in *C. elegans*. Programs of reproductive growth would be initiated only when the sterol availability was appropriate to support such growth. Under conditions of limited sterol availability such as population overcrowding and starvation, the absence of cholestenoic acid-like molecules available to act as a DAF-12 ligand would lead DAF-12 to direct programs of dauer arrest. LXR acts in a complex signaling cascade involving several other nuclear receptors (Berkenstam et al., 2004). Many nuclear receptors, including *nhr-41* and *nhr-85* (Gissendanner et al., 2004), play a role in dauer formation and another, *nhr-39*, is involved in lipid metabolism. Future research will evaluate if these nuclear receptors regulate lipid homeostasis in a cascade downstream of DAF-12 in a manner similar to what has been described in mammals.

Ecdysone receptor signaling cascades and *C. elegans*

One potential nuclear receptor signaling cascade with which DAF-12 may be involved is the ecdysone receptor signaling pathway. Studies on *Drosophila* nuclear receptors have demonstrated the importance of ecdysteroids and juvenile hormone-modulated nuclear receptor signaling cascades to invertebrate development. The similarity between ecdysone signaling and DAF-12 with respect to developmental timing has made the ecdysone pathway an important model to hypothesize how DAF-12 may be regulated.

Ecdysteroids are produced in the prothoracic glands of the fly and are released into the haemolymph where they are converted into the active form 20-hydroxyecdysone (20E). The analogous process in worms may be DAF-9 production of cholestenoic acids in the hypodermis. 20E binds a heterodimer of two nuclear receptors: the ecdysone receptor (EcR) and ultraspiracle (USP) (Koelle et al., 1991; Yao et al., 1993; Billas et al., 2003; Kumar et al., 2004). Fly transitions between larval stages are triggered by a pulse of 20E (Thummel, 2001) which modulates a cascade of many genes, including six other nuclear receptors, that act in synchrony to complete the larval stage transition (King-Jones and Thummel, 2005). On the other hand, juvenile hormone III (JH III), which functions during development to ensure growth of the larva and prevent metamorphosis, has a less clear mode of action. It weakly binds (Jones et al., 2001), transactivates (Xu et al., 2002), and induces DNA binding (Jones and Sharp, 1997) by USP, but the crystal structure of the USP LBD shows that a bacterial-derived phospholipid fills the ligand binding pocket rather than a juvenile hormone (Clayton et al., 2001; Billas et al., 2001). Recently, however, the EcR and USP were shown to heterodimerize together on several DNA response elements suggesting that they do interact (Perera et al., 2005) in a ligand-dependent manner (Bergman et al., 2004). Interestingly, RXR is an ortholog of USP and EcR is an ortholog of FXR and LXR, which are known to interact. Other *Drosophila* nuclear receptors important for development are DHR38 which dimerizes with USP (Sutherland et al., 1995; Kozlova et al., 1998) and binds a set of ecdysones (Baker et al., 2003), and the putative repressor DHR78 which binds a subset of EcR-USP DNA binding sites and can inhibit 20E-induced reporter-gene transcription in cell culture (Zelhof et al., 1995).

Attempts to map the *Drosophila* ecdysone signaling cascade in *C. elegans* have met with significant hurdles. Bioinformatic evaluation of the genome of *C. elegans* has not revealed homologs to EcR or USP (Sluder and Maina, 2001). Additionally, although a single early report indicated the presence of ecdysteroids in *C. elegans* (Mercer et al., 1988), there have been no further reports of ecdysteroids or juvenile hormones in *C. elegans* and these compounds have few, if any, pharmacological effects when added exogenously. However, EcR, USP, and ecdysteroids are present in filarial and parasitic nematodes closely related to *C. elegans* (Mendis et al., 1983; Cleator et al., 1987; O'Hanlon et al., 1991; Fleming, 1993; Shea et al., 2004). Future proteomic analysis of DAF-12 binding proteins may reveal an RXR/USP-like binding partner that is untractable by bioinformatics.

Though the ligand and receptor components of the ecdysone signaling pathway are not present in *C. elegans*, the downstream nuclear receptors in the ecdysone cascade are present and have an oscillating, reiterated pattern of expression corresponding to molting that is reminiscent of the pulsed pattern of ecdysone signaling in *Drosophila* (Gissendanner et al., 2004). The relationship of these receptors to DAF-12 has not been established, but it would be exciting if DAF-12 were the worm replacement for the EcR, and cholestenoic acid were the worm analog of ecdysone and/or juvenile hormone. This would provide a clear mechanism for DAF-12's role in maintaining normal developmental timing. Interestingly, two of these ecdysone nuclear receptor homologs (*nhr-41* and *nhr-85*) are involved in molting, but only the specific molt leading to dauer. This dauer specificity supports DAF-12 directing dauer programs via this ecdysone-like cascade (Gissendanner et al., 2004). Future studies quantitating cholestenoic acid during

development may reveal that cholestenoic acid or cholestenoic acid regioisomers are pulsed in a similar manner to ecdysone to drive these signaling pathways. Several experiments have determined that the dauer decision is made just after the L1 molt and future research will determine the precise window of cholestenoic acid treatment that determines dauer formation (Swanson and Riddle, 1981; Antebi et al., 1998).

Multiple DAF-12 ligands?

One unanswered question about DAF-12's mechanism of action is whether there are separate DAF-12 ligands for different DAF-12 functions that occur at different developmental periods. Our data suggest that several regioisomers of cholestenoic acid are present in worm extracts and that perhaps different ligands are utilized. We hypothesize, based on the rescue of lathosterol, that Δ^7 cholestenoic acid is the most likely candidate to be a high affinity dauer-rescuing DAF-12 ligand. While this thesis was in preparation, a paper was published that identified the 3-keto sterol acids Δ^7 3-one-cholestenoic acid as well as Δ^4 3-one-cholestenoic acid as DAF-12 ligands (Motola et al., 2006). These differ from the 3-hydroxy-cholestenoic acid compounds that we have found since they are 3-keto-cholestenoic acids.

Our data overlap significantly with that of Motola *et al.* (2006). For example, these authors also believe that the Δ^7 version is the most potent dauer-rescuing ligand, though this group has not synthesized it either. Both of our sets of data find that a carboxyl is important for DAF-12 binding. Furthermore, we both find that this carboxyl must be on a C27 sterol backbone, not the common C24 bile acid structure. Our derivatization bioassay data do suggest that a hydroxyl is important for the DAF-12

ligand by preventing bioactivity, but this modification may affect a non-specific factor unrelated to ligand binding such as uptake or proper metabolism. We did not more fully evaluate this finding nor did we investigate the importance of a keto group to bioactivity due to toxicity of the reagents. Our data parallel that of Motola *et al.* (2006) since we each provide evidence that DAF-9 does act as a CYP27A1 enzyme catalyzing carboxylation at the C27 position; however, they find that DAF-9 uses 3-keto sterols, and not 3-hydroxy sterols as we have hypothesized, as substrates. Interestingly, 3-keto sterols were not identified in a comprehensive analysis of *C. elegans*' sterols nor were they described by this group. Nevertheless, Motola *et al.* (2006) synthesize Δ^4 3-one-cholestenoic acid and provide significant biochemical evidence that it binds to DAF-12 with high affinity and transactivates DAF-12 in a cell-based assay. They also demonstrate that Δ^4 3-one-cholestenoic acid rescues the Daf-c phenotype of *daf-2(e1368)* and also show that it even rescues the Daf-c phenotype of the ligand-insensitive *daf-12(rh273)* though it does not rescue the gonadal migration defect. This suggests that there may be a separate DAF-12 ligand specific for gonad formation. Based on the nanomolar dissociation constant that Motola *et al.* (2006) find for 3-keto-cholestenoic acids and the ability, unlike Δ^5 cholestenoic acid, to rescue the Daf-c phenotype of *daf-12(rh273)*, it is likely that the 3-keto-cholestenoic acids are more potent and bioactive than the 3-hydroxy-cholestenoic acids.

When we re-examined our data in light of this publication we did find peaks that have an *m/z* 428 molecular ion that an esterified version of 3-keto-cholestenoic acids would have (data not shown). These also have a major fragment ion of *m/z* 271 that would correspond to loss of the side chain (data not shown). These peaks were of very

low abundance and were only detected by looking at the extracted ion chromatogram. Interestingly, they were only present in our *daf-12(m20)* bioactive extracts and not present in extracts from *daf-9(gk160) daf-12(m20)* which would be expected of the DAF-12 ligand. One possibility may be that both 3-keto and 3-hydroxy versions of cholestenoic acid are present in worms and act as ligands. However, if DAF-9 metabolizes only 3-keto sterols it is unclear how 3-hydroxy-cholestenoic acids would be produced. Potentially, the worm may metabolize 3-keto-cholestenoic acids to 3-hydroxy-cholestenoic acids and interconvert them. This is a future question that will need to be answered and will provide a better understanding of worm metabolism since the 3-hydroxy version may be the first step in metabolizing the DAF-12 ligand to an inactive form similar to the role of ecdysonoic acids in *Drosophila*.

Another possibility is that the 3-hydroxy-cholestenoic acids that we detect may simply be an artifact of the derivatization process for GC-MS during either the esterification or silylation procedure. Motola *et al.* (2006) analyzed underivatized samples by LC-MS and atmospheric pressure ionization. If the 3-keto group of a keto sterol were derivatized to a TMSO group it would become the identical compound to a 3-hydroxy sterol that was trimethylsilylated. Since 3-keto-cholestenoic acids are not commercially available, we derivatized both Δ^5 and Δ^7 3-keto sterols to see if they became the TMS version of cholesterol and lathosterol under our derivatization conditions (Figure 6.1 A-E). In the underivatized condition, the keto sterols, which do not need to be derivatized to be analyzed by GC-MS, are in high abundance (Figure 6.1 A). Dotriacontane (C32) is used as an internal standard for normalization. After both

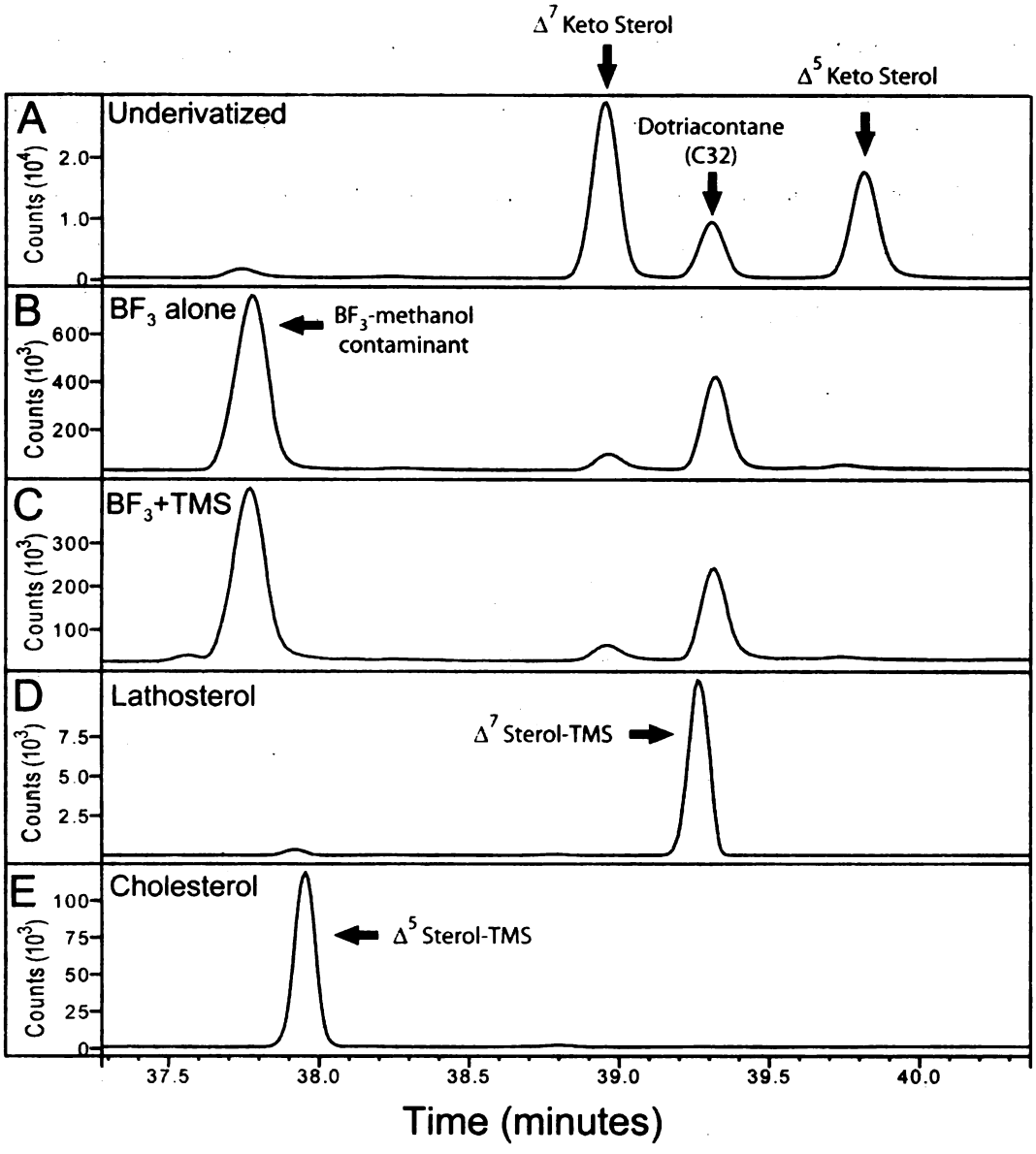
Δ7 Keto Sterol
Δ5 Keto Sterol
A
Underivatized
Dotriacontane
(C32)
Counts (10^4)
2.0
1.0
0
B
BF3 alone
BF3-methanol
contaminant
Counts (10^3)
600
400
200
C
BF3+TMS
Counts (10^3)
300
200
100
D
Lathosterol
Δ7 Sterol-TMS
Counts (10^3)
7.5
5.0
2.5
E
Cholesterol
Δ5 Sterol-TMS
Counts (10^3)
100
75
50
25
0
37.5
38.0
38.5
39.0
39.5
40.0
Time (minutes)

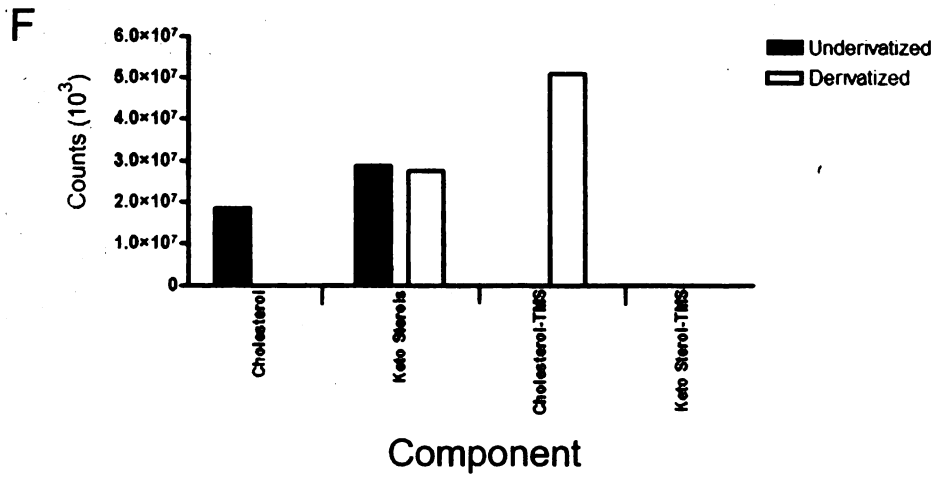
F
Counts (10^3)
6.0x10^7
5.0x10^7
4.0x10^7
3.0x10^7
2.0x10^7
1.0x10^7
0
Underivatized
Derivatized
Cholesterol
Keto Sterols
Cholesterol-TMS
Keto Sterol-TMS
Component

Figure 6.1 3-keto groups are not modified into a TMSO group by our esterification and silylation derivatization procedure. Δ^7 keto sterol and Δ^5 keto sterol were derivatized with BF_3 and BSTFA. TIC chromatogram of (A) Underivatized, (B) BF_3 esterified, and (C) BF_3 esterified and BSTFA silylated keto sterols. If silylated, these compounds would turn into lathosterol (Δ^7 sterol TMS) and cholesterol (Δ^5 sterol-TMS) and the retention of these compounds are shown in (D) and (E) respectively. (F) The peak areas of cholesterol and keto sterols and their respective TMS derivatives under underivatized and fully derivatized (BF_3 plus BSTFA) conditions.

BF_3-methanol and BSTFA derivatization (Figure 6.1 C), there is no trace of the TMS versions of the 3-keto sterols, TMS-lathosterol (Figure 6.1 D) or TMS-cholesterol (Figure 6.1 E), confirming that 3-hydroxy cholestenoic acids are not a derivatization artifact of 3-keto cholestenoic acids. However, this derivatization analysis did reveal that after BF_3-methanol treatment alone keto sterols are degraded significantly, which may explain why we only see a small amount of the compounds identified by Motola *et al.* (2006). Figure 6.1 F summarizes that 3-hydroxy sterols are only detected in underivatized conditions and are found completely in the TMS-derivatized form after our derivatization procedure. 3-keto sterols, on the other hand, are only found in their underivatized form (if not degraded by acetylation) even after derivatization. Future investigations using a less severe acetylation condition should help improve detection of 3-keto-cholestenoic acids along with 3-hydroxy-cholestenoic acids. Discovering 3-keto sterols and the steroid dehydrogenases that convert them from 3-hydroxy sterols will certainly provide important insight into worm development and lifespan regulation. Using stable isotope labeled sterols (Shoda et al., 1993) and GC-MS may be an ideal way to answer some of these questions.

It is clear that there is still a lot of work to be done to understand DAF-12 regulation of dauer formation, gonad migration, and longevity. Identification of cholestenoic acid as a DAF-12 ligand that rescues dauer formation and is also present in worm extracts is a step towards this goal. However, there are many new questions to be answered about the regulation of these ligands. With cholestenoic acid as the first orphan nuclear receptor ligand identified in *C. elegans* there are still 283 orphan receptors left to explore.

REFERENCE LIST

Agarwal,M.K. (1978). Physical characterisation of cytoplasmic gluco- and mineralo-steroid receptors. FEBS Lett. *85*, 1-8.

Ailion,M. and Thomas,J.H. (2000). Dauer formation induced by high temperatures in Caenorhabditis elegans. Genetics *156*, 1047-1067.

Albert,P.S., Brown,S.J., and Riddle,D.L. (1981). Sensory control of dauer larva formation in Caenorhabditis elegans. J Comp Neurol. *198*, 435-451.

Albert,P.S. and Riddle,D.L. (1988). Mutants of Caenorhabditis elegans that form dauer-like larvae. Dev. Biol *126*, 270-293.

Antebi,A., Culotti,J.G., and Hedgecock,E.M. (1998). daf-12 regulates developmental age and the dauer alternative in Caenorhabditis elegans. Development *125*, 1191-1205.

Antebi,A., Yeh,W.H., Tait,D., Hedgecock,E.M., and Riddle,D.L. (2000). daf-12 encodes a nuclear receptor that regulates the dauer diapause and developmental age in C. elegans. Genes Dev. *14*, 1512-1527.

Ao,W., Gaudet,J., Kent,W.J., Muttumu,S., and Mango,S.E. (2004). Environmentally induced foregut remodeling by PHA-4/FoxA and DAF-12/NHR. Science *305*, 1743-1746.

Arantes-Oliveira,N., Apfeld,J., Dillin,A., and Kenyon,C. (2002). Regulation of life-span by germ-line stem cells in Caenorhabditis elegans. Science *295*, 502-505.

Axelson,M., Mork,B., Aly,A., Walldius,G., and Sjovall,J. (1989a). Concentrations of cholestenoic acids in plasma from patients with reduced intestinal reabsorption of bile acids. J Lipid Res *30*, 1883-1887.

Axelson,M., Mork,B., Aly,A., Wisen,O., and Sjovall,J. (1989b). Concentrations of cholestenoic acids in plasma from patients with liver disease. J Lipid Res *30*, 1877-1882.

Axelson,M., Mork,B., and Everson,G.T. (1991). Bile acid synthesis in cultured human hepatoblastoma cells. J Biol Chem. *266*, 17770-17777.

Axelson,M., Mork,B., and Sjovall,J. (1988). Occurrence of 3 beta-hydroxy-5-cholestenoic acid, 3 beta,7 alpha-dihydroxy-5-cholestenoic acid, and 7 alpha-hydroxy-3-oxo-4-cholestenoic acid as normal constituents in human blood. J Lipid Res *29*, 629-641.

Baker,K.D., Shewchuk,L.M., Kozlova,T., Makishima,M., Hassell,A., Wisely,B., Caravella,J.A., Lambert,M.H., Reinking,J.L., Krause,H., Thummel,C.S., Willson,T.M., and Mangelsdorf,D.J. (2003). The Drosophila orphan nuclear receptor DHR38 mediates an atypical ecdysteroid signaling pathway. Cell *113*, 731-742.

Batta,A.K. and Salen,G. (1999). Gas chromatography of bile acids. J Chromatogr. B Biomed. Sci Appl. *723*, 1-16.

Bergman,T., Henrich,V.C., Schlattner,U., and Lezzi,M. (2004). Ligand control of interaction in vivo between ecdysteroid receptor and ultraspiracle ligand-binding domain. Biochem J *378*, 779-784.

Berkenstam,A., Farnegardh,M., and Gustafsson,J.A. (2004). Convergence of lipid homeostasis through liver X and thyroid hormone receptors. Mech. Ageing Dev. *125*, 707-717.

Berman,J.R. and Kenyon,C. (2006). Germ-cell loss extends C. elegans life span through regulation of DAF-16 by kri-1 and lipophilic-hormone signaling. Cell *124*, 1055-1068.

Billas,I.M., Iwema,T., Garnier,J.M., Mitschler,A., Rochel,N., and Moras,D. (2003). Structural adaptability in the ligand-binding pocket of the ecdysone hormone receptor. Nature *426*, 91-96.

Billas,I.M., Moulinier,L., Rochel,N., and Moras,D. (2001). Crystal structure of the ligand-binding domain of the ultraspiracle protein USP, the ortholog of retinoid X receptors in insects. J Biol Chem. *276*, 7465-7474.

Birnby,D.A., Link,E.M., Vowels,J.J., Tian,H., Colacurcio,P.L., and Thomas,J.H. (2000). A Transmembrane Guanylyl Cyclase (DAF-11) and Hsp90 (DAF-21) Regulate a Common Set of Chemosensory Behaviors in *Caenorhabditis elegans*. Genetics *155*, 85-104.

Bitsch,F., Aichholz,R., Kallen,J., Geisse,S., Fournier,B., and Schlaeppi,J.M. (2003). Identification of natural ligands of retinoic acid receptor-related orphan receptor alpha ligand-binding domain expressed in Sf9 cells--a mass spectrometry approach. Anal. Biochem *323*, 139-149.

Blumberg,B., Bolado,J., Jr., Derguini,F., Craig,A.G., Moreno,T.A., Chakravarti,D., Heyman,R.A., Buck,J., and Evans,R.M. (1996). Novel retinoic acid receptor ligands in Xenopus embryos. Proc. Natl. Acad. Sci U. S. A *93*, 4873-4878.

Blumberg,B., Kang,H., Bolado,J., Jr., Chen,H., Craig,A.G., Moreno,T.A., Umesono,K., Perlmann,T., De Robertis,E.M., and Evans,R.M. (1998). BXR, an embryonic orphan nuclear receptor activated by a novel class of endogenous benzoate metabolites. Genes Dev. *12*, 1269-1277.

Bogan,A.A., Cohen,F.E., and Scanlan,T.S. (1998). Natural ligands of nuclear receptors have conserved volumes. Nat Struct. Biol *5*, 679-681.

Bortolini,O., Medici,A., and Poli,S. (1997). Biotransformations on steroid nucleus of bile acids. Steroids *62*, 564-577.

Boudjelal,M., Wang,Z., Voorhees,J.J., and Fisher,G.J. (2000). Ubiquitin/proteasome pathway regulates levels of retinoic acid receptor gamma and retinoid X receptor alpha in human keratinocytes. Cancer Res *60*, 2247-2252.

Bourguet,W., Ruff,M., Chambon,P., Gronemeyer,H., and Moras,D. (1995). Crystal structure of the ligand-binding domain of the human nuclear receptor RXR-alpha. Nature *375*, 377-382.

Bramlett,K.S., Houck,K.A., Borchert,K.M., Dowless,M.S., Kulanthaivel,P., Zhang,Y., Beyer,T.P., Schmidt,R., Thomas,J.S., Michael,L.F., Barr,R., Montrose,C., Eacho,P.I., Cao,G., and Burris,T.P. (2003). A natural product ligand of the oxysterol receptor, liver X receptor. J Pharmacol. Exp. Ther. *307*, 291-296.

Bun-Ya,M., Maebuchi,M., Hashimoto,T., Yokota,S., and Kamiryo,T. (1997). A second isoform of 3-ketoacyl-CoA thiolase found in *Caenorhabditis elegans*, which is similar to sterol carrier protein x but lacks the sequence of sterol carrier protein 2. Eur. J Biochem *245*, 252-259.

Bun-Ya,M., Maebuchi,M., Togo,S.H., Kurosawa,T., Hashimoto,T., and Kamiryo,T. (2000). Metabolic significance and expression of *Caenorhabditis elegans* type II 3-oxoacyl-CoA thiolase. Cell Biochem Biophys. *32 Spring*, 291-293.

C. elegans Sequencing Consortium (1998). Genome sequence of the nematode *C. elegans*: a platform for investigating biology. Science *282*, 2012-2018.

Cali,J.J., Hsieh,C.L., Francke,U., and Russell,D.W. (1991). Mutations in the bile acid biosynthetic enzyme sterol 27-hydroxylase underlie cerebrotendinous xanthomatosis. J Biol Chem. *266*, 7779-7783.

Cali,J.J. and Russell,D.W. (1991). Characterization of human sterol 27-hydroxylase. A mitochondrial cytochrome P-450 that catalyzes multiple oxidation reaction in bile acid biosynthesis. J Biol Chem. *266*, 7774-7778.

Carmi,I., Kopczynski,J.B., and Meyer,B.J. (1998). The nuclear hormone receptor SEX-1 is an X-chromosome signal that determines nematode sex. Nature *396*, 168-173.

Cassada,R.C. and Russell,R.L. (1975). The dauerlarva, a post-embryonic developmental variant of the nematode *Caenorhabditis elegans*. Dev. Biol *46*, 326-342.

Cavailles,V., Dauvois,S., L'Horset,F., Lopez,G., Hoare,S., Kushner,P.J., and Parker,M.G. (1995). Nuclear factor RIP140 modulates transcriptional activation by the estrogen receptor. EMBO J *14*, 3741-3751.

Cazon Narvaez,A.V. and Suhring,S.S. (1999). A technique for extraction and thin layer chromatography visualization of fecal bile acids applied to neotropical felid scats. Rev. Biol Trop. *47*, 245-249.

Chawla,A., Repa,J.J., Evans,R.M., and Mangelsdorf,D.J. (2001). Nuclear receptors and lipid physiology: opening the X-files. Science *294*, 1866-1870.

Chen,J.H., Kabbouh,M., Fisher,M.J., and Rees,H.H. (1994). Induction of an inactivation pathway for ecdysteroids in larvae of the cotton leafworm, *Spodoptera littoralis*. Biochem J *301 (Pt 1)*, 89-95.

Chiang,J.Y. (2002). Bile acid regulation of gene expression: roles of nuclear hormone receptors. Endocr. Rev. *23*, 443-463.

Child,P. and Kuksis,A. (1979). Characterization of a wide range of isomeric natural and synthetic bile acids as the methyl ester acetates using thin-layer and gas-liquid chromaography. Natural Sciences *1*, 51-66.

Child,P., Kuksis,A., and Marai,L. (1979a). Preparation and mass spectral behaviour of some 5 beta-cholenoic acids. Can. J Biochem *57*, 216-225.

Child,P., Kuksis,A., and Myher,J.J. (1979b). Resolution of saturated and unsaturated 5 beta-cholanoic acids by gas-liquid and thin-layer chromatography. Can. J Biochem *57*, 639-644.

Chitwood,D.J. (1999). Biochemistry and function of nematode steroids. Crit Rev. Biochem Mol Biol *34*, 273-284.

Chitwood,D.J. and Lusby,W.R. (1991). Metabolism of plant sterols by nematodes. Lipids *26*, 619-627.

Chitwood,D.J., Lusby,W.R., Lozano,R., Thompson,M.J., and Svoboda,J.A. (1983). Novel nuclear methylation of sterols by the nematode *Caenorhabditis elegans*. Steroids *42*, 311-319.

Christensen,M., Estevez,A., Yin,X., Fox,R., Morrison,R., McDonnell,M., Gleason,C., Miller,D.M., III, and Strange,K. (2002). A primary culture system for functional analysis of *C. elegans* neurons and muscle cells. Neuron *33*, 503-514.

Chrivia,J.C., Kwok,R.P., Lamb,N., Hagiwara,M., Montminy,M.R., and Goodman,R.H. (1993). Phosphorylated CREB binds specifically to the nuclear protein CBP. Nature *365*, 855-859.

Clayton,G.M., Peak-Chew,S.Y., Evans,R.M., and Schwabe,J.W. (2001). The structure of the ultraspiracle ligand-binding domain reveals a nuclear receptor locked in an inactive conformation. Proc. Natl. Acad. Sci U. S. A *98*, 1549-1554.

Cleator,M., Delves,C.J., Howells,R.E., and Rees,H.H. (1987). Identity and tissue localization of free and conjugated ecdysteroids in adults of *Dirofilaria immitis* and *Ascaris suum*. Mol Biochem Parasitol. *25*, 93-105.

Cooper,A.D. (1997). Bile salt biosynthesis: an alternate synthetic pathway joins the mainstream. Gastroenterology *113*, 2005-2008.

Crowder,C.M., Westover,E.J., Kumar,A.S., Ostlund,R.E., Jr., and Covey,D.F. (2001). Enantiospecificity of cholesterol function in vivo. J Biol Chem. *276*, 44369-44372.

Dahlback,H. and Holmberg,I. (1990). Oxidation of 5 beta-cholestane-3 alpha,7 alpha, 12 alpha-triol into 3 alpha,7 alpha,12 alpha-trihydroxy-5 beta-cholestanoic acid by cytochrome P-450(26) from rabbit liver mitochondria. Biochem Biophys. Res Commun. *167*, 391-395.

Darimont,B.D., Wagner,R.L., Apriletti,J.W., Stallcup,M.R., Kushner,P.J., Baxter,J.D., Fletterick,R.J., and Yamamoto,K.R. (1998). Structure and specificity of nuclear receptor-coactivator interactions. Genes Dev. *12*, 3343-3356.

de Urquiza,A.M., Liu,S., Sjoberg,M., Zetterstrom,R.H., Griffiths,W., Sjovall,J., and Perlmann,T. (2000). Docosahexaenoic acid, a ligand for the retinoid X receptor in mouse brain. Science *290*, 2140-2144.

Dhe-Paganon,S., Duda,K., Iwamoto,M., Chi,Y.I., and Shoelson,S.E. (2002). Crystal structure of the HNF4 alpha ligand binding domain in complex with endogenous fatty acid ligand. J Biol Chem. *277*, 37973-37976.

Diekman,J. and Djerassi,C. (1967). Mass spectrometry in structural and stereochemical problems. CXXV. Mass spectrometry of some steroid trimethylsilyl ethers. J Org. Chem. *32*, 1005-1012.

Dillin,A., Crawford,D.K., and Kenyon,C. (2002). Timing requirements for insulin/IGF-1 signaling in *C. elegans*. Science *298*, 830-834.

Dinkova,T.D., Keiper,B.D., Korneeva,N.L., Aamodt,E.J., and Rhoads,R.E. (2005). Translation of a small subset of *Caenorhabditis elegans* mRNAs is dependent on a specific eukaryotic translation initiation factor 4E isoform. Mol Cell Biol *25*, 100-113.

Dowell,P., Otto,T.C., Adi,S., and Lane,M.D. (2003). Convergence of peroxisome proliferator-activated receptor gamma and Foxo1 signaling pathways. J Biol Chem. *278*, 45485-45491.

Duane,W.C. and Javitt,N.B. (1999). 27-hydroxycholesterol: production rates in normal human subjects. J Lipid Res *40*, 1194-1199.

Dussault,I., Yoo,H.D., Lin,M., Wang,E., Fan,M., Batta,A.K., Salen,G., Erickson,S.K., and Forman,B.M. (2003). Identification of an endogenous ligand that activates pregnane X receptor-mediated sterol clearance. Proc. Natl. Acad. Sci U. S. A *100*, 833-838.

Eadon,G., Popov,S., and Djerassi,C. (1972). Mass spectrometry in structural and stereochemical problems. CCXI. The effect of structural variations on the electron impact induced fragmentations of steroid hydrocarbons. J Am. Chem. Soc. *94*, 1282-1292.

Eckers,C., New,A.P., East,P.B., and Haskins,N.J. (1990). The use of tandem mass spectrometry for the differentiation of bile acid isomers and for the identification of bile acids in biological extracts. Rapid Commun. Mass Spectrom. *4*, 449-453.

Eckner,R., Ewen,M.E., Newsome,D., Gerdes,M., DeCaprio,J.A., Lawrence,J.B., and Livingston,D.M. (1994). Molecular cloning and functional analysis of the adenovirus E1A-associated 300-kD protein (p300) reveals a protein with properties of a transcriptional adaptor. Genes Dev. *8*, 869-884.

Egea,P.F., Mitschler,A., Rochel,N., Ruff,M., Chambon,P., and Moras,D. (2000). Crystal structure of the human RXRalpha ligand-binding domain bound to its natural ligand: 9-cis retinoic acid. EMBO J *19*, 2592-2601.

Elviri,L., Zagnoni,I., Careri,M., Cavazzini,D., and Rossi,G.L. (2001). Non-covalent binding of endogenous ligands to recombinant cellular retinol-binding proteins studied by mass spectrometric techniques. Rapid Commun. Mass Spectrom. *15*, 2186-2192.

Eneroth,P., Gordon,B., Ryhage,R., and Sjovall,J. (1966). Identification of mono- and dihydroxy bile acids in human feces by gas-liquid chromatography and mass spectrometry. J Lipid Res *7*, 511-523.

Entchev,E.V. and Kurzchalia,T.V. (2005). Requirement of sterols in the life cycle of the nematode *Caenorhabditis elegans*. Semin. Cell Dev. Biol *16*, 175-182.

Farnegardh,M., Bonn,T., Sun,S., Ljunggren,J., Ahola,H., Wilhelmsson,A., Gustafsson,J.A., and Carlquist,M. (2003). The three-dimensional structure of the liver X receptor beta reveals a flexible ligand-binding pocket that can accommodate fundamentally different ligands. J Biol Chem. *278*, 38821-38828.

Fisher,A.L. and Lithgow,G.J. (2006). The nuclear hormone receptor DAF-12 has opposing effects on *Caenorhabditis elegans* lifespan and regulates genes repressed in multiple long-lived worms. Aging Cell *5*, 127-138.

Fleming,M.W. (1993). Ecdysteroids during development in the ovine parasitic nematode, *Haemonchus contortus*. Comp Biochem Physiol B *104*, 653-655.

Forman,B.M., Goode,E., Chen,J., Oro,A.E., Bradley,D.J., Perlmann,T., Noonan,D.J., Burka,L.T., McMorris,T., Lamph,W.W., Evans,R.M., and Weinberger,C. (1995a). Identification of a nuclear receptor that is activated by farnesol metabolites. Cell *81*, 687-693.

Forman,B.M., Tontonoz,P., Chen,J., Brun,R.P., Spiegelman,B.M., and Evans,R.M. (1995b). 15-Deoxy-delta 12, 14-prostaglandin J2 is a ligand for the adipocyte determination factor PPAR gamma. Cell *83*, 803-812.

Fradera,X. and Mestres,J. (2004). Guided docking approaches to structure-based design and screening. Curr. Top. Med. Chem. *4*, 687-700.

Freedman,L.P. (1999). Increasing the complexity of coactivation in nuclear receptor signaling. Cell *97*, 5-8.

Fu,M., Wang,C., Zhang,X., and Pestell,R.G. (2004). Acetylation of nuclear receptors in cellular growth and apoptosis. Biochem Pharmacol. *68*, 1199-1208.

Fu,X., Menke,J.G., Chen,Y., Zhou,G., Macnaul,K.L., Wright,S.D., Sparrow,C.P., and Lund,E.G. (2001). 27-hydroxycholesterol is an endogenous ligand for liver X receptor in cholesterol-loaded cells. J Biol Chem. *276*, 38378-38387.

Galli,G. and Maroni,S. (1967). Mass spectrometric investigations of some unsaturated sterols biosynthetically related to cholesterol. Steroids *10*, 189-197.

Gampe,R.T., Jr., Montana,V.G., Lambert,M.H., Miller,A.B., Bledsoe,R.K., Milburn,M.V., Kliewer,S.A., Willson,T.M., and Xu,H.E. (2000). Asymmetry in the PPARgamma/RXRalpha crystal structure reveals the molecular basis of heterodimerization among nuclear receptors. Mol Cell *5*, 545-555.

Gehring,U. and Hotz,A. (1983). Photoaffinity labeling and partial proteolysis of wild-type and variant glucocorticoid receptors. Biochemistry *22*, 4013-4018.

Gems,D., Sutton,A.J., Sundermeyer,M.L., Albert,P.S., King,K.V., Edgley,M.L., Larsen,P.L.. and Riddle,D.L. (1998). Two pleiotropic classes of *daf-2* mutation affect larval arrest, adult behavior, reproduction and longevity in *Caenorhabditis elegans*. Genetics *150*, 129-155.

Gerisch,B. and Antebi,A. (2004). Hormonal signals produced by DAF-9/cytochrome P450 regulate *C. elegans* dauer diapause in response to environmental cues. Development *131*, 1765-1776.

Gerisch,B., Weitzel,C., Kober-Eisermann,C., Rottiers,V., and Antebi,A. (2001). A hormonal signaling pathway influencing *C. elegans* metabolism, reproductive development, and life span. Dev. Cell *1*, 841-851.

Gerst,N., Ruan,B., Pang,J., Wilson,W.K., and Schroepfer,G.J., Jr. (1997). An updated look at the analysis of unsaturated C27 sterols by gas chromatography and mass spectrometry. J Lipid Res *38*, 1685-1701.

Giguere,V., Yang,N., Segui,P., and Evans,R.M. (1988). Identification of a new class of steroid hormone receptors. Nature *331*, 91-94.

Gill,M.S., Held,J.M., Fisher,A.L., Gibson,B.W., and Lithgow,G.J. (2004). Lipophilic regulator of a developmental switch in Caenorhabditis elegans. Aging Cell *3*, 413-421.

Gissendanner,C.R., Crossgrove,K., Kraus,K.A., Maina,C.V., and Sluder,A.E. (2004). Expression and function of conserved nuclear receptor genes in *Caenorhabditis elegans*. Dev. Biol *266*, 399-416.

Gissendanner,C.R. and Sluder,A.E. (2000). nhr-25, the *Caenorhabditis elegans* ortholog of ftz-f1, is required for epidermal and somatic gonad development. Dev. Biol *221*, 259-272.

Glass,C.K. and Rosenfeld,M.G. (2000). The coregulator exchange in transcriptional functions of nuclear receptors. Genes Dev. *14*, 121-141.

Golden,J.W. and Riddle,D.L. (1982). A pheromone influences larval development in the nematode *Caenorhabditis elegans*. Science *218*, 578-580.

Golden,J.W. and Riddle,D.L. (1984). The *Caenorhabditis elegans* dauer larva: developmental effects of pheromone, food, and temperature. Dev. Biol *102*, 368-378.

Goldstein,J.T., Dobrzyn,A., Clagett-Dame,M., Pike,J.W., and DeLuca,H.F. (2003). Isolation and characterization of unsaturated fatty acids as natural ligands for the retinoid-X receptor. Arch. Biochem Biophys. *420*, 185-193.

Goto,J., Murao,N., Nakada,C., Motoyama,T., Oohashi,J., Yanagihara,T., Niwa,T., and Ikegawa,S. (1998). Separation and characterization of carboxyl-linked glucuronides of bile acids in incubation mixture of rat liver microsomes. Steroids *63*, 186-192.

Gottlieb,S. and Ruvkun,G. (1994). daf-2, daf-16 and daf-23: genetically interacting genes controlling Dauer formation in Caenorhabditis elegans. Genetics *137*, 107-120.

Grau,V. and Lafont,R. (1994). Metabolism of ecdysone and 20-hydroxyecdysone in adult *Drosophila melanogaster*. Insect Biochem Mol Biol *24*, 49-58.

Griffiths,W.J. (2003). Tandem mass spectrometry in the study of fatty acids, bile acids, and steroids. Mass Spectrom. Rev. *22*, 81-152.

Grosshans,H., Johnson,T., Reinert,K.L., Gerstein,M., and Slack,F.J. (2005). The temporal patterning microRNA *let-7* regulates several transcription factors at the larval to adult transition in *C. elegans*. Dev. Cell *8*, 321-330.

Hammer,G.D., Krylova,I., Zhang,Y., Darimont,B.D., Simpson,K., Weigel,N.L., and Ingraham,H.A. (1999). Phosphorylation of the nuclear receptor SF-1 modulates cofactor recruitment: integration of hormone signaling in reproduction and stress. Mol Cell *3*, 521-526.

Handschin,C. and Meyer,U.A. (2005). Regulatory network of lipid-sensing nuclear receptors: roles for CAR, PXR, LXR, and FXR. Arch. Biochem Biophys. *433*, 387-396.

Hashimoto,T. (1999). Peroxisomal beta-oxidation enzymes. Neurochem. Res *24*, 551-563.

Hayakawa,S. (1982). Microbial transformation of bile acids. A unified scheme for bile acid degradation, and hydroxylation of bile acids. Z. Allg. Mikrobiol. *22*, 309-326.

Hieb,W.F. and Rothstein,M. (1968). Sterol requirement for reproduction of a free-living nematode. Science *160*, 778-780.

Hoerer,S., Schmid,A., Heckel,A., Budzinski,R.M., and Nar,H. (2003). Crystal structure of the human liver X receptor beta ligand-binding domain in complex with a synthetic agonist. J Mol Biol *334*, 853-861.

Hofmann,A.F. (1999). The continuing importance of bile acids in liver and intestinal disease. Arch. Intern. Med. *159*, 2647-2658.

Hofmann,A.F. and Small,D.M. (1967). Detergent properties of bile salts: correlation with physiological function. Annu. Rev. Med. *18*, 333-376.

Hollenberg,S.M., Weinberger,C., Ong,E.S., Cerelli,G., Oro,A., Lebo,R., Thompson,E.B., Rosenfeld,M.G., and Evans,R.M. (1985). Primary structure and expression of a functional human glucocorticoid receptor cDNA. Nature *318*, 635-641.

Hsin,H. and Kenyon,C. (1999). Signals from the reproductive system regulate the lifespan of *C. elegans*. Nature *399*, 362-366.

Ichimiya,H., Egestad,B., Nazer,H., Baginski,E.S., Clayton,P.T., and Sjovall,J. (1991). Bile acids and bile alcohols in a child with hepatic 3 beta-hydroxy-delta 5-C27-steroid dehydrogenase deficiency: effects of chenodeoxycholic acid treatment. J Lipid Res *32*, 829-841.

Isaac,R.E., Milner,N.P., and Rees,H.H. (1983). Identification of ecdysonoic acid and 20-hydroxyecdysonoic acid isolated from developing eggs of *Schistocerca gregaria* and pupae of *Spodoptera littoralis*. Biochem J *213*, 261-265.

Isaac,R.E. and Rees,H.H. (1984). Isolation and identification of ecdysteroid phosphates and acetylecdysteroid phosphates from developing eggs of the locust, *Schistocerca gregaria*. Biochem J *221*, 459-464.

Jacobs,M.N., Dickins,M., and Lewis,D.F. (2003). Homology modelling of the nuclear receptors: human oestrogen receptorbeta (hERbeta), the human pregnane-X-receptor (PXR), the Ah receptor (AhR) and the constitutive androstane receptor (CAR) ligand binding domains from the human oestrogen receptor alpha (hERalpha) crystal structure, and the human peroxisome proliferator activated receptor alpha (PPARalpha) ligand binding domain from the human PPARgamma crystal structure. J Steroid Biochem Mol Biol *84*, 117-132.

Janowski,B.A., Willy,P.J., Devi,T.R., Falck,J.R., and Mangelsdorf,D.J. (1996). An oxysterol signalling pathway mediated by the nuclear receptor LXR alpha. Nature *383*, 728-731.

Javitt,N.B. (2000). Biologic role(s) of the 25(R),26-hydroxycholesterol metabolic pathway. Biochim. Biophys. Acta *1529*, 136-141.

Javitt,N.B. (2002a). 25R,26-Hydroxycholesterol revisited: synthesis, metabolism, and biologic roles. J Lipid Res *43*, 665-670.

Javitt,N.B. (2002b). Cholesterol, hydroxycholesterols, and bile acids. Biochem Biophys. Res Commun. *292*, 1147-1153.

Javitt,N.B., Kok,E., Carubbi,F., Blizzard,T., Gut,M., and Byon,C.Y. (1986). Bile acid synthesis. Metabolism of 3 beta-hydroxy-5-cholenoic acid to chenodeoxycholic acid. J Biol Chem. *261*, 12486-12489.

Jeong,P.Y., Jung,M., Yim,Y.H., Kim,H., Park,M., Hong,E., Lee,W., Kim,Y.H., Kim,K., and Paik,Y.K. (2005). Chemical structure and biological activity of the *Caenorhabditis elegans* dauer-inducing pheromone. Nature *433*, 541-545.

Jia,K., Albert,P.S., and Riddle,D.L. (2002). DAF-9, a cytochrome P450 regulating *C. elegans* larval development and adult longevity. Development *129*, 221-231.

Johnson,S.M., Lin,S.Y., and Slack,F.J. (2003). The time of appearance of the *C. elegans let-7* microRNA is transcriptionally controlled utilizing a temporal regulatory element in its promoter. Dev. Biol *259*, 364-379.

Jones,G. and Sharp,P.A. (1997). Ultraspiracle: an invertebrate nuclear receptor for juvenile hormones. Proc. Natl. Acad. Sci U. S. A *94*, 13499-13503.

Jones,G., Wozniak,M., Chu,Y., Dhar,S., and Jones,D. (2001). Juvenile hormone III-dependent conformational changes of the nuclear receptor ultraspiracle. Insect Biochem Mol Biol *32*, 33-49.

Kaluzny,M.A., Duncan,L.A., Merritt,M.V., and Epps,D.E. (1985). Rapid separation of lipid classes in high yield and purity using bonded phase columns. J Lipid Res *26*, 135-140.

Katzenellenbogen,B.S., Montano,M.M., Ediger,T.R., Sun,J., Ekena,K., Lazennec,G., Martini,P.G., McInerney,E.M., Delage-Mourroux,R., Weis,K., and Katzenellenbogen,J.A. (2000). Estrogen receptors: selective ligands, partners, and distinctive pharmacology. Recent Prog. Horm. Res *55*, 163-193.

Katzenellenbogen,J.A., O'Malley,B.W., and Katzenellenbogen,B.S. (1996). Tripartite steroid hormone receptor pharmacology: interaction with multiple effector sites as a basis for the cell- and promoter-specific action of these hormones. Mol Endocrinol *10*, 119-131.

Kenyon,C. (2005). The plasticity of aging: insights from long-lived mutants. Cell *120*, 449-460.

Khan,M.A., Wang,Y., Heidelberger,S., Alvelius,G., Liu,S., Sjovall,J., and Griffiths,W.J. (2006). Analysis of derivatised steroids by matrix-assisted laser desorption/ionisation and post-source decay mass spectrometry. Steroids *71*, 42-53.

King-Jones,K. and Thummel,C.S. (2005). Nuclear receptors--a perspective from *Drosophila*. Nat Rev. Genet. *6*, 311-323.

Kliewer,S.A., Lenhard,J.M., Willson,T.M., Patel,I., Morris,D.C., and Lehmann,J.M. (1995). A prostaglandin J2 metabolite binds peroxisome proliferator-activated receptor gamma and promotes adipocyte differentiation. Cell *83*, 813-819.

Knapp,F.F., Jr. and Schroepfer,G.J., Jr. (1976). Mass spectrometry of sterols. Electron ionization induced fragmentation of C-4-alkylated cholesterols. Chem. Phys. Lipids *17*, 466-500.

Knapp,F.F., Wilson,M.S., and Schroepfer,G.J., Jr. (1976). Mass spectral fragmentation of 5alpha-hydroxysteroids. Chem. Phys. Lipids *16*, 31-59.

Kniazeva,M., Crawford,Q.T., Seiber,M., Wang,C.Y., and Han,M. (2004). Monomethyl branched-chain fatty acids play an essential role in *Caenorhabditis elegans* development. PLoS Biol *2*, E257.

Koelle,M.R., Talbot,W.S., Segraves,W.A., Bender,M.T., Cherbas,P., and Hogness,D.S. (1991). The *Drosophila* EcR gene encodes an ecdysone receptor, a new member of the steroid receptor superfamily. Cell *67*, 59-77.

Kostrouchova,M., Krause,M., Kostrouch,Z., and Rall,J.E. (2001). Nuclear hormone receptor CHR3 is a critical regulator of all four larval molts of the nematode *Caenorhabditis elegans*. Proc. Natl. Acad. Sci U. S. A *98*, 7360-7365.

Kozlova,T., Pokholkova,G.V., Tzertzinis,G., Sutherland,J.D., Zhimulev,I.F., and Kafatos,F.C. (1998). *Drosophila* hormone receptor 38 functions in metamorphosis: a role in adult cuticle formation. Genetics *149*, 1465-1475.

Kralli,A., Bohen,S.P., and Yamamoto,K.R. (1995). LEM1, an ATP-binding-cassette transporter, selectively modulates the biological potency of steroid hormones. Proc. Natl. Acad. Sci U. S. A *92*, 4701-4705.

Krumrine,J., Raubacher,F., Brooijmans,N., and Kuntz,I. (2003). Principles and methods of docking and ligand design. Methods Biochem Anal. *44*, 443-476.

Krylova,I.N., Sablin,E.P., Moore,J., Xu,R.X., Waitt,G.M., MacKay,J.A., Juzumiene,D., Bynum,J.M., Madauss,K., Montana,V., Lebedeva,L., Suzawa,M., Williams,J.D., Williams,S.P., Guy,R.K., Thornton,J.W., Fletterick,R.J., Willson,T.M., and Ingraham,H.A. (2005). Structural analyses reveal phosphatidyl inositols as ligands for the NR5 orphan receptors SF-1 and LRH-1. Cell *120*, 343-355.

Kuervers,L.M., Jones,C.L., O'Neil,N.J., and Baillie,D.L. (2003). The sterol modifying enzyme LET-767 is essential for growth, reproduction and development in *Caenorhabditis elegans*. Mol Genet. Genomics *270*, 121-131.

Kuksis,A. and Child,P. (1980). Analysis and structure determination of unsaturated 5 beta - cholanoic acids. Lipids *15*, 770-782.

Kulkarni,B. and Javitt,N.B. (1982). Chenodeoxycholic acid synthesis in the hamster: a metabolic pathway via 3 beta, 7 alpha-dihydroxy-5-cholen-24-oic acid. Steroids *40*, 581-589.

Kumar,M.B., Potter,D.W., Hormann,R.E., Edwards,A., Tice,C.M., Smith,H.C., Dipietro,M.A., Polley,M., Lawless,M., Wolohan,P.R., Kethidi,D.R., and Palli,S.R. (2004). Highly flexible ligand binding pocket of ecdysone receptor: a single amino acid change leads to discrimination between two groups of nonsteroidal ecdysone agonists. J Biol Chem. *279*, 27211-27218.

Lachaise,F. and Lafont,R. (1984). Ecdysteroid metabolism in a crab: *Carcinus maenas L.* Steroids *43*, 243-259.

Lafont,R., Blais,C., Beydon,P., Modde,J., Enderle,U., and Koolman,J. (1983). Conversion of ecdysone and 20-hydroxyecdysone into 26-OIC derivatives is a major pathway in larvae and pupae of species from three insect orders. Arch. Insect Biochem Physiol *1*, 41-58.

Larsen,P.L., Albert,P.S., and Riddle,D.L. (1995). Genes that regulate both development and longevity in *Caenorhabditis elegans*. Genetics *139*, 1567-1583.

Lehmann,J.M., Kliewer,S.A., Moore,L.B., Smith-Oliver,T.A., Oliver,B.B., Su,J.L., Sundseth,S.S., Winegar,D.A., Blanchard,D.E., Spencer,T.A., and Willson,T.M. (1997). Activation of the nuclear receptor LXR by oxysterols defines a new hormone response pathway. J Biol Chem. *272*, 3137-3140.

Lemonde,H.A., Johnson,A.W., and Clayton,P.T. (1999). The identification of unusual bile acid metabolites by tandem mass spectrometry: use of low-energy collision-induced dissociation to produce informative spectra. Rapid Commun. Mass Spectrom. *13*, 1159-1164.

Lengqvist,J., Alvelius,G., Jornvall,H., Sjovall,J., Perlmann,T., and Griffiths,W.J. (2005a). Electrospray mass spectrometry for the direct accurate mass measurement of ligands in complex with the retinoid X receptor alpha ligand binding domain. J Am. Soc. Mass Spectrom. *16*, 1631-1640.

Lengqvist,J., Mata,d.U., Perlmann,T., Sjovall,J., and Griffiths,W.J. (2005b). Specificity of receptor-ligand interactions and their effect on dimerisation as observed by electrospray mass spectrometry: bile acids form stable adducts to the RXRalpha. J Mass Spectrom. *40*, 1448-1461.

Li,J., Brown,G., Ailion,M., Lee,S., and Thomas,J.H. (2004). NCR-1 and NCR-2, the *C. elegans* homologs of the human Niemann-Pick type C1 disease protein, function upstream of DAF-9 in the dauer formation pathways. Development *131*, 5741-5752.

Lindblom,T.H., Pierce,G.J., and Sluder,A.E. (2001). A *C. elegans* orphan nuclear receptor contributes to xenobiotic resistance. Curr. Biol *11*, 864-868.

Ludewig,A.H., Kober-Eisermann,C., Weitzel,C., Bethke,A., Neubert,K., Gerisch,B., Hutter,H., and Antebi,A. (2004). A novel nuclear receptor/coregulator complex controls *C. elegans* lipid metabolism, larval development, and aging. Genes Dev. *18*, 2120-2133.

Maebuchi,M., Togo,S.H., Yokota,S., Ghenea,S., Bun-Ya,M., Kamiryo,T., and Kawahara,A. (1999). Type-II 3-oxoacyl-CoA thiolase of the nematode *Caenorhabditis elegans* is located in peroxisomes, highly expressed during larval stages and induced by clofibrate. Eur. J Biochem *264*, 509-515.

Mak,H.Y. and Ruvkun,G. (2004). Intercellular signaling of reproductive development by the *C. elegans* DAF-9 cytochrome P450. Development *131*, 1777-1786.

Makishima,M., Okamoto,A.Y., Repa,J.J., Tu,H., Learned,R.M., Luk,A., Hull,M.V., Lustig,K.D., Mangelsdorf,D.J., and Shan,B. (1999). Identification of a nuclear receptor for bile acids. Science *284*, 1362-1365.

Malone,E.A., Inoue,T., and Thomas,J.H. (1996). Genetic analysis of the roles of daf-28 and age-1 in regulating Caenorhabditis elegans dauer formation. Genetics *143*, 1193-1205.

Mammato,D.C. and Eadon,G.A. (1975). Concerning the mechanism of the characteristic ring D fragmentation of steroids. J Org. Chem. *40*, 1784-1792.

Mangelsdorf,D.J. and Evans,R.M. (1995). The RXR heterodimers and orphan receptors. Cell *83*, 841-850.

Matyash,V., Entchev,E.V., Mende,F., Wilsch-Brauninger,M., Thiele,C., Schmidt,A.W., Knolker,H.J., Ward,S., and Kurzchalia,T.V. (2004). Sterol-derived hormone(s) controls entry into diapause in *Caenorhabditis elegans* by consecutive activation of DAF-12 and DAF-16. PLoS Biol *2*, e280.

Matyash,V., Geier,C., Henske,A., Mukherjee,S., Hirsh,D., Thiele,C., Grant,B., Maxfield,F.R., and Kurzchalia,T.V. (2001). Distribution and transport of cholesterol in *Caenorhabditis elegans*. Mol Biol Cell *12*, 1725-1736.

McKenna,N.J., Lanz,R.B., and O'Malley,B.W. (1999a). Nuclear receptor coregulators: cellular and molecular biology. Endocr. Rev. *20*, 321-344.

McKenna,N.J., Nawaz,Z., Tsai,S.Y., Tsai,M.J., and O'Malley,B.W. (1998). Distinct steady-state nuclear receptor coregulator complexes exist in vivo. Proc. Natl. Acad. Sci U. S. A *95*, 11697-11702.

McKenna,N.J., Xu,J., Nawaz,Z., Tsai,S.Y., Tsai,M.J., and O'Malley,B.W. (1999b). Nuclear receptor coactivators: multiple enzymes, multiple complexes, multiple functions. J Steroid Biochem Mol Biol *69*, 3-12.

Meaney,S., Babiker,A., Lutjohann,D., Diczfalusy,U., Axelson,M., and Bjorkhem,I. (2003). On the origin of the cholestenoic acids in human circulation. Steroids *68*, 595-601.

Mendis,A.H., Rose,M.E., Rees,H.H., and Goodwin,T.W. (1983). Ecdysteroids in adults of the nematode, *Dirofilaria immitis*. Mol Biochem Parasitol. *9*, 209-226.

Menke,J.G., Macnaul,K.L., Hayes,N.S., Baffic,J., Chao,Y.S., Elbrecht,A., Kelly,L.J., Lam,M.H., Schmidt,A., Sahoo,S., Wang,J., Wright,S.D., Xin,P., Zhou,G., Moller,D.E., and Sparrow,C.P. (2002). A novel liver X receptor agonist establishes species differences in the regulation of cholesterol 7alpha-hydroxylase (CYP7a). Endocrinology *143*, 2548-2558.

Mercer,J.G., Munn,A.E., and Rees,H.H. (1988). *Caenorhabditis elegans*: occurrence and metabolism of ecdysteroids in adults and dauer larvae. Comp Biochem Physiol B *90*, 261-267.

Merris,M., Kraeft,J., Tint,G.S., and Lenard,J. (2004). Long-term effects of sterol depletion in *C. elegans*: sterol content of synchronized wild-type and mutant populations. J Lipid Res *45*, 2044-2051.

Merris,M., Wadsworth,W.G., Khamrai,U., Bittman,R., Chitwood,D.J., and Lenard,J. (2003). Sterol effects and sites of sterol accumulation in *Caenorhabditis elegans*: developmental requirement for 4alpha-methyl sterols. J Lipid Res *44*, 172-181.

Mi,L.Z., Devarakonda,S., Harp,J.M., Han,Q., Pellicciari,R., Willson,T.M., Khorasanizadeh,S., and Rastinejad,F. (2003). Structural basis for bile acid binding and activation of the nuclear receptor FXR. Mol Cell *11*, 1093-1100.

Miller,W.L. (1988). Molecular biology of steroid hormone synthesis. Endocr. Rev. *9*, 295-318.

Mims,D. and Hercules,D. (2003). Quantification of bile acids directly from urine by MALDI-TOF-MS. Anal. Bioanal. Chem. *375*, 609-616.

Mims,D. and Hercules,D. (2004). Quantification of bile acids directly from plasma by MALDI-TOF-MS. Anal. Bioanal. Chem. *378*, 1322-1326.

Mooijaart,S.P., Brandt,B.W., Baldal,E.A., Pijpe,J., Kuningas,M., Beekman,M., Zwaan,B.J., Slagboom,P.E., Westendorp,R.G., and van Heemst,D. (2005). *C. elegans* DAF-12, Nuclear Hormone Receptors and human longevity and disease at old age. Ageing Res Rev. *4*, 351-371.

Moss,E.G. and Tang,L. (2003). Conservation of the heterochronic regulator Lin-28, its developmental expression and microRNA complementary sites. Dev. Biol *258*, 432-442.

Motola,D.L., Cummins,C.L., Rottiers,V., Sharma,K.K., Li,T., Li,Y., Suino-Powell,K., Xu,H.E., Auchus,R.J., Antebi,A., and Mangelsdorf,D.J. (2006). Identification of ligands

for DAF-12 that govern dauer formation and reproduction in *C. elegans*. Cell *124*, 1209-1223.

Nasal,A., Siluk,D., and Kaliszan,R. (2003). Chromatographic retention parameters in medicinal chemistry and molecular pharmacology. Curr. Med. Chem. *10*, 381-426.

Nelson,D.R. (1998). Metazoan cytochrome P450 evolution. Comp Biochem Physiol C. Pharmacol. Toxicol. Endocrinol *121*, 15-22.

Nelson,D.R. (1999). Cytochrome P450 and the individuality of species. Arch. Biochem Biophys. *369*, 1-10.

Nicolaou,K.C., Evans,R.M., Roecker,A.J., Hughes,R., Downes,M., and Pfefferkorn,J.A. (2003). Discovery and optimization of non-steroidal FXR agonists from natural product-like libraries. Org. Biomol. Chem. *1*, 908-920.

Nishimaki-Mogami,T., Une,M., Fujino,T., Sato,Y., Tamehiro,N., Kawahara,Y., Shudo,K., and Inoue,K. (2004). Identification of intermediates in the bile acid synthetic pathway as ligands for the farnesoid X receptor. J Lipid Res *45*, 1538-1545.

Nolte,R.T., Wisely,G.B., Westin,S., Cobb,J.E., Lambert,M.H., Kurokawa,R., Rosenfeld,M.G., Willson,T.M., Glass,C.K., and Milburn,M.V. (1998). Ligand binding and co-activator assembly of the peroxisome proliferator-activated receptor-gamma. Nature *395*, 137-143.

Nwokoro,N.A., Wassif,C.A., and Porter,F.D. (2001). Genetic disorders of cholesterol biosynthesis in mice and humans. Mol Genet. Metab *74*, 105-119.

O'Hanlon,G.M., Cleator,M., Mercer,J.G., Howells,R.E., and Rees,H.H. (1991). Metabolism and fate of ecdysteroids in the nematodes *Ascaris suum* and *Parascaris equorum*. Mol Biochem Parasitol. *47*, 179-187.

O'Malley,B. (1990). The steroid receptor superfamily: more excitement predicted for the future. Mol Endocrinol *4*, 363-369.

Oftebro,H., Bjorkhem,I., Skrede,S., Schreiner,A., and Pederson,J.I. (1980). Cerebrotendinous xanthomatosis: a defect in mitochondrial 26-hydroxylation required for normal biosynthesis of cholic acid. J Clin. Invest *65*, 1418-1430.

Ohkura,K., Suzuki,N., Ishihara,T., and Katsura,I. (2003). SDF-9, a protein tyrosine phosphatase-like molecule, regulates the L3/dauer developmental decision through hormonal signaling in *C. elegans*. Development *130*, 3237-3248.

Onate,S.A., Tsai,S.Y., Tsai,M.J., and O'Malley,B.W. (1995). Sequence and characterization of a coactivator for the steroid hormone receptor superfamily. Science *270*, 1354-1357.

Ory,D.S. (2004). Nuclear receptor signaling in the control of cholesterol homeostasis: have the orphans found a home? Circ Res *95*, 660-670.

Otte,K., Kranz,H., Kober,I., Thompson,P., Hoefer,M., Haubold,B., Remmel,B., Voss,H., Kaiser,C., Albers,M., Cheruvallath,Z., Jackson,D., Casari,G., Koegl,M., Paabo,S., Mous,J., Kremoser,C., and Deuschle,U. (2003). Identification of farnesoid X receptor beta as a novel mammalian nuclear receptor sensing lanosterol. Mol Cell Biol *23*, 864-872.

Pagano,M., Mirshahi,M., Mirshahi,F., Monnot,M., Lazar,G., Chassaing,C.G., Fermandjian,S., and Agarwal,M.K. (1994). Properties of the mineralocorticoid receptor immunopurified from bovine kidney. Biochem Pharmacol. *48*, 1163-1169.

Parks,D.J., Blanchard,S.G., Bledsoe,R.K., Chandra,G., Consler,T.G., Kliewer,S.A., Stimmel,J.B., Willson,T.M., Zavacki,A.M., Moore,D.D., and Lehmann,J.M. (1999). Bile acids: natural ligands for an orphan nuclear receptor. Science *284*, 1365-1368.

Parmentier,G.G., Janssen,G.A., Eggermont,E.A., and Eyssen,H.J. (1979). C27 bile acids in infants with coprostanic acidemia and occurrence of a 3 alpha,7 alpha,12 alpha-tridhydroxy-5 beta-C29 dicarboxylic bile acid as a major component in their serum. Eur. J Biochem *102*, 173-183.

Partridge,L.G. and Djerassi,C. (1977). Mass spectrometry in structural and stereochemical problems. 250. Characteristic fragmentations of cholesterol acetate. J Org. Chem. *42*, 2799-2805.

Partridge,L.G., Midgley,I., and Djerassi,C. (1977). Mass spectrometry in structural and stereochemical problems. 249. Elucidation of the course of the characteristic ting D fragmentation of unsaturated steroids. J Am. Chem. Soc. *99*, 7686-7695.

Patterson,G.I. and Padgett,R.W. (2000). TGF[beta]-related pathways: roles in *Caenorhabditis elegans* development. Trends in Genetics *16*, 27-33.

Pelillo,M., Galletti,G., and Lercker,G. (2000). Mass spectral fragmentations of cholesterol acetate oxidation products. Rapid Commun. Mass Spectrom. *14*, 1275-1279.

Perera,S.C., Zheng,S., Feng,Q.L., Krell,P.J., Retnakaran,A., and Palli,S.R. (2005). Heterodimerization of ecdysone receptor and ultraspiracle on symmetric and asymmetric response elements. Arch. Insect Biochem Physiol *60*, 55-70.

Perissi,V., Staszewski,L.M., McInerney,E.M., Kurokawa,R., Krones,A., Rose,D.W., Lambert,M.H., Milburn,M.V., Glass,C.K., and Rosenfeld,M.G. (1999). Molecular determinants of nuclear receptor-corepressor interaction. Genes Dev. *13*, 3198-3208.

Perwaiz,S., Tuchweber,B., Mignault,D., Gilat,T., and Yousef,I.M. (2001). Determination of bile acids in biological fluids by liquid chromatography-electrospray tandem mass spectrometry. J Lipid Res *42*, 114-119.

Pikuleva,I. and Javitt,N.B. (2003). Novel sterols synthesized via the CYP27A1 metabolic pathway. Arch. Biochem Biophys. *420*, 35-39.

Pikuleva,I.A., Babiker,A., Waterman,M.R., and Bjorkhem,I. (1998). Activities of recombinant human cytochrome P450c27 (CYP27) which produce intermediates of alternative bile acid biosynthetic pathways. J Biol Chem. *273*, 18153-18160.

Pollack,J.D., Clark,D.S., and Somerson,N.L. (1971). Four-directional-development thin-layer chromatography of lipids using trimethyl borate. J Lipid Res *12*, 563-569.

Popov,S., Carlson,R.M., Wegmann,A., and Djerassi,C. (1976). Minor and trace sterols in marine invertebrates. 1. General methods of analysis. Steroids *28*, 699-732.

Potier,N., Billas,I.M., Steinmetz,A., Schaeffer,C., van Dorsselaer,A., Moras,D., and Renaud,J.P. (2003). Using nondenaturing mass spectrometry to detect fortuitous ligands in orphan nuclear receptors. Protein Sci *12*, 725-733.

Pulfer,M.K. and Murphy,R.C. (2004). Formation of biologically active oxysterols during ozonolysis of cholesterol present in lung surfactant. J Biol Chem. *279*, 26331-26338.

Qin,H. and Powell-Coffman,J.A. (2004). The Caenorhabditis elegans aryl hydrocarbon receptor, AHR-1, regulates neuronal development. Dev. Biol. *270*, 64-75.

Rachez,C., Suldan,Z., Ward,J., Chang,C.P., Burakov,D., Erdjument-Bromage,H., Tempst,P., and Freedman,L.P. (1998). A novel protein complex that interacts with the vitamin D3 receptor in a ligand-dependent manner and enhances VDR transactivation in a cell-free system. Genes Dev. *12*, 1787-1800.

Rastinejad,F., Perlmann,T., Evans,R.M., and Sigler,P.B. (1995). Structural determinants of nuclear receptor assembly on DNA direct repeats. Nature *375*, 203-211.

Reinhart.B.J., Slack,F.J., Basson,M., Pasquinelli,A.E., Bettinger,J.C., Rougvie,A.E., Horvitz,H.R., and Ruvkun,G. (2000). The 21-nucleotide *let-7* RNA regulates developmental timing in *Caenorhabditis elegans*. Nature *403*, 901-906.

Riddle,D.L. and Albert,P.S. (1997). Genetic and environmental regulation of dauer larva development. In C. elegans II, (Cold Spring Harbor, NY: Cold Spring Harbor Laboratory Press), pp. 739-768.

Riddle,D.L., Swanson,M.M., and Albert,P.S. (1981). Interacting genes in nematode dauer larva formation. Nature *290*, 668-671.

Russell,D.W. (1999). Nuclear orphan receptors control cholesterol catabolism. Cell *97*, 539-542.

Russell,D.W. (2003). The enzymes, regulation, and genetics of bile acid synthesis. Annu. Rev. Biochem *72*, 137-174.

Ryhage,R. and stenhagen,E. (1960). Mass spectrometry in lipid research. J Lipid Res *1*, 361-390.

Scalia,S. (1995). Bile acid separation. J Chromatogr. B Biomed. Appl. *671*, 299-317.

Schapira,M., Raaka,B.M., Das,S., Fan,L., Totrov,M., Zhou,Z., Wilson,S.R., Abagyan,R., and Samuels,H.H. (2003). Discovery of diverse thyroid hormone receptor antagonists by high-throughput docking. Proc. Natl. Acad. Sci U. S. A *100*, 7354-7359.

Schwarz,M., Russell,D.W., Dietschy,J.M., and Turley,S.D. (1998). Marked reduction in bile acid synthesis in cholesterol 7alpha-hydroxylase-deficient mice does not lead to diminished tissue cholesterol turnover or to hypercholesterolemia. J Lipid Res *39*, 1833-1843.

Seggerson,K., Tang,L., and Moss,E.G. (2002). Two genetic circuits repress the *Caenorhabditis elegans* heterochronic gene lin-28 after translation initiation. Dev. Biol *243*, 215-225.

Seol,W., Choi,H.S., and Moore,D.D. (1996). An orphan nuclear hormone receptor that lacks a DNA binding domain and heterodimerizes with other receptors. Science *272*, 1336-1339.

Setchell,K.D., Lawson,A.M., Tanida,N., and Sjovall,J. (1983). General methods for the analysis of metabolic profiles of bile acids and related compounds in feces. J Lipid Res *24*, 1085-1100.

Setchell,K.D., Schwarz,M., O'Connell,N.C., Lund,E.G., Davis,D.L., Lathe,R., Thompson,H.R., Weslie,T.R., Sokol,R.J., and Russell,D.W. (1998). Identification of a new inborn error in bile acid synthesis: mutation of the oxysterol 7alpha-hydroxylase gene causes severe neonatal liver disease. J Clin. Invest *102*, 1690-1703.

Setoguchi,T., Salen,G., Tint,G.S., and Mosbach,E.H. (1974). A biochemical abnormality in cerebrotendinous xanthomatosis. Impairment of bile acid biosynthesis associated with incomplete degradation of the cholesterol side chain. J Clin. Invest *53*, 1393-1401.

Shea,C., Hough,D., Xiao,J., Tzertzinis,G., and Maina,C.V. (2004). An rxr/usp homolog from the parasitic nematode, *Dirofilaria immitis*. Gene *324*, 171-182.

Shiau,A.K., Barstad,D., Loria,P.M., Cheng,L., Kushner,P.J., Agard,D.A., and Greene,G.L. (1998). The structural basis of estrogen receptor/coactivator recognition and the antagonism of this interaction by tamoxifen. Cell *95*, 927-937.

Shim,Y.H., Chun,J.H., Lee,E.Y., and Paik,Y.K. (2002). Role of cholesterol in germ-line development of *Caenorhabditis elegans*. Mol Reprod. Dev. *61*, 358-366.

Shoda,J., Axelson,M., and Sjovall,J. (1993). Synthesis of potential C27-intermediates in bile acid biosynthesis and their deuterium-labeled analogs. Steroids *58*, 119-125.

Shostak,Y., Van Gilst,M.R., Antebi,A., and Yamamoto,K.R. (2004). Identification of *C. elegans* DAF-12-binding sites, response elements, and target genes. Genes Dev. *18*, 2529-2544.

Simons,S.S., Jr. and Thompson,E.B. (1981). Dexamethasone 21-mesylate: an affinity label of glucocorticoid receptors from rat hepatoma tissue culture cells. Proc. Natl. Acad. Sci U. S. A *78*, 3541-3545.

Sluder,A.E. and Maina,C.V. (2001). Nuclear receptors in nematodes: themes and variations. Trends Genet. *17*, 206-213.

Sluder,A.E., Mathews,S.W., Hough,D., Yin,V.P., and Maina,C.V. (1999). The nuclear receptor superfamily has undergone extensive proliferation and diversification in nematodes. Genome Res *9*, 103-120.

Snow,M.I. and Larsen,P.L. (2000). Structure and expression of *daf-12*: a nuclear hormone receptor with three isoforms that are involved in development and aging in *Caenorhabditis elegans*. Biochim. Biophys. Acta *1494*, 104-116.

Song,C. and Liao,S. (2000). Cholestenoic acid is a naturally occurring ligand for liver X receptor alpha. Endocrinology *141*, 4180-4184.

Soontjens,C.D., Rafter,J.J., and Gustafsson,J.A. (1996). Ligands for orphan receptors? J Endocrinol *150 Suppl*, S241-S257.

Stehlin,C., Wurtz,J.M., Steinmetz,A., Greiner,E., Schule,R., Moras,D., and Renaud,J.P. (2001). X-ray structure of the orphan nuclear receptor RORbeta ligand-binding domain in the active conformation. EMBO J *20*, 5822-5831.

Street,J.M., Trafford,D.J., and Makin,H.L. (1983). The quantitative estimation of bile acids and their conjugates in human biological fluids. J Lipid Res *24*, 491-511.

Su,M., Merz,D.C., Killeen,M.T., Zhou,Y., Zheng,H., Kramer,J.M., Hedgecock,E.M., and Culotti,J.G. (2000). Regulation of the UNC-5 netrin receptor initiates the first reorientation of migrating distal tip cells in *Caenorhabditis elegans*. Development *127*, 585-594.

Subramaniam,N., Leong,G.M., Cock,T.A., Flanagan,J.L., Fong,C., Eisman,J.A., and Kouzmenko,A.P. (2001). Cross-talk between 1,25-dihydroxyvitamin D3 and transforming growth factor-beta signaling requires binding of VDR and Smad3 proteins to their cognate DNA recognition elements. J Biol Chem. *276*, 15741-15746.

Sutherland,J.D., Kozlova,T., Tzertzinis,G., and Kafatos,F.C. (1995). *Drosophila* hormone receptor 38: a second partner for *Drosophila* USP suggests an unexpected role for nuclear receptors of the nerve growth factor-induced protein B type. Proc. Natl. Acad. Sci U. S. A *92*, 7966-7970.

Svensson,S., Ostberg,T., Jacobsson,M., Norstrom,C., Stefansson,K., Hallen,D., Johansson,I.C., Zachrisson,K., Ogg,D., and Jendeberg,L. (2003). Crystal structure of the heterodimeric complex of LXRalpha and RXRbeta ligand-binding domains in a fully agonistic conformation. EMBO J *22*, 4625-4633.

Swanson,M.M. and Riddle,D.L. (1981). Critical periods in the development of the *Caenorhabditis elegans* dauer larva. Dev. Biol *84*, 27-40.

Sym,M., Basson,M., and Johnson,C. (2000). A model for niemann-pick type C disease in the nematode *Caenorhabditis elegans*. Curr. Biol *10*, 527-530.

Szczepanik,P.A., Hachey,D.L., and Klein,P.D. (1976). Characterization of bile acid methyl ester acetate derivatives using gas-liquid chromatography, electron impact, and chemical ionization mass spectrometry. J Lipid Res *17*, 314-334.

Tatar,M., Bartke,A., and Antebi,A. (2003). The endocrine regulation of aging by insulin-like signals. Science *299*, 1346-1351.

Thompson,M.J., Svoboda,J.A., Lozano,R., and Wilzer,K.R. (1988). Profile of free and conjugated ecdysteroids and ecdysteroid acids during embryonic development of *Manduca sexta (L.)* following maternal inorporation of [14-C] cholesterol. Arch. Insect Biochem Physiol *7*, 157-172.

Thummel,C.S. (2001). Molecular mechanisms of developmental timing in *C. elegans* and *Drosophila*. Dev. Cell *1*, 453-465.

Toll,A., Shoda,J., Axelson,M., Sjovall,J., and Wikvall,K. (1992). 7 alpha-hydroxylation of 26-hydroxycholesterol, 3 beta-hydroxy-5-cholestenoic acid and 3 beta-hydroxy-5-cholenoic acid by cytochrome P-450 in pig liver microsomes. FEBS Lett. *296*, 73-76.

Van Gilst,M.R., Hadjivassiliou,H., Jolly,A., and Yamamoto,K.R. (2005a). Nuclear hormone receptor NHR-49 controls fat consumption and fatty acid composition in C. elegans. PLoS. Biol. *3*, e53.

Van Gilst,M.R., Hadjivassiliou,H., and Yamamoto,K.R. (2005b). A Caenorhabditis elegans nutrient response system partially dependent on nuclear receptor NHR-49. Proc. Natl. Acad. Sci. U. S. A *102*, 13496-13501.

Vowels,J.J. and Thomas,J.H. (1992). Genetic analysis of chemosensory control of dauer formation in *Caenorhabditis elegans*. Genetics *130*, 105-123.

Wagner,R.L., Apriletti,J.W., McGrath,M.E., West,B.L., Baxter,J.D., and Fletterick,R.J. (1995). A structural role for hormone in the thyroid hormone receptor. Nature *378*, 690-697.

Warren,J.T., Petryk,A., Marques,G., Jarcho,M., Parvy,J.P., Dauphin-Villemant,C., O'Connor,M.B., and Gilbert,L.I. (2002). Molecular and biochemical characterization of

two P450 enzymes in the ecdysteroidogenic pathway of *Drosophila melanogaster*. Proc. Natl. Acad. Sci U. S. A *99*, 11043-11048.

Webb,P., Nguyen,N.H., Chiellini,G., Yoshihara,H.A., Cunha Lima,S.T., Apriletti,J.W., Ribeiro,R.C., Marimuthu,A., West,B.L., Goede,P., Mellstrom,K., Nilsson,S., Kushner,P.J., Fletterick,R.J., Scanlan,T.S., and Baxter,J.D. (2003). Design of thyroid hormone receptor antagonists from first principles. J Steroid Biochem Mol Biol *83*, 59-73.

Weinberger,C., Hollenberg,S.M., Ong,E.S., Harmon,J.M., Brower,S.T., Cidlowski,J., Thompson,E.B., Rosenfeld,M.G., and Evans,R.M. (1985). Identification of human glucocorticoid receptor complementary DNA clones by epitope selection. Science *228*, 740-742.

White,K.P., Hurban,P., Watanabe,T., and Hogness,D.S. (1997). Coordination of *Drosophila* metamorphosis by two ecdysone-induced nuclear receptors. Science *276*, 114-117.

White,T., Bursten,S., Federighi,D., Lewis,R.A., and Nudelman,E. (1998). High-resolution separation and quantification of neutral lipid and phospholipid species in mammalian cells and sera by multi-one-dimensional thin-layer chromatography. Anal. Biochem *258*, 109-117.

Wightman,B., Ha,I., and Ruvkun,G. (1993). Posttranscriptional regulation of the heterochronic gene *lin-14* by *lin-4* mediates temporal pattern formation in *C. elegans*. Cell *75*, 855-862.

Williams,S., Bledsoe,R.K., Collins,J.L., Boggs,S., Lambert,M.H., Miller,A.B., Moore,J., McKee,D.D., Moore,L., Nichols,J., Parks,D., Watson,M., Wisely,B., and Willson,T.M. (2003). X-ray crystal structure of the liver X receptor beta ligand binding domain: regulation by a histidine-tryptophan switch. J Biol Chem. *278*, 27138-27143.

Wurtz,J.M., Bourguet,W., Renaud,J.P., Vivat,V., Chambon,P., Moras,D., and Gronemeyer,H. (1996). A canonical structure for the ligand-binding domain of nuclear receptors. Nat Struct. Biol *3*, 87-94.

Wurtz,J.M., Guillot,B., Fagart,J., Moras,D., Tietjen,K., and Schindler,M. (2000). A new model for 20-hydroxyecdysone and dibenzoylhydrazine binding: a homology modeling and docking approach. Protein Sci *9*, 1073-1084.

Wyllie,S.G., Amos,B.A., and Tokes,L. (1977). Electron impact induced fragmentation of cholesterol and related C-5 unsaturated steroids. J Org. Chem. *42*, 725-732.

Xu,H.E., Lambert,M.H., Montana,V.G., Parks,D.J., Blanchard,S.G., Brown,P.J., Sternbach,D.D., Lehmann,J.M., Wisely,G.B., Willson,T.M., Kliewer,S.A., and Milburn,M.V. (1999). Molecular recognition of fatty acids by peroxisome proliferator-activated receptors. Mol Cell *3*, 397-403.

Xu,Y., Fang,F., Chu,Y., Jones,D., and Jones,G. (2002). Activation of transcription through the ligand-binding pocket of the orphan nuclear receptor ultraspiracle. Eur. J Biochem *269*, 6026-6036.

Yanagisawa,J., Yanagi,Y., Masuhiro,Y., Suzawa,M., Watanabe,M., Kashiwagi,K., Toriyabe,T., Kawabata,M., Miyazono,K., and Kato,S. (1999). Convergence of transforming growth factor-beta and vitamin D signaling pathways on SMAD transcriptional coactivators. Science *283*, 1317-1321.

Yang,Y., Griffiths,W.J., Nazer,H., and Sjovall,J. (1997). Analysis of bile acids and bile alcohols in urine by capillary column liquid chromatography-mass spectrometry using fast atom bombardment or electrospray ionization and collision-induced dissociation. Biomed. Chromatogr. *11*, 240-255.

Yao,T.P., Forman,B.M., Jiang,Z., Cherbas,L., Chen,J.D., McKeown,M., Cherbas,P., and Evans,R.M. (1993). Functional ecdysone receptor is the product of EcR and Ultraspiracle genes. Nature *366*, 476-479.

Yoshinaga,S.K., Peterson,C.L., Herskowitz,I., and Yamamoto,K.R. (1992). Roles of SWI1, SWI2, and SWI3 proteins for transcriptional enhancement by steroid receptors. Science *258*, 1598-1604.

Yuan,C.X., Ito,M., Fondell,J.D., Fu,Z.Y., and Roeder,R.G. (1998). The TRAP220 component of a thyroid hormone receptor- associated protein (TRAP) coactivator complex interacts directly with nuclear receptors in a ligand-dependent fashion. Proc. Natl. Acad. Sci U. S. A *95*, 7939-7944.

Zelhof,A.C., Yao,T.P., Evans,R.M., and McKeown,M. (1995). Identification and characterization of a *Drosophila* nuclear receptor with the ability to inhibit the ecdysone response. Proc. Natl. Acad. Sci U. S. A *92*, 10477-10481.

Zeng,Z., Allan,G.F., Thaller,C., Cooney,A.J., Tsai,S.Y., O'Malley,B.W., and Tsai,M.J. (1994). Detection of potential ligands for nuclear receptors in cellular extracts. Endocrinology *135*, 248-252.

Zhao,Q., Khorasanizadeh,S., Miyoshi,Y., Lazar,M.A., and Rastinejad,F. (1998). Structural elements of an orphan nuclear receptor-DNA complex. Mol Cell *1*, 849-861.

APPENDIX A

```
                 ++++++H3++++++              ++++H4+++++  ++++++H5++++++
DAF-12     557 IMDVTMRRFVKVAKGVFAFREVSQEGKFSLLKGGMIEMLTVRGVTRYDASTN 608
LXRα       260 LAIVSVQEIVDFAKQLPGFLQLSREDQIALLKTSAIEVMLLETSRRYNPGSE 311
LXRβ       274 LAIISVQEIVDFAKQVPGFLQLGREDQIALLKASTIEIMLLETARRYNHETE 325
FXR        287 MATNHVQVLVEFTKKLPGFQTLDHEDQIALLKGSAVEAMFLRSAEIFNKKLP 338
PXR        246 MSTYMFKGIISFAKVISYFRDLPIEDQISLLKGAAFELCQLRFNTVFNAETG 297
VDR        233 LVSYSIQKVIGFAKMIPGFRDLTSEDQIVLLKSSAIEVIMLRSNESFTMDDM 284
CAR        164 INTFMVLQVIKFTKDLPVFRSLPIEDQISLLKGAAVEICHIVLNTTFCLQTQ 215
EAR1α      442 SFTPAVREVVEFAKHIPGFRDLSQHDQVTLLKAGTFEVLMVRFASLFNVKDQ 493
EAR1β      408 SFTPAVKEVVEFAKRIPGFRDLSQHDQVNLLKAGTFEVLMVRFASLFDAKER 459
TRα        221 IITPAITRVVDFAKKLPMFSELPCEDQIILLKGCCMEIMSLRAAVRYDPESD 272
TRβ        275 IITPAITRVVDFAKKLPMFCELPCEDQIILLKGCCMEIMSLRAAVRYDPESE 326
RARβ       112 LATKCIIKIVEFAKRLPGFTGLTIADQITLLKAACLDILILRICTRYTPEQD 163
RARα       231 LSTKCIIKTVEFAKQLPGFTTLTIADQITLLKAACLDILILRICTRYTPEQD 282
RARγ       233 LATKCIIKIVEFAKRLPGFTGLSIADQITLLKAACLDILMLRICTRYTPEQD 284
RORα       326 KITEAIQYVVEFAKRIDGFMELCQNDQIVLLKAGSLEVVFIRMCRAFDSQNN 377

                    +H12+
DAF-12     740 EAEELPGEFFKIK- 753
LXRα       434 KLPPLLSEIWDVHE 447
LXRβ       448 KLPPLLSEIWDVHE 461
FXR        460 KFTPLLCEIWDVQ- 472
PXR        421 FATPLMQELFGITG 434
VDR        414 KLTPLVIEVFGNEI 427
CAR        338 AMMPLLQEICS--- 348
TRα        477 ADSPSSSEEEPEVC 490
TRβ        452 LFPP----LFLEVF 461
RARβ       323 SISPSSVENSGVSQ 336
RARα       449 SLSPSSNRSSPATH 462
RARγ       441 DEVPGG-QGKGGLK 454
RORα       510 HFPPLYKELFTSEF 523
```

DAF-12 alignment of regions corresponding to H3-5 and H12 with other nuclear receptors based on bioinformatics data by Mooijaart *et al.* (2005). This alignment uses the same protein sequences and as close to the same alignment parameters as possible to generate an appropriate alignment. Abbreviations not in the body of the text are progesterone receptor (PXR), vitamin D receptor (VDR), constitutive androgen receptor (CAR), estrogen receptor related 1 (EAR1), retinoid acid receptor (RAR), and retinoid acid receptor related orphan receptor (ROR). Amino acids corresponding to helix regions are noted at the top of the alignment.

APPENDIX B

SOLVENT LIST

Acetonitrile (#9255-02, JT Baker)

Chloroform (#270636, Sigma)

Diethyl ether (#9259-02, JT Baker)

DMSO (#115560010, Acros Organics)

Ethanol (#E7023, Sigma)

Ethyl Acetate (#270520, Sigma)

Glacial Acetic Acid (#AX0073-14, EM Bioscience)

Hexane (#217-1, Burdick & Jackson)

Isopropanol (#323-1, Burdick & Jackson)

Methanol (#230-1, JT Baker)

Toluene (#347-1, Burdick & Jackson)

Trimethyl Borate (#32569, Alfa Aesar)